**REPUBLIQUE ALGERIENNE DEMOCRATIQUE ET POPULAIRE**
**MINISTERE DE L'ENSEIGNEMENT SUPERIEUR ET DE LA RECHERCHE SCIENTIFIQUE**
**UNIVERSITE ECHAHID HAMMA LAKHDAR D'EL OUED**

**F**aculté de la **T**echnologie
**D**épartement de **G**énie **M**écanique
**L**aboratoire de **V**alorisation des **T**echnologies des **R**essources **S**ahariennes
LVTRS

# Thèse de Doctorat

N° d'ordre :
N° de série :

Présentée par :

## HADJADJ Abdessamia

En vue de l'obtention du diplôme de **DOCTORAT LMD** en **:**
**Filière : Génie mécanique**
**Option : Energétique**

# Etude de la faisabilité technique et économique de l'installation d'un échangeur de chaleur géothermique dans la région d'El Oued-Algérie-

**Soutenue le 06/ 01/ 2021, devant le jury composé de :**

| | | | | |
|---|---|---|---|---|
| Pr | Fethi BOURAS | Professeur | UHL El-Oued | Président |
| Dr | Ali BOUKHARI | MCA | UHL El-Oued | Examinateur |
| Pr | Djamel BECHKI | Professeur | UKM Ouargla | Examinateur |
| Pr | Abdelghani BOUBEKRI | Professeur | UMK Ouargla | Examinateur |
| Pr | Boubaker BENHAOUA | Professeur | UHL El-Oued | Dir. de Thèse |
| Dr | Abdelmalek ATIA | MCA | UHL El-Oued | Co dir. de Thèse |
| Dr | Ridha MENECEUR | MCB | UHL El-Oued | Invité |

**DEMOCRATIC AND POPULAR REPUBLIC OF ALGERIA**
**MINISTRY OF HIGHER EDUCATION AND SCIENTIFIC RESEARCH**
**UNIVERSITY ECHAHID HAMMA LAKHDAR OF EL-OUED**

**F**aculty of **T**echnology
**D**epartment of **M**echanical **E**ngineering
**L**aboratory of **V**alorization and **T**echnology of **S**aharaian **R**esources
**LVTRS**

# Doctoral thesis

N° order :
N° series :

Presented by:

**HADJADJ Abdessamia**

Thesis with a view to obtaining the **DOCTORATE** degree in**:**
**Mechanical Engineering**
**Speciality: Energetic**

# Technical- economic study of feasibility and realization of geothermal heat exchanger in El-Oued region – Alegria-

**Defended on 06/ 01/ 2021, in front of the jury composed of:**

| | | | | |
|---|---|---|---|---|
| Dr | Fethi BOURAS | Professeur | UHL El-Oued | President |
| Dr | Ali BOUKHARI | MCA | UHL El-Oued | Examiner |
| Dr | Djamel BECHKI | Professeur | UKM Ouargla | Examiner |
| Dr | Abdelghani BOUBEKRI | Professeur | UMK Ouargla | Examiner |
| Dr | Boubaker BENHAOUA | Professeur | UHL El-Oued | Thesis Director |
| Dr | Abdelmalek ATIA | MCA | UHL El-Oued | Thesis Co-director |
| Dr | Ridha MENECEUR | MCB | UHL El-Oued | Invited |

# ACKNOWLEDGMENTS

I want to express my sincere gratitude to my supervisor **Pr. Boubaker BENHAOUA** and my Co-Supervisor **Dr. Abdelmalek ATIA**, for their excellent guidance, valuable advice, strong support, and continuous encouragement throughout the course of this research work at El Oued University. It has been a great pleasure and privilege to work under their supervision toward completion of this research.

I greatly acknowledge the supervising committee members, **Pr. Fethi BOURAS, Dr. Ali BOUKHARI** and **Dr. Ridha MENECEUR** from El Oued University; and **Pr**. **Djamel BECHKI and Pr. Abdelghani BOUBEKRI** from university of Ouargla. I would also like to appreciate all their guidance, suggestions and comments for improving this thesis.

I wish to express my deepest gratitude to VTRS Laboratory (El Oued university) and LENREZA Laboratory (Ouargla University) for their helpful support.

My special acknowledges go to **Dr.Müslüm Arici** (Kocaeli University, Turkey) for his excellent guidance, precious help and valuable advices.

I wish to express my deepest gratitude to all staff and my colleagues of Mechanical Engineering Department at El Oued University, for their helpful technical discussions and suggestions during the preparation of my thesis.

## Nomenclature

| | |
|---|---|
| Cp | Specific heat capacity, J kg$^{-1}$ K$^{-1}$ |
| D | Exchanger diameter, m |
| DT1 to DT7 | Temperature of air along the HWAHE pipe length, °C |
| $E_x$ | Exergy rate, W |
| h | Enthalpy, kJ kg$^{-1}$ |
| L | Exchanger lengths, m |
| ṁ | Mass flow rate, kg s$^{-1}$ |
| Q | Heat exchange rate, W |
| Re | Reynold number |
| s | Entropy, kJ kg$^{-1}$ °C $^{-1}$ |
| A | Surface area, m$^2$ |
| T | Temperature, °C |
| U | Overall heat transfer coefficient, W m$^{-2}$ °C$^{-1}$ |
| V | Air velocity inside the pipe, m s$^{-1}$ |
| $W_{me}$ | Uncertainty of measurement, % |
| $W_{an}$ | Uncertainty in Rotameter reading, % |
| $W_{sl}$ | Uncertainty associated with system leakages, % |
| $W_{te}$ | Uncertainty of the thermocouple, % |
| $W_T$ | Total uncertainty in measurement of temperature, % |
| $W_{\dot{m}}$ | Total uncertainty in measurement of mass flow rate, % |
| Z | Depth of soil, m |
| ΔP | Pressure loss, Pa |
| ΔT | Temperature difference between the inlet and outlet, °C |
| LMTD | Log mean temperature difference, °C |

**Greek letters**

| | |
|---|---|
| λ | Thermal conductivity, W m$^{-1}$ K$^{-1}$ |
| α | Thermal diffusivity of the soil, m$^2$.s$^{-1}$ |
| ρ | Density, kg m$^{-3}$ |
| ε | Thermal efficiency, % |
| η | Exergy efficiency, % |
| Λ | Linear loss ratio of load |
| ζ | Singular loss ratio of load |
| μ | Dynamic viscosity of air, N s m$^{-2}$ |

**Subscripts**

| | |
|---|---|
| amb | Ambient |
| in | Inlet |
| out | Outlet |
| wat | Water |
| lin | Linear |
| sin | Singular |
| des | Destruction |
| Ej | Exajoule |
| IP | Inputb power |
| P.P | Pumping power |

# Contents

# List of Tables

# List of Figures

# General introduction

## Context

The buildings sector is a major consumer of energy globally. It constitutes a third of the world's energy use, according to the International Energy Agency. In particular, between 2000 and 2010, the amount of energy used for air conditioning increased by about 60 % . The cooling of the premises in Algeria comes mainly from electrical energy. This energy represents 46.6% of the total consumption of energy in the country. Furthermore, this proportion is continuously growing with the development of dwellings, without taking environmental conditions into account, and with the increase in living standards. Indeed, the forecast was conducted by the Ministry of Energy(ME) [10], of the final demand for energy by sector.

It indicates that the buildings sector will be the most energy-consuming field by 2030. This reflects a very high energy bill.

In addition to this energetic existence, the increase in the usage of this energy is followed by an increase in the amount of emissions pollution.

As a result, it is necessary to replace the current conditioning devices, which are major energy consumers, with other resource new technologies having better energy efficiency. This can only be guaranteed by developing the use of renewable energies.

The type of renewable energy most appropriate for heating and cooling buildings is surface or underground geothermal energy. In Algeria, the surface geothermal potential is very important. Indeed, measurements of the soil temperature at the site of El Oued, approximately three-meter deep, are in the order of 22 $^oC$ in winter and 25 $^oC$ in summer.

So, the ground can be seen as a gigantic heat reservoir from which excess heat can be drawn or rejected upon the need via a heat exchanger. The air-ground heat exchanger is a geothermal installation consisted mainly of an underground pipe in which the outside ventilation air is pumped. The air will lose or gain heat depending on whether its temperature is high or low compared to the temperature of the soil at the burial depth.

Holicoidal Water Air Heat Exchangers (HWAHEs) are chosen according to the energy needs of the buildings to be conditioned. Indeed, a single unit is sufficient for a room or a small house, while for large houses, larger areas, several HWAHEs must be used.

The interest of Algeria in exploiting geothermal energy opens up new possibilities for economic growth, especially since it is an energy source that can help reducing the problems of large energy consumption in the sector buildings.

## Objective of this study

The objective of this thesis is to initiate and test the exploitation, in Algeria, of the thermal potential of the ground and especially the surface geothermal energy, for air conditioning individual premises. An experimental study of the performance of such systems in the climatic conditions of our country can allow us to conclude wether feasibility of geothermal energy, in our country, may be done;

- A new geometry that consists of a helicoid exchanger may be thougth as development design. This design helps the geothermal heat exchanger to reduce the installation area and ensure the transfer of heat.
- In order to assess the evolution of the air temperature inside the buried exchanger a need to propose analytical and numerical models for the principle of energy balances.
- Experimental validation of the developed models takes place from the measurements throught an installed system in El Oued region.
- The electricity consumption for a house cooling and heating will be calculated with and without the HWAHE system, after having determined the energy usage for cooling and heating the house.

# Organization of the thesis

This thesis contains sixth chapters:

- In the first chapter entitled "**General information on geothermal energy**" in wich a brief overview is given on the energetic state in Algeria. Next, a description of geothermal energy as a renewable energy is presented with an emphasis on its applications in the field of housing in particular, geothermal heat pumps and air-to-ground heat exchangers.
- The second chapter entitled "**State of art on geothermal heat exchanger systems**" provides an overview of the various works carried out around the world under different operating conditions of the air-to-ground geothermal heat exchanger. In this context, analysis of previous works will allow us to predict the challenges to be taken into account in the next chapters;
- .In the third chapter entitled "**Study of thermal heat transfer**" Various theoretical balances used to calculate the variation of quantities will be described;
- The experimental study is presented in the fourth chapter. The existing experimental setup taken considerations was done in El Oued region at the South-East of (Algeria), is presented. The monitoring set up for this experimental part of system energy performance is helicoidally Water Air Heat Exchanger (HWAHE);
- The fifth chapter is reserved for the exposure, evaluation and interpretation of the various obtained results;
- In the sixth chapter "**Techno-economic study**",a modelling analysis into the reduction of the cooling and heating energy consumption of a specific house, coupled with the HWAHE device under the designed conditions, will be presented;
- finaly a general conculsion about this work will take place in this munscript.

# Chapter I

# General information on geothermal energy

## I.1 Introduction

firstly,this chapter deals with Algeria's energy situation from an economic point of view, then it will talk about geothermal energy as well as clean and renewable energy and their different applications, in particular in the field of geothermal energy.The emphasis is on application of air-ground heat exchangers wich a known as Canadian wells depending on the use for heating or cooling buildings.

## I.2 Global energy demand

The world energy demand is growing, it is satisfied by a very predominantly carbon supply. In 2000, global final energy consumption was 394 Ej (IEA, 2000) and primary energy consumption was 583 Ej (BP, 2019) the [1, 11], whose world population was 7.8 billion inhabitants (PRB, 2019) [12]. The difference between primary energy and final energy comes on the one hand from the energy consumption of the industries of the production system, transport and distribution of energy (mines, refineries), losses in transport (electric lines, gas pipelines) and especially energy losses linked to the transformation of heat into electricity in thermal power plants (conventional or nuclear).

It is interesting to know the primary and final energy consumption under two aspects: the primary energy consumption by product and the final energy consumption by energy product and by sector of activity.

## I.3 Primary energy consumption by form of energy

Despite the determination of the international community to reduce and decarbonize (that is, to favor low-carbon sources that emit less greenhouse gases), the demand for primary energy has increased by more than 52% from 2000 to 2019, and the share of hydrocarbons remained dominant at almost 87%, as illustrated in Figure I.1.

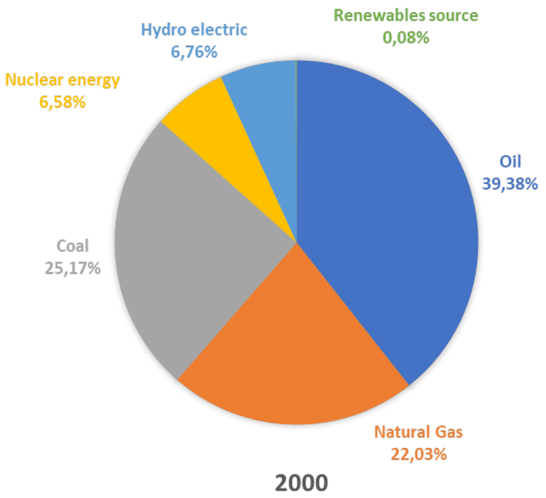


(a)

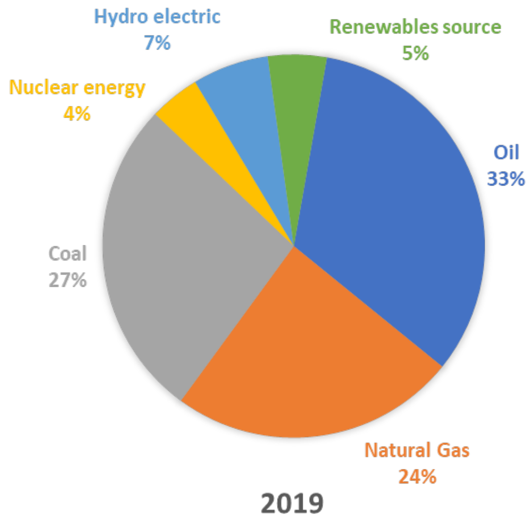


(b)

Figure I.1: Breakdown of overall output of primary energy by form of energy [1]

Fossil fuels are dominant: the first consumed source is petroleum (33%), followed by coal (27%); the share of natural gas is around 24% of primary consumption. Production from renewable sources, dominated by hydraulics (7%), is higher than that of nuclear (4% in 2014). World consumption of primary energy is around 583 Ej in 2019 (see Appendix A). A significant part (40%) of primary energy consumption is devoted to the production of electricity.

## I.4 Energy consumption in Algeria

Final consumption includes all final energy uses, reached 48.1 Mtoe in 2018, reflecting an increase of 3.5 Mtoe, or (+ 7.8%) compared to 2017. The evolution of final consumption by product and by sector of activity is detailed entited below [2, 10, 13].

### I.4.1 By energy product

Strong increase (17.4%) in natural gas consumption to 16.0 Mtoe, which has become the main form of energy consumed and was boosted after its first place in the final energy mix of 33.3%, induced by the growing needs of Sonelgaz customers, particularly those of buildings. Petroleum products energy consumed, with 32.2% of final consumption (15.5 Mtoe) a slight recovery (1.2%) in the consumption of petroleum products per day after two years of decline. Electricity consumption growth (4.9%) to reach 13.9 Mtoe, following the increase in demand from Sonelgaz customers. Finally, growth in demand for LPG (+ 11%) to 2.6 Mtoe, driven by that of LPG / C which experienced a strong increase (42%) (see Figure I.2).

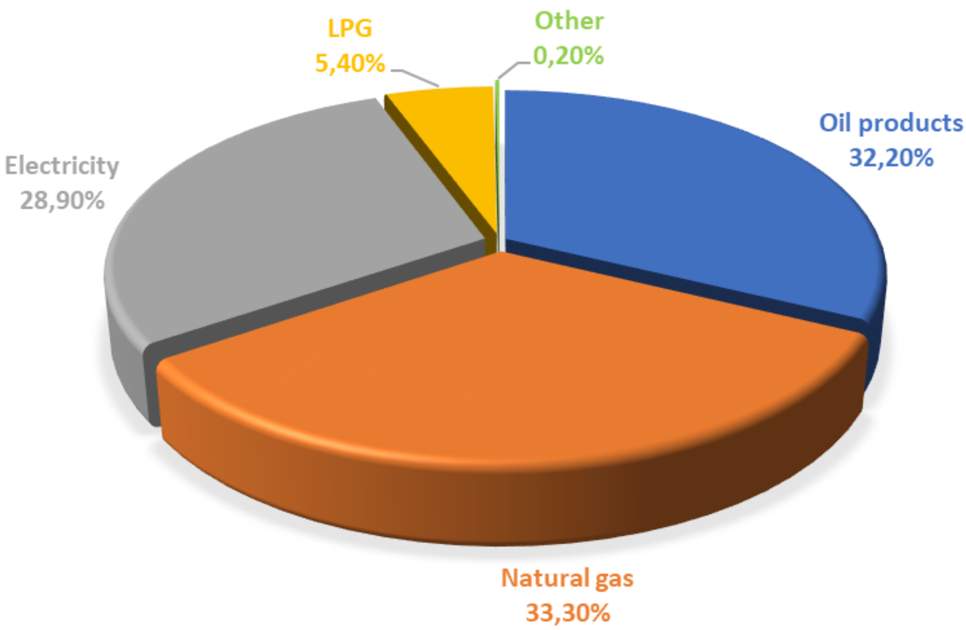


Figure I.2: Breakdown of final consumption by energy product for 2018 [2]

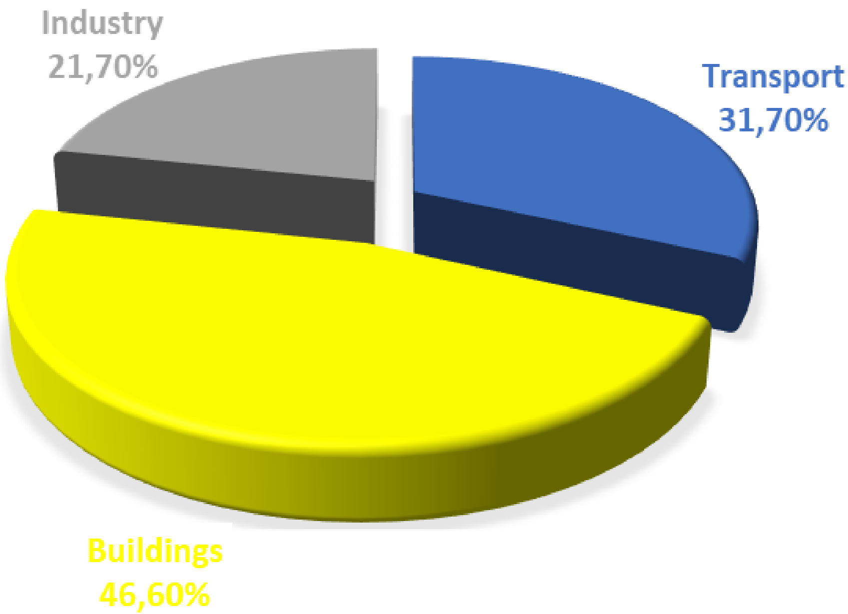


Figure I.3: Breakdown of final consumption by sector of activity for 2018 [2]

### I.4.2 By sector of activity

The detail of final consumption, by sector of activity, is given in the figure I.3 below: According to the National Agency for the Promotion and Rationalization of the Use of Energy (APRUE), in its report on the final energy consumption of Algeria, for the year 2018, the most consumer sector of energy is the buildings sector of 46.6 %, then industry with 21.7 % and finally transport with 31.7% [2].

### I.4.3 Energy consumption in the buildings sector in Algeria

Figure I.4 represents energy consumption in the building sector in Algeria wich was probably multiplied by five between the years 2009-2018. Electricity, natural gas, fuel, coal, wood and even electric batteries are energy carriers of the domestic sector. The different types of energy serve us globally for four different uses,heating, lighting, domestic hot and cooking.

Heating represents the largest expenditure for around 60% of household energy; Lighting, appliances.

- Lighting, audiovisual appliances and air conditioning account for almost 20% of energy;

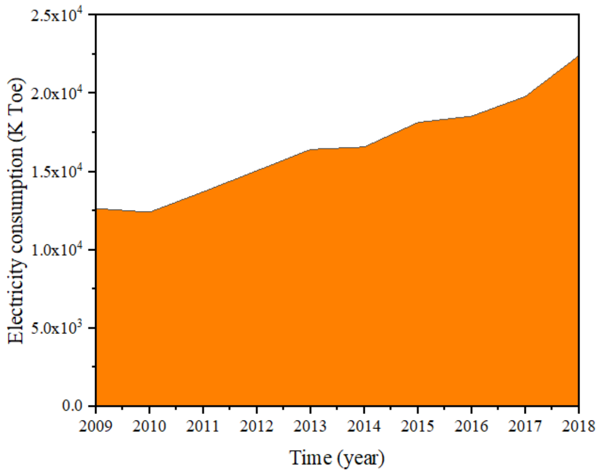


Figure I.4: Evolution of national electricity consumption in the household sector

- The domestic hot water required represents almost 15%;
- Cooking represents almost 5%.

Figure I.4 presents final energy consumption per citizen is 0.48 toe in 1990, its evolution will increase from 0.71 toe in 2000 to 1.35 toe in 2010 and to 1.88 toe in 2020. Today, Algeria energy needs are met almost exclusively by hydrocarbons [2, 10, 13–22].

## I.5 Consumption of natural gas and electricity in Algeria

Domestic natural gas consumption started in 1961 at a rate of 156 million $m^3$ and reached 1.4 billion $m^3$ in 2000. According to statistical data obtained from SONELGAZ services figure I.5, it shows an evolution in gas consumption, with an average consumption of 8.5 Billion $m^3$ in 2010, and continued consumption of gas in 2018, when it reached 16.9 billion $m^3$, and the expected development of gas consumption contenus to groo.

Electricity consumption and production between 1980 and 2012 increased by 41.5 % and 61.5%. In recent years, electricity consumption in Algeria has risen by 4.9 % year and long-term demand for electricity has been forecast to rise by 7 % per year in the long term. Furthermore, in recent years the distribution of electricity has experienced

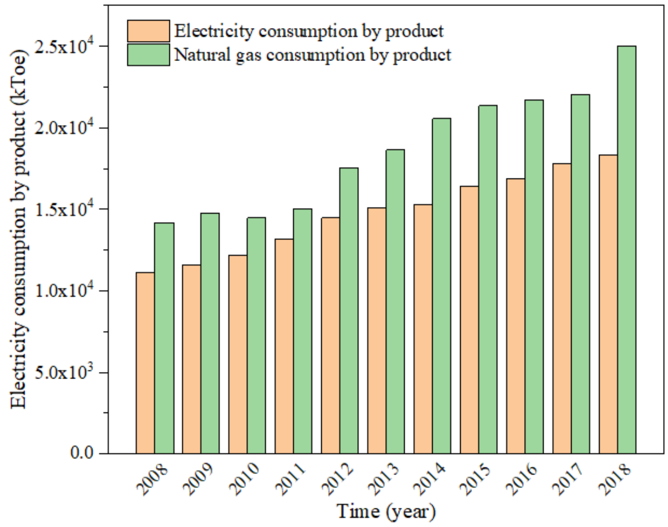


Figure I.5: National consumption by form of energy

significant disruptions due to rising domestic demand, mainly due to the increased use of air conditioners, especially in the residential sectors [2, 10, 13–22].

## I.6 Climatic data

### I.6.1 Geographical data

Algeria is distinguished by a variety of climatic zones which can be divided into three categories:

1. The Tell: temperate humid climate of Mediterranean type;
2. The High Plains: continental climate;
3. The Sahara: arid and dry climate.

Algeria is located between latitude $18^o$ and $38^o$ North, and between $9^o$ West longitude and $12^o$ East longitude, with the international meridian $0^o$ Greenwich passing near the town of Mostaganem. The distances between north and south, east and west vary from 2000 to 1600 km, respectively [23].

### I.6.2 Climatic zones in Algeria

Algeria has an area of 2.381,741 $km^2$ , with great geographic and climatic diversity, from the coast to the desert. The main climatic regions are illustrated in figure I.6 :

- **Zone A (Coastal Zones):** the maritime coast whose climate is particularly temperate with mild and rainy winters and hot, humid summers;
- **Zone B (Internal areas):** the mountain coastline, which has a cold climate in winter, but the summer is hot and less humid;
- **Zone C (Upper Highlands):** heights characterized by cold and fairly long winters of the same height as zones A and B and hot and dry summers;
- **Zone D (Saharan zones):** it represents the desert climate which is characterized by a large solar reserve and low humidity, the winter period is shorter with moderate days and cold nights, and the summer is very hot when the temperatures reach $45^oC$ in the shade.

The thermal behavior of a building depends on external stresses such as the temperature of the external air, the radiative exchange with its surroundings and mass transfer. A building is made of interconnected elements and heat transfer takes place concurrently by conduction, convection and radiation [24].

### I.6.3 Climate of the El Oued region

The region of EL Oued is characterized by a Saharan climate, with a very reduced rainfall, high temperatures, high evaporation and a weak biological life of the ecosystem (See Appendix A Table I.1). The average monthly temperatures recorded in the hottest month (July) are $34.3^oC$. While those of the coldest month (January) are $11.6^oC$. Precipitation is rare and irregular, and ranges from 0.3 mm to 12 mm. Annual average rainfall at El Oued is 6.65 $mm.year^{-1}$. (Hot and dry wind) with a speed of up to 4.44 $m.s^{-1}$ can be remarked at any time of year. Relative humidity levels vary from 25 to 70 % [25] .

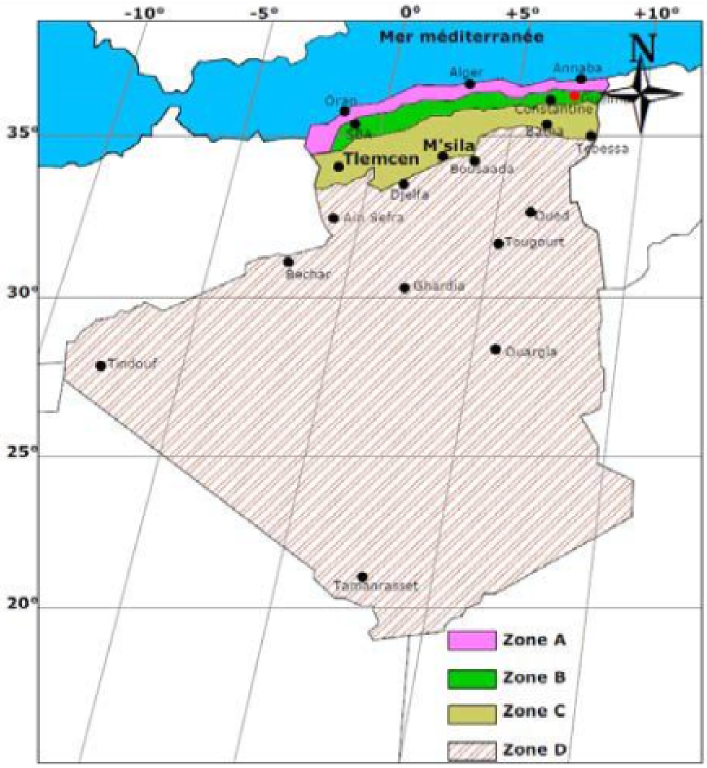


Figure I.6: Classification of climate in Algeria [23]

The quantitative study of the climate of El Oued region climate reveals that the climate is exactly, of arid type, in conformity with the theory of "De Martonne". According to the climatic conditions of the region of El Oued region and the tables of Mahoney [26], three main areas can be distinguished:

**The sub-heating zone**, which spreads both day and night during the winter season, and only at night during the spring season (Mars and April) and autumn (October and November).

**The comfort zone**, present in the months of March, April, October and November by day, and the months of May and September by night.

**Finally, the overheating zone**, which lasts during the summer during the day and the days for the months of May and September.

## I.7 Integration of renewable energies in Algeria

The development of new energy resources remains one of the main concerns of the public authorities in Algeria. Actually, the combination of renewable energies in the

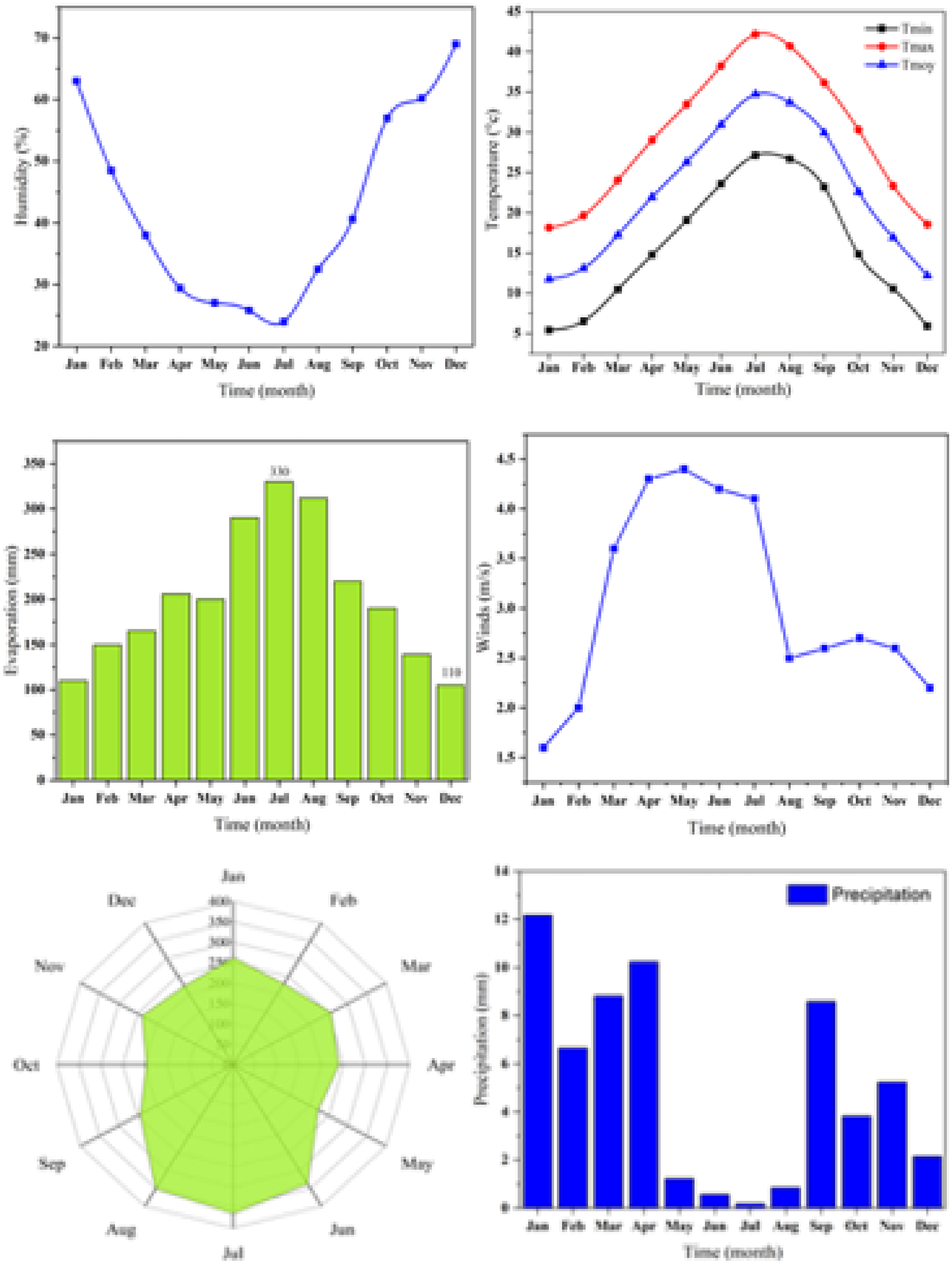


Figure I.7: Interpretation of climatic data for the El Oued region (2008-2018)

national energy mix constitutes a major challenge in the preservation of fossil resources by diversification of electricity production sectors and contribution to sustainable development In 2011, our country adopted an ambitious renewable energy production program. This program provided the foundations, the means for its implementation and a timetable for 2030.

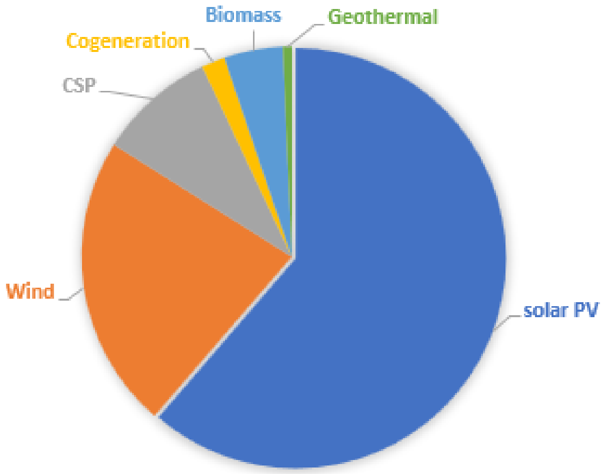


Figure I.8: Distribution of the National Renewable Energy Program [3]

The objective of this program is to produce 22 GW of renewable energy electricity by 2030, of which 12 GW will be devoted to national demand and 10 GW to export. This program focuses on the development of photovoltaic and large-scale wind energy, the introduction of biomass (waste valuation), cogeneration and geothermal energy, and also the postponement of the development of solar thermal energy (CSP) until 2021.

The completion of this figure I.8 will make it possible to achieve, by 2030, a share of renewables of almost 27% in the national electricity production balance sheet [3].

## I.8 Geothermal energy

The European renewable energy Directive 2009 (2009/28 / EC) defines geothermal energy as "energy stored as heat below the solid earth surface." Geothermal energy is on the surface of the globe all over. It is due to a temperature gradient (increase in depth temperature), averaging 3 $^{o}C$ per 100 meters deep. Regional variations in the geothermal gradients were observed though. It can be related to the age and composition of 1 or similar geological structures.

This energy is exploited by extracting heat, which makes it possible, depending on the quantities and temperatures obtained, to produce electricity, to supply collective or individual heating networks (individual houses, residences collective, heating of service or industrial buildings, ...).

Geothermal energy use dates from the 19th century for non-electric uses such as heating or cooling. Geothermal energy is currently the thermal source of applications in agriculture, aquaculture, district heating, and also for heating and cooling in the residential and industrial sectors [27]. The output is also assured at a pace from 100 to 300 years that could be sustained for a long time [28]. Therefore, geothermal systems contribute to the efficiency of sustainable development and the benefits of a geothermal system are multiple: simple, safe, adaptable, capable of responding to a load continuously, variable or for peak [29].

## I.8.1 Geothermal energy falls into three categories

### I.8.1.1 High geothermal energy

High energy geothermal resources with a temperature above 150 $^oC$ are located between 1500 and 3000 m below sea level in geographical areas with an abnormally high geothermal gradient. They correspond to volcanic regions located close to the borders of the lithospheric plates: the Pacific "fire belt", the Lesser Antilles arc, the Mediterranean arc, or the great African rift. This type of geothermal energy is then used to power thermal springs, heat houses, or even produce electricity.

### I.8.1.2 Medium geothermal energy

Present in many parts of the world, medium-energy resources (90 to 150 $^oC$) are found in the same geological setting as high-energy geothermal energy, at a shallower depth (less than 1000 m). But they are also hidden in sedimentary basins at depths ranging from 2000 to 4000 m. Medium energy geothermal energy also occurs in many of the very localized regions where discontinuities in the rocks occur, faults through which water can easily rise to the surface, indicating its presence through hot source.

### I.8.1.3 Low-energy geothermal energy

Low energy geothermal energy is based on the direct use of hot water heat contained in deep aquifers, with a temperature between 30 and 150 $^oC$. It is present in many regions of the world: The Amazon and Rio Plata basin in South America, the Boise region

(Idaho) and the Mississippi-Missouri basin in the USA, the Pannonian basin in Hungary, the Paris and Aquitaine basins in France, the Artesian basin in Australia, the Beijing region and Central Asia.

#### I.8.1.4 Very low energy geothermal energy

It is an energy that is located a few meters below the ground surface and whose temperature is lower 30 $^oC$. Everywhere and at any point, including in the crystalline basement regions, the heat stored in the ground surface layers (few meters deep) can be captured and converted by the 'through a heat transfer fluid for heating and cooling individual buildings. For collective or commercial buildings, it is important to implement heat pumps which use this energy at low temperatures to increase it to a sufficient temperature for heating [30].

## I.9 Types of operation and application

The General exploitation of geothermal energy depends on the temperature of the subsoil, which in turn depends on the depth where the heat exchangers will be installed. The minimum depth (also called minimum production depth (km)) is the depth that corresponds to a temperature of the surface of the ground of about 40 $^oC$. The map of the minimum production depth of the world is represented on figure I.9, (in respect the this figure for Algeria, it is clear that the minimum production depth is between 1 and 1.5 km) [31] .

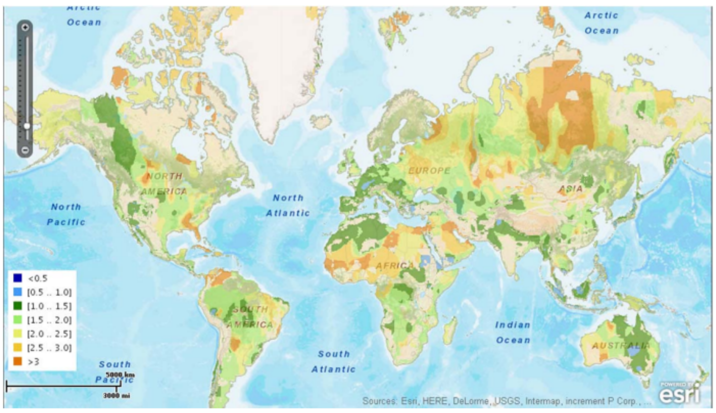


Figure I.9: Map of minimum production depth

## I.10 Geothermal potential in Algeria

Geothermal energy occupies an important part of renewable energy sources in Algeria. The uses of this energy are many and varied. They range from direct uses, such as fish farming, greenhouse heating, and balneotherapy to industrial uses, such as power generation. The geothermal resources of Algeria are of low energy type, they are mainly located in the North and in the Sahara [31].

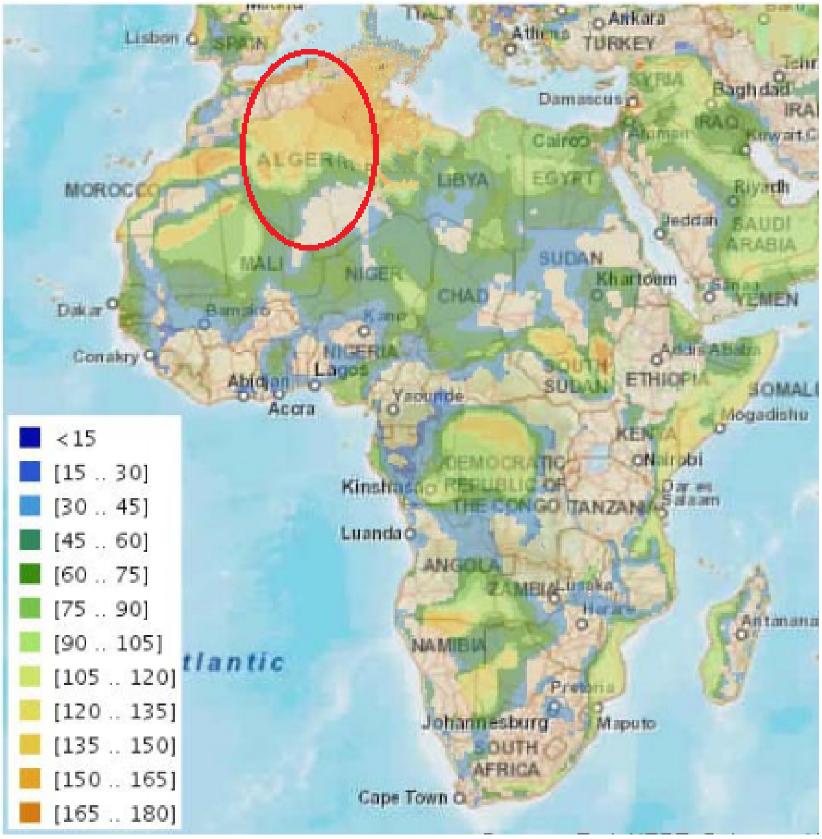


Figure I.10: Minimum production depth map

The maximum temperature extracted for a depth of 3 km or less is shown in Figure I.9 for Algeria.the later has better geothermal as see in Figure I.10 shows that Algeria has better geothermal potential compared to African countries. Indeed, the maximum temperature extracted for depth less than or equal to 3 km is between 100-150 $^oC$ [31].

Gouareh et al. [32] have elaborated on a geothermal gradient map showing the temperature variation as a function of depth over the Algerian national territory. Three zones with a strong geothermal gradient are highlighted: in the North-East, more particularly in the Constantine regions, in the North-West (the Oran regions), in addition to the numerous thermal springs in the Algerian South and more exactly in the South-West. In these regions, the value of the geothermal gradient can be as high as 7 $^oC/$ 100 m (see Figure I.11).

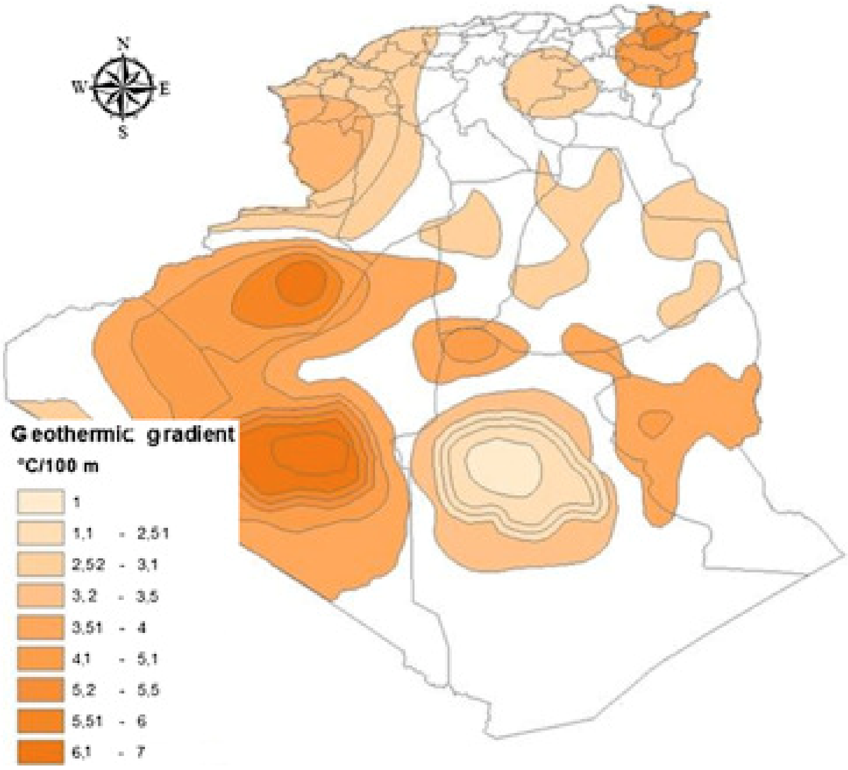


Figure I.11: Geothermal gradient map in Algeria

# I.11 Geothermal energy capture system

Geothermal energy collection systems are made up of exchangers, (also called sensors) buried in the ground according to their arrangement, there are three types of exchanger: horizontal, vertical and helical.

## I.11.1 Horizontal heat exchanger

These are tubes (generally made of polyethylene) installed and buried horizontally at a shallow depth (0.6 m to 1.2 m). The fluid circulating in the exchanger tubes is called refrigerant. Horizontal exchangers are installed in-ground, exposed to the sun, next to

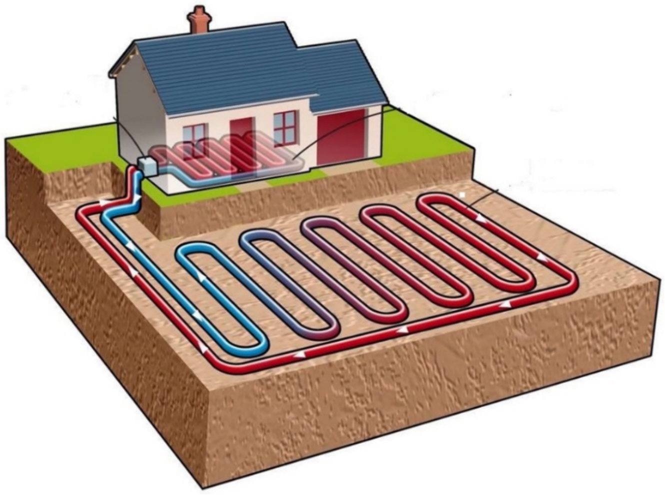

Figure I.12: Geothermal heat pump diagram using a horizontal sensor

the building, they must be placed more than 2 m from trees and 3 m from foundations, wells, septic tanks, and drainage systems in shown Figure I.12.

## I.11.2 Vertical heat exchanger

### I.11.2.1 Exchangers Vertically Buried

Exchangers Vertically Buried: A borehole is carried out in which a sensor containing a heat transfer fluid is mounted (U-shaped tube, or double U in polyethylene). With cement and bentonite, it is then sealed. It can achieve a drilling depth of up to 100 m. In theory, two geothermal probes spaced at least 10 m apart will heat a house with 120 $m^2$ of living space as shown in figure I.13. In general, this type of exchanger is more costly to mount, but on the other hand, it is less costly on the piping side than horizontal exchangers [33].

### I.11.2.2 Vertical exchanger on ground water

Vertical exchangers are called "ground water" when the capture of geothermal energy is guaranteed by the water figure I.14. The heat of the subsoil is that contained in the water of shallow aquifers captured by drilling.

In the case of vertical exchangers on ground water, the ground water with drawn (suction well) is discharged (into another river or discharge well). This type of exchanger

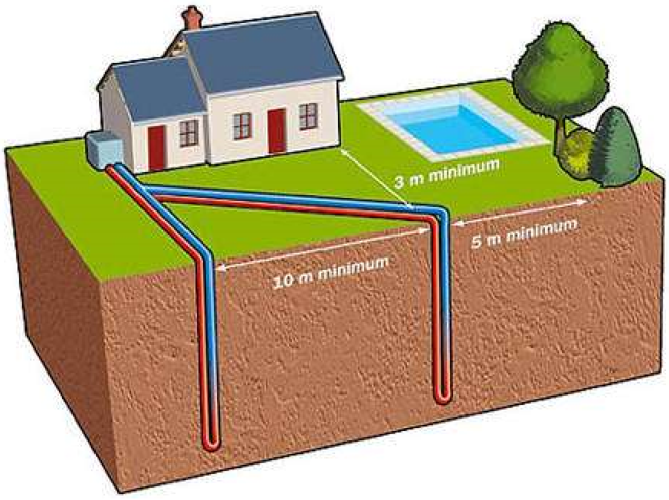


Figure I.13: Geothermal heat pump diagram with vertical sensor (geothermal probe)

is interesting from a point of view cost since a single borehole provides air conditioning to collective or tertiary buildings [33].

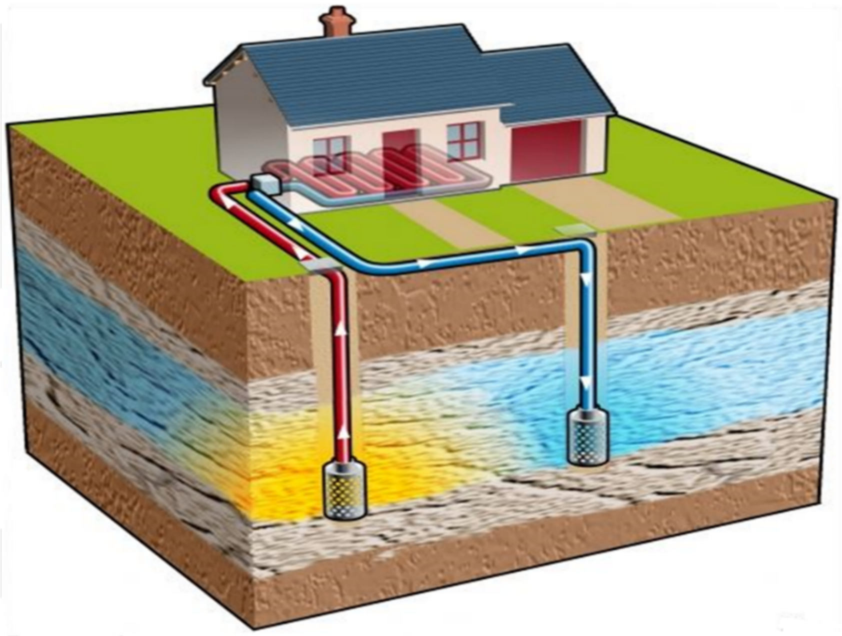

Figure I.14: Geothermal heat pump diagram with groundwater

### I.11.3 Helicoidal heat exchanger

As mentioned previously, geothermal probes require substantial investment in the high cost of drilling, and horizontal geothermal sensors need large, well-off ground surfaces. Faced with these constraints, other geometries and forms were developed, mainly the

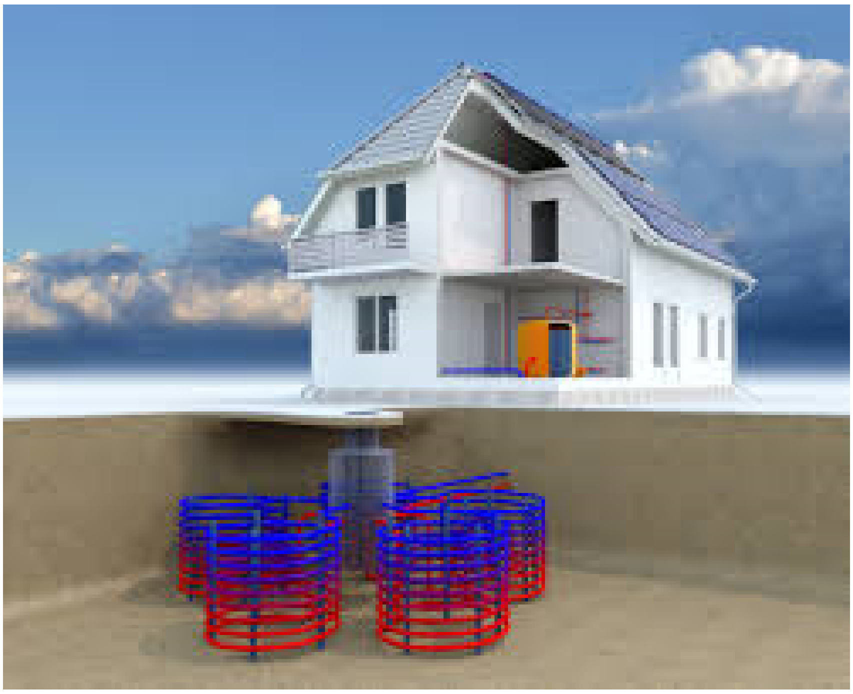

Figure I.15: Schematic representation of helical sensors

circular helix shape, also known as the helicoidal. The geothermal heat exchanger which takes this form is generally called "a geothermal basket "(Moch, 2013) and presented in figure I.15. Its particularity lies in its spiral form which allows it to occupy small ground area compared to the horizontal sensors, the helical exchangers are more practical to install than the horizontal sensors, but also more economical than the vertical sensors, since the cost of the installations of the exchangers entered is linked to the depth of the drilling [34, 35].

## I.12 Earth-to-air heat exchanger (Canadien well)

Air -earth heat exchangner (or Canadian underground tube): The idea of utilizing the earth as a heat sink was known in ancient times. In about 3000 B.C., Iranian architects used wind towers and underground air tunnels for passive cooling. Underground Air Tunnels (UAT) systems, nowadays also known as earth to air heat exchangers (EAHE). EAHE system is a very low energy geothermal heat exchanger used to cool or heat the ventilated air in a building.It has been in use for years in developed countries due to their higher energy utilization performances compared to conventional heating and cooling

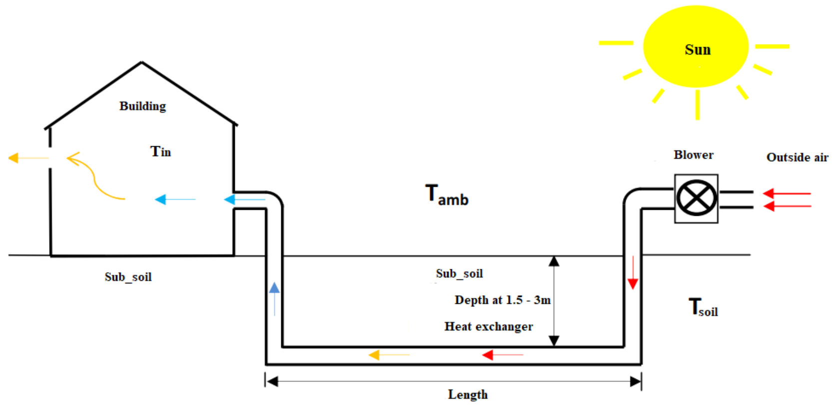


Figure I.16: Earth to air heat exchanger in operation during summer season

systems. EAHE is a passive climate control technique that has application in buildings and agriculture homes using the underground soil temperature that stays fairly constant at a depth of about 2.53 m [36, 37].

The principle is simple, pass a pipe of good thermal conductivity (steel, PVC, etc.) at a certain depth where the annual temperature of the subsoil remains constant temperature during the season of the year [37]. The air generally used as a working fluid transfers heat during its passage through the tube wher the subsoil presents a source of heat gain or loss due to its thermal capacity to store heat or coolness [38].

Through the day and the summer period ( see Figure I.16), the external air temperature T$ext$ is higher than the temperature of the ground. The air is forced naturally (by the blower the air) inside the buried tube or it carries out heat exchange with the layer which surrounds the tube by conduction and convection or the basement plays the role of a source of dissipation. The air loses some degree temperatures during the passage and it will be injected directly into the building which improves cooling or natural ventilation [39].

In the winter season (see Figure I.17), the outside air temperature is lower than the air temperature within the house. The underground soil as a source of heat gain increases the temperature of the air passing through the system. Tair out > Tair in. The result is building preheating and more induced flow which enhances thermal comfort. The ability to work during all seasons of the year (winter and summer) shows the potential of this technique in improving thermal comfort [40].

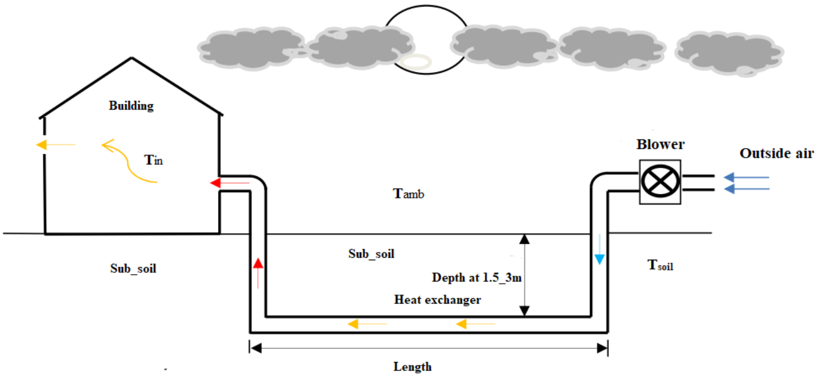


Figure I.17: Earth to air heat exchanger in operation during winter season

### I.12.1 Types of heat exchangers

There are two different types of earth to air heat exchangers. The first, with an "open-loop" where the outside air is absorbed through tubes in order to ventilate the building, and the second with "closed-loop" where the air is absorbed from the building before being recycled through the tubes. The last type is less used in the residential sector because it does not meet the requirements for air quality. The important aspects that determine the efficiency of an earth to air exchanger are the nature of the climate, the thermophysical properties of the soil, the depth of the source rock, and the water table. This information is essential for the dimensioning of the air-ground exchanger system. Also, there is Hybrid system: EAHE is used with air conditioning systems to minimize energy consumption and increase the system efficiency coefficient. Renewable methods can also be combined with EAHE such as wind towers, solar chimney, etc (see Figure I.18).

1. **Arrangement of buried tubes:**

    - single tube system;
    - Multiple tube system.

2. **Alignment of buried tubes:**

    - horizontal EAHE;
    - Vertical EAHE;
    - Helicoidal EAHE.

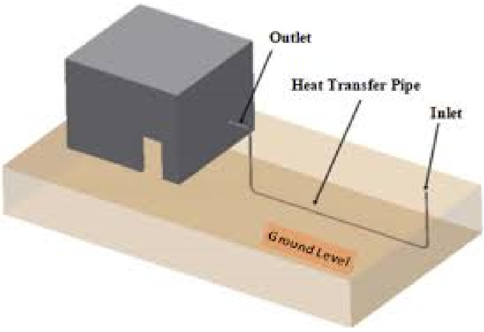


(a) Linear pipe-layout for EAHE systems

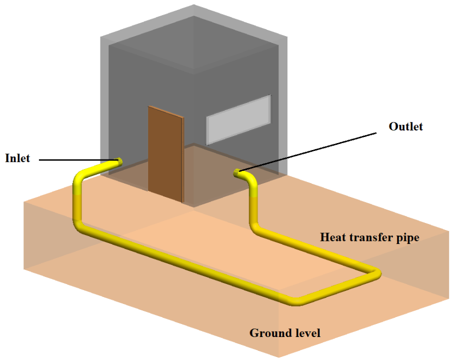


(b) Closed loop for EAHE system

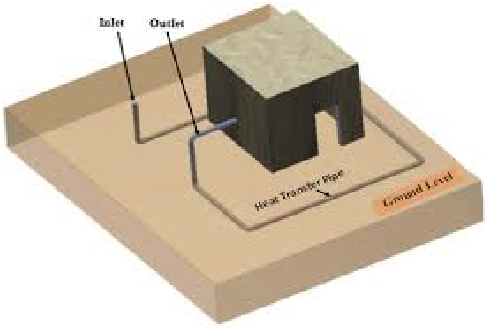


(c) EAHE systems with spiral pipe layouts

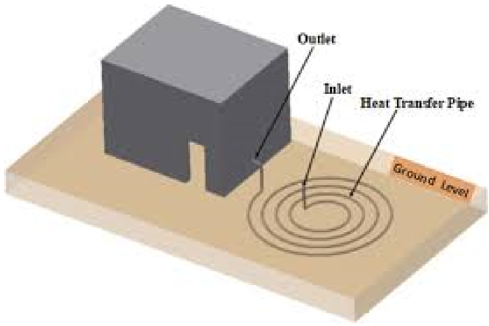


(d) Ring pipe-layout for EAHE systems

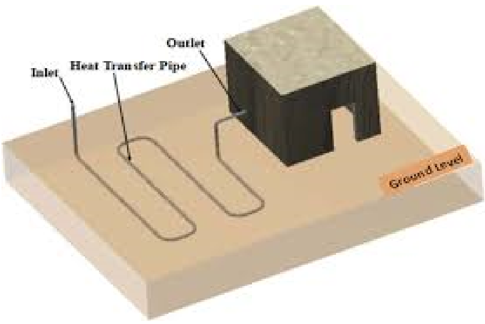


(e) Grid pipe-layout for EAHE system

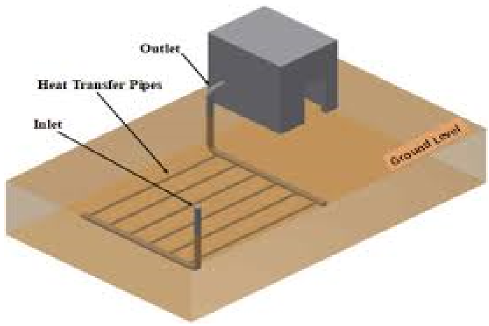


(f) Serpentine pipe-layout for EAHE systems

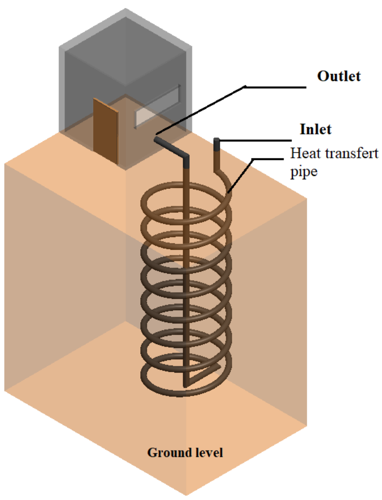


(g) Helical vertical-coil pipe-layout for a EAHE systems

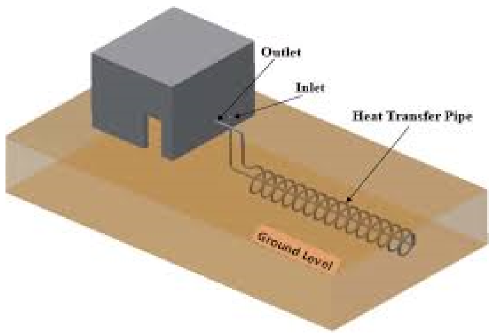


(h) Helical horizontal-coil pipe-layout for a EAHE

Figure I.18: Diagram of Heat Exchanger Forms

### I.12.2 Factors affecting the performance and operation of air-to-ground heat exchangers

factors that affect the efficiency and operation of air-to-ground heat exchangers are listed as bellow:

- Geographic location;
- Composition and treatment of the soil surface covering the ground (climatic conditions);
- Physical properties of the soil (humidity, density of the soil, mineral composition of the soil, the form of the particles making up the soil);
- Physical and thermal properties of the soil (thermal conductivity of the soil, thermal diffusivity of the soil);
- Bonding of soil with pipes;
- Temperature and velocity of the inlet air;
- Relative humidity of the air;
- Parameters related to the pipe: material (PVC, steel... etc.), length of the pipe, diameter, thickness;
- Depth of the buried pipe;
- Spacing between the pipes;
- Pipe roughness;
- Thermal insulation at the outlet of the pipe;
- Operating time;
- Sensitive and latent heat transfer.

### I.12.3 Advantages and disadvantages of earth to air heat exchanger

The earth to air heat exchanger has the following advantages:

- Simplicity of dessing and installation;
- They consume less energy to operate the system;
- Adaptation to several types of soil;
- It is expected that air pollution problems will be minimized by using EAHE for passive cooling and heating purposes;
- Requires less maintenance with lower costs;
- No pollution or greenhouse effect due to the absence of any source of combustion;
- They do not use compressor, or any refrigerant;
- Air uses as working fluid;
- They have a simpler design and consequently less maintenance;
- They do not require the unit to be located where it is exposed to weathering;
- Does not require energy for its operation in case of wind velocity high;
- They have lower initial cost than GSHPs and ISAHP.

Despite these advantages, the technique has the following disadvantages:

- High installation price.
- Phenomenon of condensation inside the exchanger tube and possible development of microorganisms which lowers the quality of indoor air.
- Air outlet temperature is non-uniform.
- High dependence on local climatic conditions in the presence of the upper parts of the exchanger above the ground, which directly and indirectly

- convection of fan noise via pipes to the far away living space.

Air vapor condensation discharge from EAHE is considered as problem. Useful solution for solving condensed water vapor discharge problem in the underground air tunnel, there is a way to pump out any water in the pipe, that is, a small submersible pump is located at the lowest point. but, this solution will increase the total energy consumption of the system.

# Chapter II

# State of Art on geothermal heat exchanger systems

## II.1 Introduction

Several types of air-to - ground exchangers have been developed and tested by several researchers around the world, with the primary objective of releasing and/or recovering the maximum amount of thermal energy at low financial costs and evaluating the air exchanger's thermal efficiency. This party aims to give an overview of the implementation of geothermal Heat Exchanger for passive air conditioning for any applications. The overview switches focus to systems which utilize the ground as a heat source, this covers general definitions and the most factors inuencing on heat exchanger performances, which need to be considered from ground thermal properties to piping materials. numerous experimental, theoretical and simulation studies have been carried out to investigate the different parameters. Different modes of operation have been performance reviewed on the efficiency of earth air tunnel heat exchanger systems, the effect of thermo-physical parameters of soil, thermal and flow parameters of air, geometrical and material properties of pipes. Significant work has recently been discussed to achieve these targets. In this chapter, we present some works available in the literature on the thermal phenomena of air-to- ground exchangers.

## II.2 Main factors influencing on ground heat exchanger behaviors

In literature review of previous studies, we found several factors that affecting the behavior of geothermal heat exchanger. Soil properties and moisture content such as the heat capacity, thermal conductivity and thermal diffusivity should take in consideration during the GHE implementation, because those factors have an important influence on the behavior of the GHE [41–43]. Also, the ground loop such as length, diameter and physical properties, have a consistent effect [44, 45]. Additional to all these factors, the climatic conditions play a principal role in GHE performances. Besides the selection of mechanical components, the ground loop length is the primary focus of ground source heat system design. Despite this, few investigations have considered the long-term influence of ground-loop characteristics on ground behavior or with regard to system optimization [46]. To date, the design of ground-loops is non-standardized, leading to range of ground-loop configuration, installation depths, pipe diameters and materials being used [36] . The following paragraphs present the main factors of the ground-loop influencing on the geothermal heat exchanger. The conduit of the well may consist of a single tube laid in a meander or loop around the building or be organized in the form of a network of parallel tubes installed between collectors in order to increase the ow of air circulating in the well [47]. However, the length of the tubes determines the exchange surface and the residence time of the air in the tubes. In a first approximation, the temperature profile of the air in the tubes is asymptotic. The optimum length of the exchanger will depend on the ow in the pipes. Indeed, the bibliography shows that for low ows, the minimum temperature is reached rather quickly, and that after a certain length, the exchanger no longer tempers the air: It has reached its limit of effectiveness. On the other hand, when ow increases, the tube length increases too in order to establish the ground temperature [41]. Therefore, an increase in the diameter of the tubes results in an increase in the exchange surface, but the experience demonstrated that doesn't necessarily increasing the heat exchange, this is due to the air circulating in the center of the pipe will no longer be in contact with the pipe wall's and its temperature will be little in uenced by the temperature of the ground. The choice of the material properties is important because it is directly affecting the soil / well thermal exchanges. The use of compact walls with high thermal conductivity must be favored because it allows to increase the exchanges and thus to reduce the length of the well [48] . Some other factors have low inuence on the behavior of the GHE, these include the internal roughness of the pipes, the overall geometry of the ground loop and the operating regime of the GHE [49].

## II.3 State of art on ground heat exchanger

The geothermal energy system is an environmentally friendly and inexpensive technique that is influenced by the temperature difference Tin and Tout at the level of the PVC pipe or the heat exchanger. Like any other energy system, the geothermal energy also is influenced by the solar energy [50] Many studies noted that beyond 3 m depth, the temperature can be considered almost constant [51–53]. In the studies of [5, 54], numerical simulations and experimentations were performed, and different parameters such as air flow, depth of burial, length and diameter were taken in consideration to calculate the energy performance of earth air heat exchanger (EAHE). The performance of a conventional air/water heat pump system with that of a geothermal heat pump system was compared experimentally in [55]. Comparing the two systems, the results show that the geothermal system could save 43% of the energy consumed by the traditional system during the heating period (winter) and 37% during the cooling period (summer). Several experimental and numerical models are developed for the researches have been carried out on the GHE system in literature. Al Ajmi et al [4] carried out study on the cooling potential of earthair heat exchangers for domestic buildings in a desert climate, a theoretical model of an earthair heat exchanger (EAHE) was developed for predicting the outlet air temperature and cooling potential of these devices in a hot, arid climate. A sub-soil temperature model adapted for the specific conditions in Kuwait is presented and its output compared with measurements in two locations, a typical meteorological year for Kuwait was prepared and used to predict the cooling loads of the air-conditioned dwelling with and without the assistance of the EAHE. A typical Kuwaiti domestic building of dimensions $(10 \times 10 \times 3) m^3$ was defned for testing EAHE performance. The building materials (walls, roof and oor) are in accord with the prevailing building materials and practices in the region. The building is assumed to have two windows each of area $1m^2$ in the North/South direction. The simulation carried out by Al Ajmi for the period from May to September, which is the most arid and the hottest time of the year in Kuwait. The simulation conducted for the case of the building being cooled by air-conditioning both with and without assistance from the EAHE.figure II.1,represnted the peak heat removal rate from the building with air-conditioning alone was calculated to be 4370 W while that with air conditioning and EAHE assistance was 2670 W. The peak cooling load reduction due to the operation of the EAHE was thus 1700 W (mid-July). The indoor temperature of the building for the free running" condition (that is, without air conditioning) showed a reduction of 2.8 $^oC$ in the peak hours through use of the EAHE system as illustrated [4]. Concluded that there is potential for EAHE systems to make a useful contribution to energy saving in Kuwait, and in similar desert climate locations. Moummi et al [56].

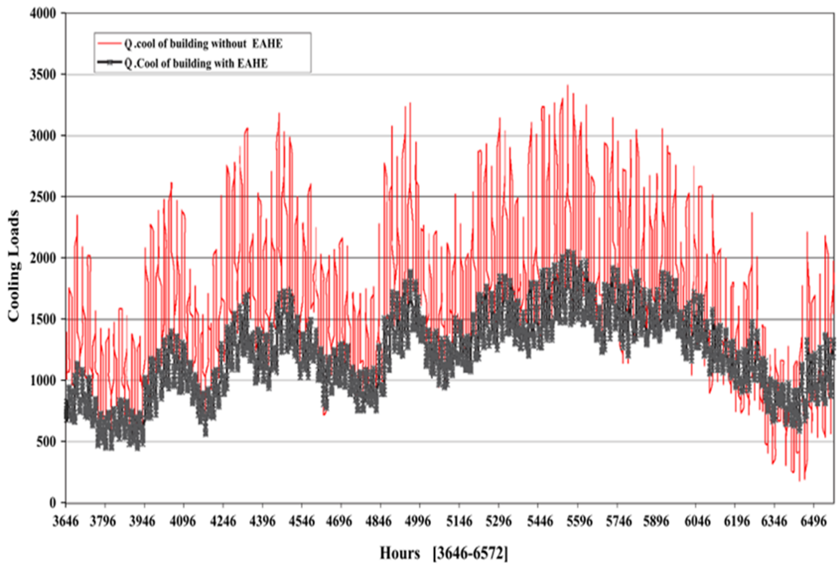


Figure II.1: Heat removed from the building by air conditioning during May September with and without EAHE assistance [4]

Presented theoretical and experimental study on refreshing by geothermal energy in Biskra area, this technique, called Canadian's well, uses air/ground heat exchanger system. They investigated the air temperature evolution at the outlet of the heat exchanger. The authors verified experimentally first the mathematical models that have been established, which give the best evolution of the air temperature in the exchanger as a function of the different structural parameters (diameter, length, ow, ground temperature, depth). The experimental tests bench was mounted on site at the University of Biskra. It is a network of four trays with a total length of about 60 m. The inner diameter of the pipe is 110 mm which is placed at a depth of 3 m under a slope of 2%. In the second stage, a synthesis and comparison study were taken place between the theoretical results developed and those obtained experimentally from the measurements.

At the end of this study and based on the results obtained, the authors found a promising vector in climate engineering as a renewable energy source can be exploited industrially. However, the experimental results compared to the analytical results allowed the authors to conclude that the presented model can be improved. Indeed, experimentally the temperature of the uid continuously decreases with the length of the exchanger.

Benhammou et al [5]. Implemented They study on simulation and characterization of a geothermal air exchanger for refreshing buildings operating in the climatic conditions of southern Algeria (Adrar). The authors obtained very encouraging results which indicate that this low-priced technique can cover an important part of our needs in domestic cooling. This study also permitted them to exanimate the inuence of several parameters of the exchanger on its daily average efficiency and on the temperature of air cooled in the outlet of the exchanger. This heat exchanger constructed from a polyethylene pipe of 50 m length and 16 cm diameterit is shown in figure II.2, buried at a depth of 3 m from the ground surface. The average air velocity in the pipe is taken to be 3.5 $m.s^{-1}$. The inuence of different parameters on the functional of the air-to-ground exchanger [5].

Based on this study the authors concluded that the temperature of the cooled air at the outlet of the exchanger is lower when the burial depth in the ground greater. Similarly, when the exchanger is longer the temperature of the cooled air is lower; however, the ow velocity has such an important effect on the functional of the geothermal exchanger. The temperature of the cooled air increases linearly with the speed of the air. Therefore, it is better to choose a speed neither very low nor very high. Concerning the diameter of the buried pipe, they found that there is an optimum diameter of 10 cm for which the temperature of the cooled air is minimal and the daily efficiency of the exchanger is maximal.

Draoui et al [57] carried out a study on the air conditioning system integrating a

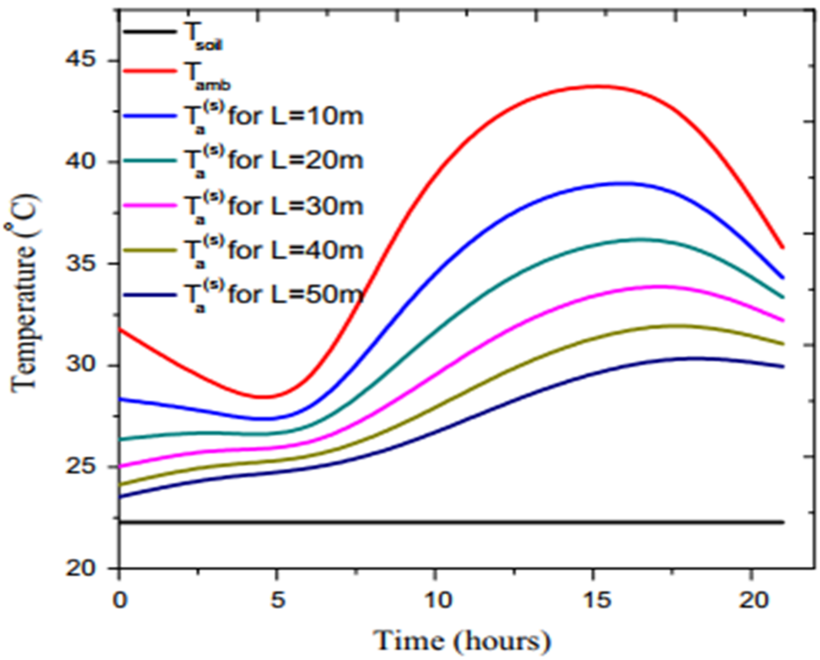


Figure II.2: Effect of pipe length on the air outlet temperature [5]

Canadian well in the arid zones, case of Bechar. In this work, they studied the performance of an air ground heat exchanger with a view to perform an analytical modeling. They first validated the model of the ground temperature and air temperature in the heat exchanger, and then analyzed the inuence of several parameters, namely depth, diameter and length of the pipe on the temperature inside the exchanger, the authors exanimated the inuence of several parameters on the functional of the air-to-ground heat exchanger, furthermore they compared their results with some work already implemented [4,56]. The results obtained by the authors make it possible to fully understand the functional of the air-ground heat exchanger during the seasons. Beloufi et al 43. Investigated the thermal performances of an earth air heat exchanger (EAHE) under transient conditions in cooling mode.

They carried out their experiments in south Algeria at the University of Biskra. They constructed a PVC pipe of 53.16 m long and 110 mm diameter buried at 3 m depth to be used. The experimental setups were tested under monitoring of 71 hours in continuous operation mode with high inlet temperatures. Therefore, a mathematical model was presented for EAHE by using the fnite differences method. They found that the continuous operation mode has no signifcant effect on the outlet air temperature and thus on the EAHE performances during operating period.

Results of the theoretical predictions were validated with the measured air temperatures along the EAHE and showed acceptable matching between numerical and experimental results. H. Boughanmi et al [6]. Studied the evaluation of soil thermal potential under Tunisian climate using a new conic basket geothermal heat exchanger, they designed geothermal heat exchangers system composed of two conic baskets serially connected. Both heat exchangers are made in polyethylene high-density material and have a length of 3 m each one. They used for greenhouse cooling and heating through a geothermal heat pump. Its conical geometry is selected to reduce the operation cost and the exploited area, compared to vertical and horizontal geothermal heat exchangers often used. It also assures the maximum of heat exchange with the soil. The aim of this study is to determine the thermal performance of one Conic Basket Geothermal Heat Exchanger (CBGHE) are shown in figure II.3, a buried at 3 m deep, in the exploitation of the soil thermal potential, in summer. A rate of heat exchange with the soil is determined and the global heat exchange of the CBGHE is assessed. Its energy and efficiencies are also evaluated using both first and second law of thermodynamic. presented the results. This work allows determining the optimal exchange surface of the CBGHE which should be used to assure the maximal exploitation of the soil thermal potential for eventual use in greenhouse heating and cooling.

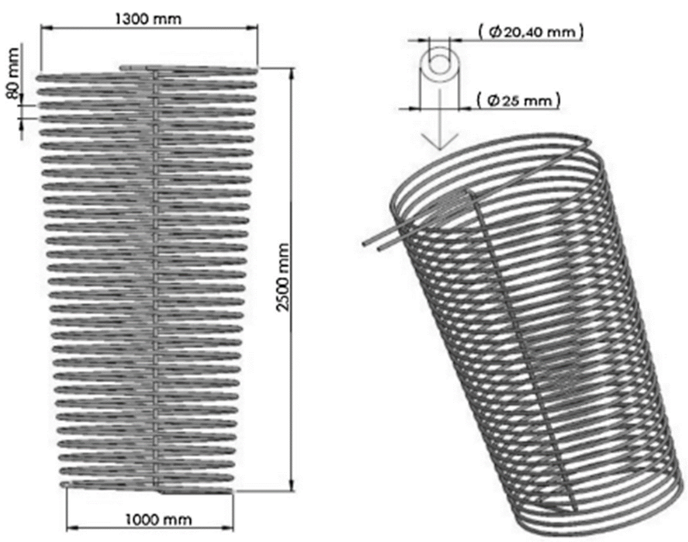


Figure II.3: schematic of the CBGHE system [6]

## II.4 Effect of thermal and flow parameters of air

Air properties such as temperature, flow rate, relative humidity are important parameters that affect EAHE system efficiency. Different studies were carried out considering the effect of air properties on the efficiency of the EAHE system. It presents the effect of different thermal and flow properties of air as presented in table II.1.

### II.4.1 Effect of Inlet air temperature

Air temperature at the EAHE tube inlet plays a significant role as the rate of heat transfer between air and soil is controlled by the difference in temperature between the air and ground soil are chown in figure II.4. Studied the impact of ambient air temperature on outlet air temperature, observed that the performance of the earth to air heat exchanger (EAHE) system highly depends on inlet air temperature. also, they noticed that with the increase in inlet air temperature, the outlet temperature of air increases [58–62].

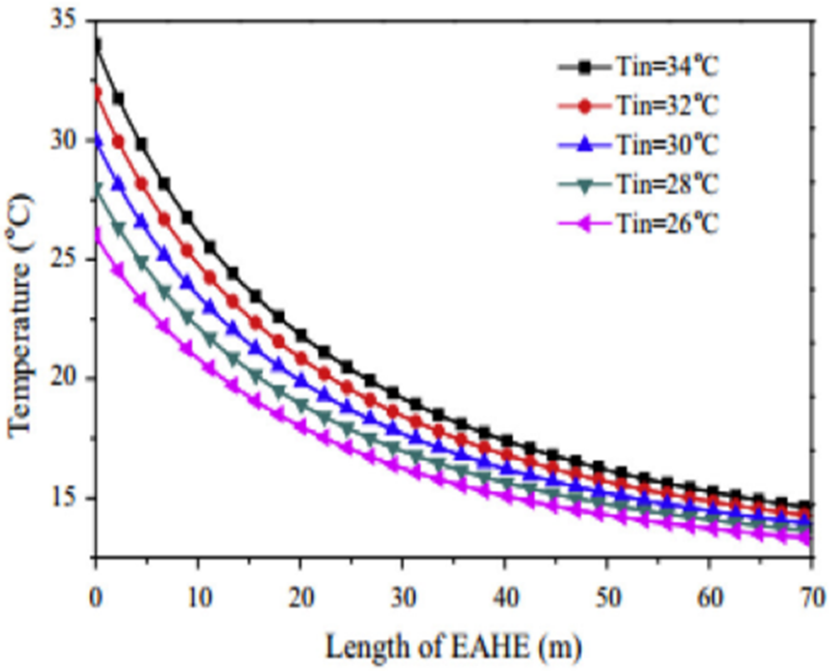


Figure II.4: EAHE performance under different inlet air temperature [7]

### II.4.2 Effect Air flow velocity

The increase in air velocity in the pipe below the soil surface also affects the efficiency of the EATHE system as evidenced by a decrease in the overall temperature differential between inlet and outlet air [60, 63–70].

Table II.1: Effect of thermal and flow properties of air on performance of EAHE system

| S. No | Properties | Findings | References |
|---|---|---|---|
| **1.** | Velocity of air | With increase of air velocity, the total temperature difference between inlet and outlet air temperature decreases but total heat gain/loss increases. | [64, 71–73] |
| **2.** | Inlet air temperature | Increasing inlet air temperature, the outlet air temperature increases but the total temperature drop increases in cooling operation, however, the total temperature rise decreases during the heating operation. | [58, 61, 62, 70, 72] |

## II.5 Effect of pipe properties on EAHE system

Geometric and thermo-physical properties of the pipe are the main parameters that significantly affect EAHE efficiency. The geometric properties include the length, diameter, thickness etc. of the pipe and thermo-physical properties include thermal conductivity, density, roughness etc. The effects of the various pipe properties on EAHE device efficiency are illustrated in Table II.2.

### II.5.1 Effect of pipe material

It can be inferred from previous studies that buried pipe content has a negligible impact on the thermal efficiency of the EAHE system, and can therefore be ignored. Pipe quality, corrosion resistance and reliability are the key considerations for selecting the pipe material of an EAHE device. In addition, the interior of the pipe must be hygienic, and an anti-microbial coating is also recommended. PVC pipe, therefore, provides a better option, as it has the advantage of low cost, greater corrosion resistance and easier installation.

### II.5.2 Effect of pipe length

The studied that pipe length is a key factor which affects EAHE efficiency. In several studies it was clearly established that the drop / rise in air temperature increases to a certain length by increasing pipe length, after which the impact of pipe length on drop/rise temperature becomes less pronounced. The pipe length should therefore be optimized to minimize the initial capital cost of the system without compromising EAHE system efficiency.

### II.5.3 Effect pipe diameter

Numerous researchers have taken into account the parametric study effect of the pipe diameter, which is the significant geometric parameter that affects the efficiency of the EAHE device. From numerous studies it is observed that by increasing the pipe diameter are represent in figure II.5, the total temperature drop / rise in the heat exchanger pipe decreases but the overall heat transfer rate increases for the given flow velocity. For the same strength the expense of large diameter pipes (0.15 m) is 6-7 times greater than that of small diameter pipes (0.05 m). It is therefore preferable to use several small diameter pipes instead of single pipes with a wide diameter.

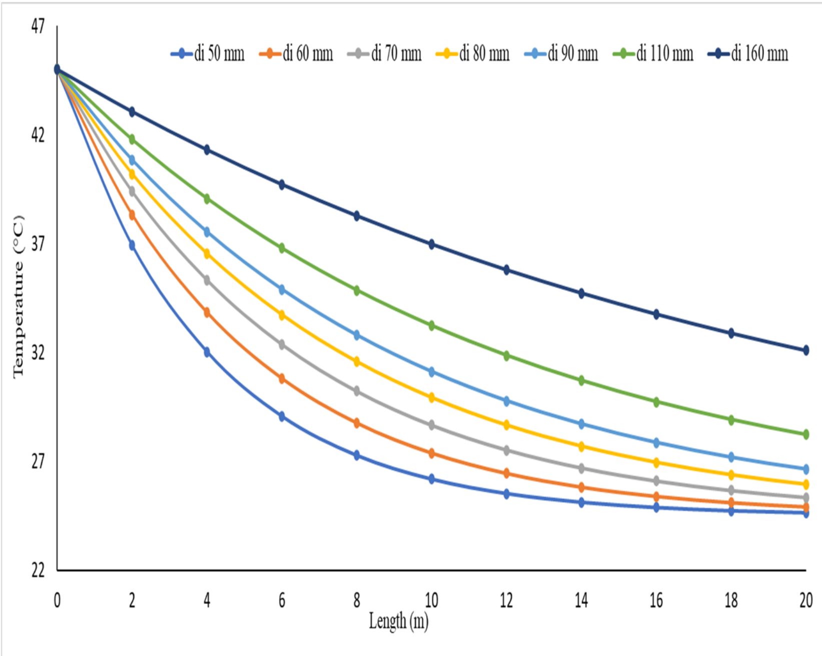


Figure II.5: EAHE performance under different diameter

### II.5.4 Buried pipe depth

Knowledge of the temperature profile at ground surface and its variation with depth is important for deciding underground heat that can be tapped for heat exchanger system design. The distribution of ground temperature is primarily influenced by the soil's physical properties and composition, and also by the soil surface cover. The studies carried out to date have shown that for different geographical and climatic conditions the optimal pipe depth of the heat exchanger device has different values. Therefore, pipe should be installed at optimum depth below the surface of the earth so as it affects the whole system efficiency.

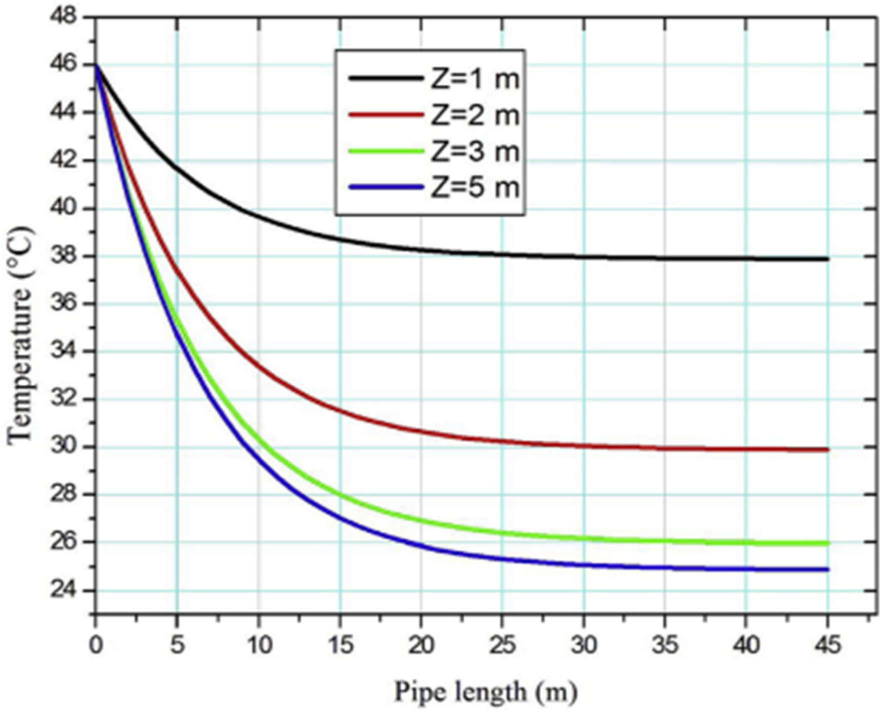


Figure II.6: Air temperature along the tube length at different depths [8]

### II.5.5 Pipe spacing (pitch)

Wide requirements for cooling/ heating loads can require the use of several pipes and make interspacing an important factor which must be greater than the thermal zone. Thermal influence zone (TIZ) described as an area in the soil layer around the heat exchanger pipe where the transfer of heat from air to soil causes a significant change in soil layer temperature (0.5 $^{O}C$ rise or drop from undisturbed soil temperature).

### II.5.6 Pipe roughness

Pipe roughness is also a critical factor that greatly influences the efficiency of the EAHE system. Experimental investigations have shown that the cooling efficiency and the decrease in temperature increases as the relative roughness of the tubes increases. Increasing the roughness of the tubing, increases not only the coefficient of heat transfer but also the pressure decrease are chown in figure II.7. The EAHE pipe should therefore be constructed to ensure optimal heat transfer with minimal pressure losses.

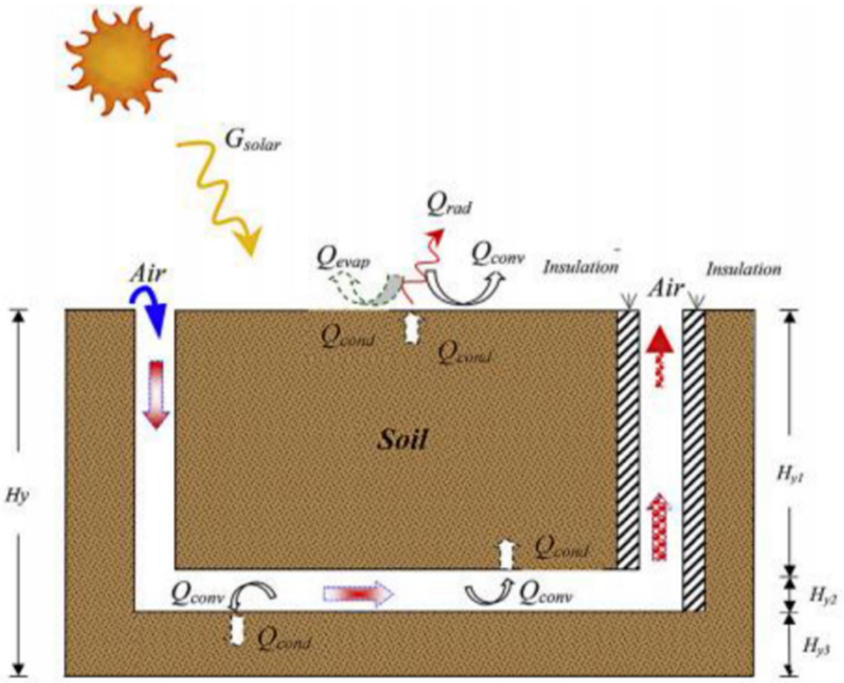


Figure II.7: EAHE with thermal insulation at pipe outlet [9]

### II.5.7 Different design

a comprehensive review of different design aspects of EAHE pipe pinpoints to create the EAHE system with suitable pipe layout and design guidelines to minimize the overall system expense. It thus becomes an inexpensive and viable passive system for applications for air heating and refrigeration [74–81].

Table II.2: Effect of pipe properties on the performance of EAHE system

| S. No | Properties | Findings | References |
|---|---|---|---|
| **1.** | Pipe length | Increasing the length of pipe, the difference between inlet and outlet air temperature increases up to a certain length beyond which no increase in heat transfer has been shown | [82–85] |
| **2.** | Pipe diameter | At given flow rate, heating, and cooling potential of EAHE increases with decreasing pipe diameter. | [71, 72, 86–90] |
| **3.** | Pipe material | Pipe material has a small influence (negligible) on the thermal performance of EAHE system | [73, 86, 90, 91], |
| **4.** | Depth of pipe | Increasing depth of EAHE pipe, heating and cooling potential increase up to a certain depth beyond which no important improvement in performance increment was observed. | [8, 71, 86, 91–93] |
| **5.** | Spacing between parallel pipes | The spacing between pipes must be equivalent to or more than thermal influence place. Smaller spacing between pipe creates a negative impact on the thermal performance of EAHE system | [82, 82, 94–97] |
| **6.** | Roughness of pipe | By increasing relative roughness of pipe, the cooling/heating efficiency increases but pumping power also increases | [98, 99] |
| **7.** | Different design | with suitable pipe layout and design guidelines become an inexpensive and viable passive system for applications for air heating and refrigeration | [74–81] |

## II.6 Conclusion

Based on various experimental, theoretical and simulation tests, the geothermal heat exchanger system is found to be an outstanding passive heating / cooling technique for buildings. The geothermal heat exchanger system helps to minimize the building's power usage because, compared to the traditional system, it uses very little power. The geothermal heat exchanger device can function effectively under various climatic conditions and can provide pre-tempered air for different applications.

Thus, it is concluded that if geothermal heat exchanger system developed with proper design guidelines it would be capable of providing sufficient heating and cooling in small as well as large buildings with significant energy savings.

# Chapter III

# Study of thermal heat transfer

## III.1 Introduction

An evaluation of a geothermal heat exchanger thermal efficiency includes suitable thermal models. In the first section, an analytical model using the general conduction equation will be established in transient conditions during this third chapter in order to estimate the ground temperature profile. In the second part of this chapter and we present to evaluate the energy and exergy performance of geothermal heat exchanger, the exchanger efficiency and the exchanger's pressure drops as a result of the air flow controlling the heat transfer.

## III.2 Mathematical modeling

In order to extract the maximum cold energy contained in the first few meters of the subsoil at a reliable economic cost, we must study the depth of penetration into the ground for the ideal location of the air/soil exchanger in the subsoil and this means where the temperature remains invariant or less sensitive to external climatic conditions over time.

### III.2.1 Modeling of the soil temperature

Soil is considered to be a homogeneous and invariant medium, characterized by constant properties such as: thermal conductivity $\lambda$ soil, the density $\rho$ soil and the specific heat capacity $Cp_{soil}$. The transfer of heat in the soil is unidirectional in the vertical direction. The temporal variation of the soil moisture rate due to water infiltration is neglected and no water table is taken into account under the area where the exchanger is installed. The mathematical model of the soil temperature is based on the heat conduction theory applied to a semi-infinite homogenous solid [100, 101]. Heat conduction in the soil is given by:

$$\frac{\partial^2 T}{\partial^2 Z} = \frac{1}{\alpha}\frac{\partial T_{soil}}{\partial t} \quad \text{(III.1)}$$

$$T(0,t) = T_{mean} + A_s \times \cos[\omega(t - t_0)] \quad \text{(III.2)}$$

$$T(\infty,t) = T_{mean} \quad \text{(III.3)}$$

Where:

$T_{mean}$: mean annual temperature ($^oC$);

$A$: Amplitude of the soil surface temperature variation ($^oC$); $t$: Time ($h$);

$Z$: Vertical coordinate ($m$);

$\alpha$: Thermal diffusivity of the soil $[\alpha = \lambda/(\rho.C_p)](m^2.s^{-1})$;

$\omega$: Annual temperature frequency, $[\omega = 2.\pi/8760](rad/hour)$ ;

$\lambda$: Thermal conductivity of the soil $(W.m^{-1}.^oC^{-1})$;

$\rho$: Density of the soil $(kg.m^{-3})$; $C_p$: The specific heat of the soil in $(J.kg^{-1}.^oC^{-1})$.

To modeling the earth/ air heat exchanger, it is necessary to know the optimal installation depth of the underground pipes in the region under study, i.e. EL Oued. The soil temperature was calculated using the following equation [102, 103].

$$T(Z,t) = T_{mean} + A_s \times \exp^{-z\sqrt{\pi/8777}\times\cos[\frac{2\pi}{8777}\times(t-t_0)-\frac{z}{2}\times\sqrt{\frac{8777}{\pi\alpha}}]} \quad \text{(III.4)}$$

## III.2.2 Analytical study of the immersed exchanger

### III.2.2.1 Power exchanged and thermal efficiency

We consider an air of temperature Tair which circulates in a buried exchanger. Considered to be a cylindrical tube of length L, immersed at a level in the water well of considered constant temperature Twat. The power exchanged through the immersed

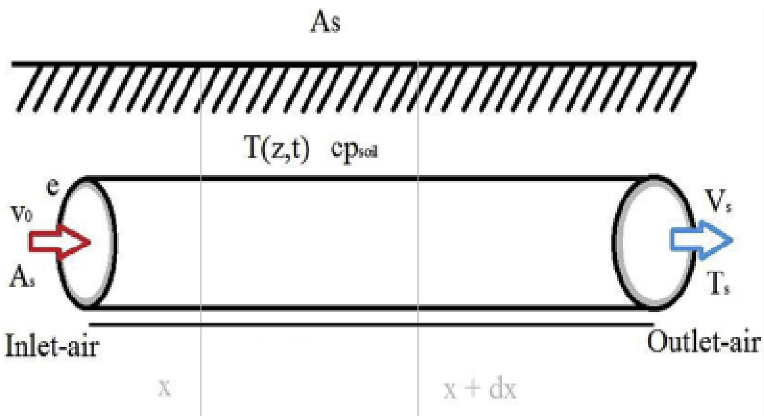


Figure III.1: Schematic diagram of the earth air heat exchanger

exchanger is a function of the air temperature Tair, the inlet ($T_{in}$) and outlet ($T_{out}$) of the exchanger, and the temperature of the water well Twat. It is also a function of the exchange coefficient U of the immersed exchanger and of the exchange surface (S). Consider an infinitesimal element of the exchanger, dx in the direction of flow.

#### III.2.2.2 Thermal analysis of a geothermal helicoidal heat exchanger

The heat flow exchanged through the dS surface element between air and water well is written. For the geometry of the helicoidal exchanger is complex we will consider the case of a cylinder with an inner radius ri and outer radius re. The analytical model was initially used to determine the outlet fluid temperature under the ground. We consider an infinitesimal element dx of a pipe in the coolant flow direction figure III.1. The analytical heat exchange rate dQ is given:

$$\partial Q = U(T_g - T_{out})\partial A \tag{III.5}$$

$$\partial Q = \dot{m}\, C_p \partial T = \dot{m}\, C_p [T_{out}(X + \partial X) - T_{out}(X)] \tag{III.6}$$

We suppose that there is no phase change.

$$\partial Q = \dot{m}\, C_p \partial T_{out} \tag{III.7}$$

$$\partial Q = \dot{m}\, C_p \partial T_{out} = U(T_g - T_{out})\partial A \tag{III.8}$$

After, rearranging Eq. (III.8)

$$\frac{\partial T_{out}}{T_g - T_{out}} = \frac{U}{\dot{m}\,C_P}\partial A \tag{III.9}$$

After, rearranging of Eq. (III.9) gives

$$\int_{T_{in}}^{T_{out}} \frac{\partial T_{out}}{T_{out} - T_g} = \frac{U}{\dot{m}\,C_P}\int_0^Z \partial A \tag{III.10}$$

$$\frac{T_{out} - T_g}{T_{in} - T_g} = \exp\left[-\frac{U}{\dot{m}\,C_P}A\right] \tag{III.11}$$

With $A = 2\pi r L$

The outlet temperature has a following expression:

$$T_{out} = (T_{in} - T_g)\exp\left(-\frac{U}{\dot{m}\,C_P}A\right) + T_g \tag{III.12}$$

The amount of heat transferred to the ground is:

$$Q_{GHE} = \dot{m}\,C_P\left[1 - \exp\left(-\frac{h}{\dot{m}\,C_P}A\right)(T_g - T_{in})\right] \tag{III.13}$$

QGHE can be formulated by following equation:

$$Q_{GHE} = UA\Delta TLM \tag{III.14}$$

where U and A denotes respectively the overall heat transfer coefficient and heat transfer area. $\Delta TLM$ is the log mean temperature difference and defined as follows:

$$\Delta TLM = \frac{T_{out} - T_{in}}{\ln\left(\frac{T_{out} - T_{in}}{T_{in} - T_g}\right)} \tag{III.15}$$

#### III.2.2.3 Temperature ratio for an earth-to-air heat exchanger

The temperature ratio RT is an important characteristic for passive cooling applications which describes the temperature damping between inlet and outlet temperature. The smaller RT is, the more cooling energy is supplied to the building mean (high conductive heat transfer between soil and pipe and high convective heat transfer between pipe and air) [104].

RT is independent of the climate if the inlet air temperature is related to same limits ($T_{in,max}$ and $T_{in,min}$):

$$RT = \frac{T_{out,max} - T_{out,min}}{T_{in,max} - T_{in,min}} \tag{III.16}$$

#### III.2.2.4 Thermal efficiency

The efficiency of the HWAHE is defined as the ratio of the air temperature drop between the outlet and the inlet of the HWAHE and the difference between water and inlet air temperatures [69,103]. The exchanger thermal efficiency is defined as the ratio of the actual exchanged Qe thermal power and the maximum theoretically possible exchange power (Qemax), expressed by:

$$\epsilon = \frac{T_{outlet} - T_{inlet}}{T_{soil} - T_{inlet}} \tag{III.17}$$

#### III.2.2.5 Energy Performance

The thermal performance of the HWAHE can be estimated in terms of the coefficient of performance (COP) [105]. COP is a ratio between the removal heat of cooling and the power input to the blower that is kept approximately constant as given by Eq.

$$COP = \frac{Q_e}{W_b} \tag{III.18}$$

Where :

$$Q_e = \dot{m}\, C_P (T_{in} - T_{out}) \tag{III.19}$$

### III.2.3 Pressure losses at the buried exchanger

An ideal heat exchanger is assumed to have infinite conductance. However, the calculation of pressure losses is essential to better quantify the heat transfer through the buried exchanger [106]. There are two types of pressure losses: The linear pressure loss

$\Delta P_{lin}$ and the singular pressure loss $\Delta P_{sin}$ . The total pressure loss is calculated using Eq

$$\Delta P_{total} = \Delta P_{lin} + \Delta P_{sin} \tag{III.20}$$

#### III.2.3.1 linear pressure loss

The linear pressure loss $\Delta P_{lin}$ describes the pressure losses by friction with the wall of pipes. They are caused by fluid viscosity, the linear pressure loss for a flow in a rectilinear control is determined in the following way

$$\Delta P_{lin} = \frac{\rho\, L\, \nu^2}{2D}\Lambda \tag{III.21}$$

With,

$\Lambda$ :Linear loss ratio of load;

$\rho$ :Density of air flowing in the pipe;

$\nu$ :Flow velocity;

D : Exchanger diameter;

L : Exchanger lengths. The calculation of the pressure drop coefficient depends on the nature of the flow, laminar or turbulent. Flow is characterized by its Reynolds number:

$$Re = \frac{\rho\, \nu\, D}{\mu} \tag{III.22}$$

Or, $\mu$ represents the dynamic viscosity of air $(1.85 \times 10^{-5} Pa.s)$

For values of Re <2000, the flow regime is laminar and the coefficient $\Lambda$ is not affected by the relative roughness. It is a function of the flow rate Q is given by the **Hangen-Poiseuille relation**: $\Lambda = \frac{64}{Re}$.

Within the limits 2000 <Re <4000, the regime is considered unstable and $\Lambda$ is determined by the Frenkel relation: $\Lambda = \frac{2.7}{Re^{0.53}}$ For 4000 < Re < 10000, the regime is considered unstable and $\Lambda$ is estimated by Blasius relation: $\Lambda = \frac{0.316}{Re^{0.25}}$

For high values of Re, the regime is completely turbulent from which results in the variation of as a function of Re and of $\frac{i}{D}$ ($\epsilon_i$: roughness index of the exchanger, it translates the amplitude of the linearity defects of the wall of the exchanger tube). Von Karman and Prandtl, Nikuradse or Colebrook and White determined $\Lambda$ by the empirical relations [106]:

Von Karman et Prandlt : $\frac{1}{\sqrt{\lambda}} = -2\log\left[\frac{2.51}{Re\sqrt{\lambda}}\right]$

Nikuradse : $\lambda = 0.0032 + \frac{0.221}{Re^{0.237}}$

Colebrook et white : $\frac{1}{\sqrt{\lambda}} = -2\log\left[\frac{\frac{\epsilon_i}{D}}{3.7} + \frac{2.51}{Re\sqrt{\lambda}}\right]$

To estimate the type of flow we calculated in the table III.1 the Reynolds number for different diameters and mass flow rates

Table III.1: Effect of pipe properties on the performance of EAHE system

| **Pipe diameter** | **30** | **40** | **60** | **80** | **100** |
|---|---|---|---|---|---|
| **Mass flow rate** ($kg.s^{-1}$) | **Reynolds number** | | | | |
| **0.02** | 63270 | 47453 | 31635 | 23726 | 18981 |
| **0.04** | 126541 | 94906 | 63270 | 47453 | 37962 |
| **0.06** | 189812 | 142359 | 94906 | 71179 | 56943 |
| **0.08** | 253083 | 189812 | 126541 | 94906 | 75925 |
| **0.1** | 316354 | 189812 | 158177 | 118632 | 94906 |

We can remark that for the range of the flow and the diameter that we study here, the flow is partially turbulent. We therefore consider for the following the pressure loss for a turbulent flow whose pressure loss coefficient can be calculated by the Blasius relation:

$$\Lambda = \frac{0.316}{Re^{0.25}} = \left(\frac{0.01}{Re}\right)^{0.25} \tag{III.23}$$

### III.2.3.2 Singular pressure loss

The singular pressure loss $\Delta P_{sin}$ is the result of velocity differences and changes of direction of the fluid and can be given as:

$$\Delta P = \xi\,\rho\frac{v^2}{2} \tag{III.24}$$

with $\xi$ represents the coefficient of the singular pressure loss [106].

### III.2.4 Exergetic study of the heat exchanger

#### III.2.4.1 HWAHE Exergy balance

The exergy is defined as the available work exists in the system with respect to the environment conditions [6, 105, 107, 108]. It is considered as a useful tool that can be used for energy system designing, performances analyzing and optimizing. The exergy balance is given as:

$$\sum E_{x,des} = \sum E_{x,in} - \sum E_{x,out} \tag{III.25}$$

Where $\sum E_{x,in}$ represents the rate of exergy gained in the tube flow. It is given by the following equation:

$$\sum E_{x,in} = \dot{m}_{in} C_P \left( T_{in} - T_{soil} - T_{soil} \ln \left( \frac{T_{in}}{T_{soil}} \right) \right) + \frac{\dot{m}_{in}}{\rho} \Delta P_{in} \tag{III.26}$$

With:

$\dot{m}_{in}$: Air inlet mass flow rate at the exchanger;

$T_{in}$ : Air inlet temperature at the exchanger;

$\Delta P_{in}$: Air inlet pressure loss at the exchanger.

$\sum E_{x,out}$ is the total exergy of geothermal heat exchanger system, and is given by the following expression:

$$\sum E_{x,out} = \dot{m}_{out} C_P \left( T_{out} - T_{soil} - T_{soil} \ln \left( \frac{T_{out}}{T_{soil}} \right) \right) + \frac{\dot{m}_{out}}{\rho} \Delta P_{out} \tag{III.27}$$

With: $\dot{m}_{out}$: Air outlet mass flow rate at the exchanger;

$T_{out}$: Air outlet temperature at the exchanger;

$\Delta P_{out}$ : Air outlet pressure loss at the exchanger.

The exergy destruction rate of the exchanger can be translated as:

$$E_{x,dest} = \sum \dot{m}_{in} \left[ (h_{in} - h_0) - T_{soil}(S_{in} - S_0) \right] - \sum \dot{m}_{out} \left[ (h_{out} - h_0) - T_{soil}(S_{out} - S_0) \right] \tag{III.28}$$

Due to conservation of mass, and the rearranging of the equation above, we can write:

$$\sum E_{x,dest} = \sum \dot{m}\left[(h_{in} - h_{out}) - T_{soil}(S_{in} - S_{out})\right] \tag{III.29}$$

$$\sum \dot{m}_{in} = \sum \dot{m}_{out} = \sum \dot{m} \tag{III.30}$$

The $\Delta h$ and $\Delta S$ expressing respectively the enthalpy and entropy of the HWAHE are calculated as follow:

$$\Delta h = h_{in} - h_{out} = C_P(T_{out} - T_{in}) - \frac{\Delta P_{in}}{\rho} \tag{III.31}$$

$$\Delta S = S_{in} - S_{out} = C_P \ln\left(\frac{T_{out}}{T_{in}}\right) \tag{III.32}$$

The exergy destruction rate of the exchanger is calculated as follows:

$$\sum E_{x,dest} = \dot{m}\, C_P\left[T_{out} - T_{in} - T_{soil}\ln\left(\frac{T_{out}}{T_{in}}\right)\right] + \frac{\dot{m}}{\rho}\Delta P_{in} \tag{III.33}$$

#### III.2.4.2 Exergy efficiency of HWAHE

The exergy efficiency of the HWAHE system is evaluated by [6, 105]:

$$\eta = \frac{\sum E_{x,out}}{\sum E_{x,in}} \tag{III.34}$$

## III.3 Conclusions

Thermal mathematical models based on the general conduction equation and the theory of energy balances have been presented in this chapter, the purpose of which is to predict the evolution of the temperature in the soil and that within the buried tube. To determine the different essential parameters that enabled us to assess the thermal efficiency of a fresh geothermal heat exchanger as a helical water air heat exchanger, a program was developed in the 'Fortran' language.

# Chapter IV

# Experimental setup

## IV.1 Location of the cell: Presenting the study site

El-Oued is an Algerian state, located in the southeastern part of Algeria; it is a desert area. This zone has abundant solar radiation throughout the year as shown in figure IV.1. The coordinates of the selected site for the completion of the solar power station are: the latitude is $33.60^o$ north, the longitude is $6.79^o$ east, and the altitude equals 42 m.

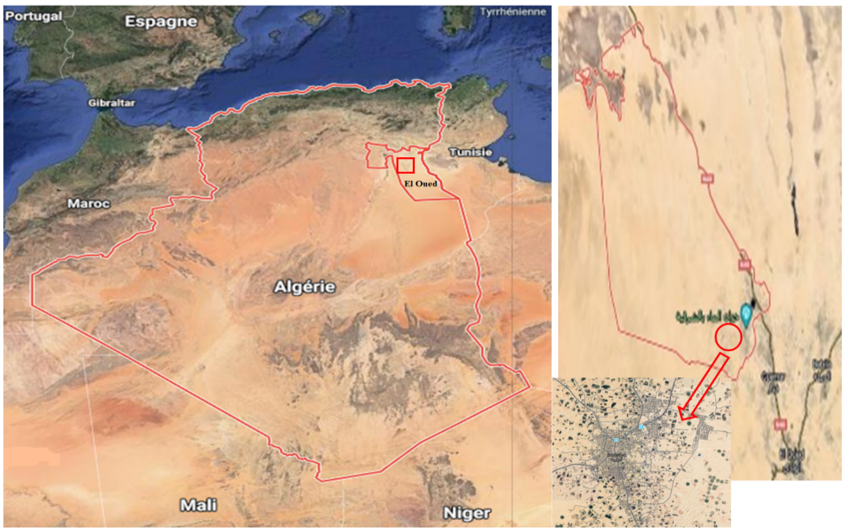


Figure IV.1: Location and geographical coordinates of the studied area

The area is shown in figure IV.1 is located in Reguiba municipality, where this chosen place is located about a 30 km away from El Oued headquarters, this region is a place in a vast desert climate covering the yellow floor and glossy. As for the climate of this region, it is hot and dry in summer, cold and dry in winter, while the spring is characterized by the seasonal wind. The agriculture of all kinds is the first economic activity of the population of this region; the trade comes in the second place, while the livestock occupies third place and finally the rest of the services.

In figure IV.2, the daily average solar radiation and day duration are presented for El-Oued region. It is obvious that El-Oued region has an average daily insolation of 6 h in December to 14.18 h in June. In addition, more than 228 $kWh.m^{-1}.month^{-1}$ of direct solar radiation in summer and about 114 $kWh.m^{-1}.month^{-1}$ in winter fall on the El-Oued region [109].

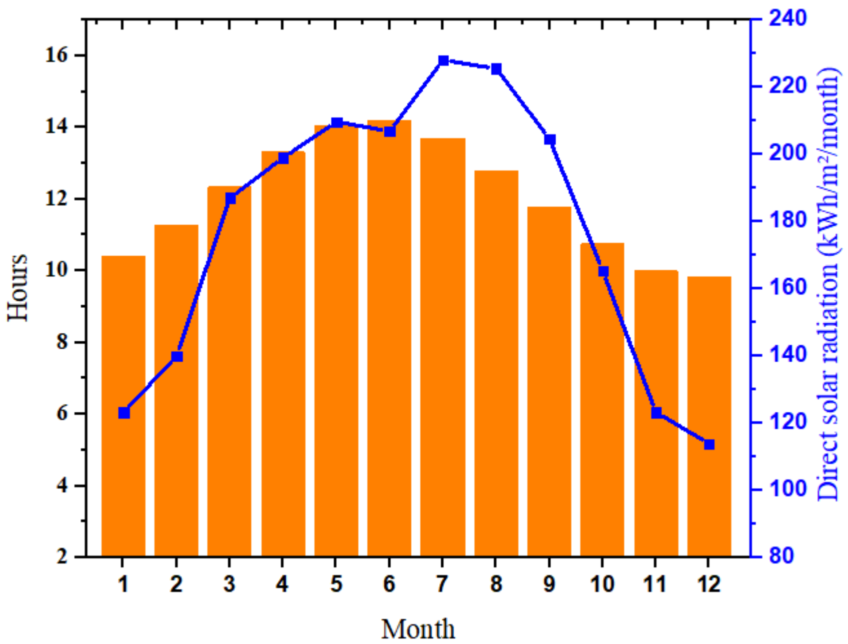


Figure IV.2: Mean daily solar radiation intensity and duration of the day and its bright sunshine insolation in El-Oued region

# Description of materials

The first geothermal system studied in the regions El Oued in the framework of this thesis consists of air duct. The geothermal heat exchanger designed and realized in El Oued region (Reguiba) which consist to of a helicoidal vertical shape as shown in figure IV.3. This configuration allows to decrease the area of installation of the geothermal heat exchanger and to assure the maximum of heat transfer from the soil to its surface due to the helicoidal shape of the vertical. The Helicoidal Water Air Heat Exchanger(HWAHE) has a helical shape with 0.8 m in diameter and 3 m in length. The heat exchanger is made of PVC pipe of 30 m length and 0.06 m diameter, and it is formed of 12 spires where the space between two consecutive spires is 0.3 m. The heat exchanger is immersed in a water well of 5 m deep as shown in figure IV.3.

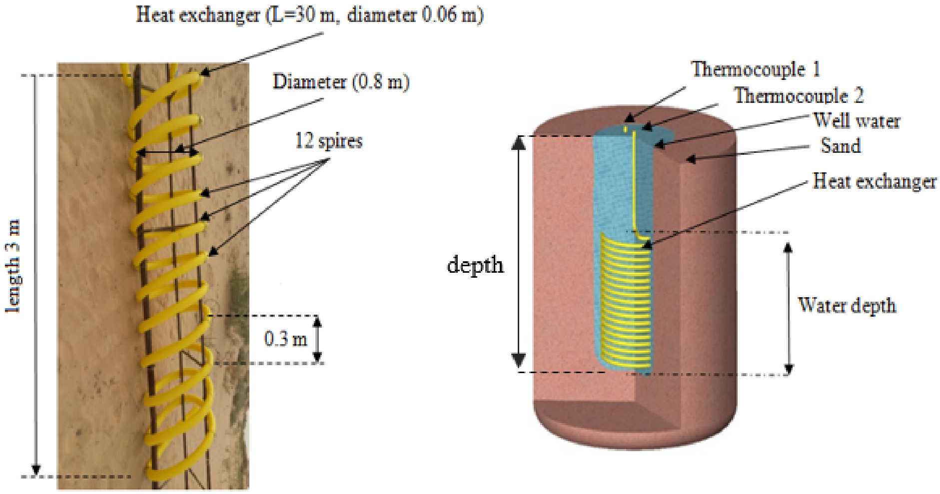


Figure IV.3: Description of the heat exchanger

### IV.1.1 Geothermal heat exchanger description

The experimental setup steps mainly consist of drilling the well, preparation of the exchanger and setting up of the heat exchanger into the water well as detailed below. Due to the low solidity of El Oued soil (sandy soil) the well drilled using the Concrete rings to avoid falling of the sand, the well drilled with 1 m diameter and 5 m depth and then filled with water, figure IV.4 shows clear picture of the drilled well.

The geothermal heat exchanger installed into the water well in the depth of 2 to 5 m as shown in IV.4. So, all the exchanger placed between the second and the fifth meter of the water well, the inlet and the outlet of the exchanger placed in small room constructed by plastic with the outlet have another option of injecting air from the outside too. In addition, a variable air flow extractor is placed at the inlet of the exchanger.

An external air intake vent with a height of 0.5 m built to avoid clogging is provided for the entry of fresh air into the duct, covered by a cap that prevents rainwater and sand from infiltrating within the duct. To prevent the intrusion of rodents, birds and insects, a fine mesh protective grid, accessible for cleaning, is installed at the entrance of each tunnel. A blower is mounted at the tube inlet to pump air within the exchanger. The flow of the blower varies. Air is continually pumped into the exchanger. No regulation is provided to start or stop the blower [69].

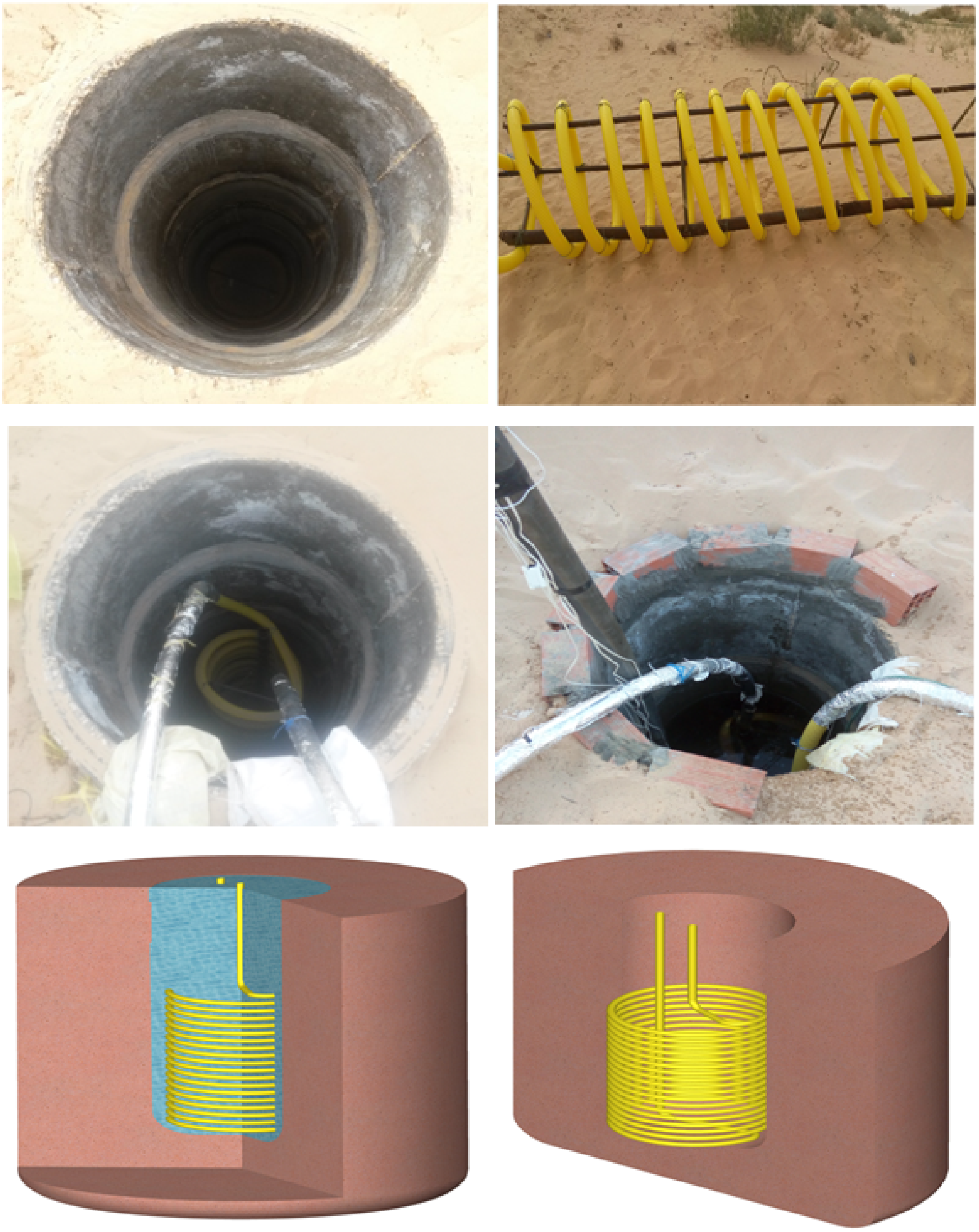

Figure IV.4: Experimental setup

The geothermal heat exchanger has a conical basket shape. Its diameter is 80 cm and the length 3 m, this exchanger made by PVC pipe with 30 m length and 6 cm diameter, it is formed of 12 spires and the space between two consecutive spires is 30 cm, Table IV.2 shows the parameter of the exchanger.

Table IV.1: Experimental parameters

| Parameters | Values |
|---|---|
| **Diameter of pipe (m)** | 0.06 |
| **Length of pipe (m)** | 30 |
| **Depth of pipe (m)** | 5 |
| **Thickness of pipe (m)** | 0.005 |
| **Mass flow rate** ($kg.s^{-1}$) | 0.035, 0.05 and 0.07 |
| **Water temperature (K)** | 297.8 |
| **Water thermal conductivity** ($W.m^{-1}.K^{-1}$) | 0.60 |
| **Water density** ($kg.m^{-3}$) | 1000 |
| **Water specific heat capacity** ($J.kg^{-1}K^{-1}$) | 4180 |
| **Ambient temperature (K)** | 311 |

### IV.1.2 Principle of operation

The principle of operation is very intuitive, the air at ambient temperature is blown into the heat exchanger by a blower at a constant velocity. It travels throughout the tube and exchanges heat with water. At the inlet and outlet at 30 m the heat exchanger, an anemometer is placed at the end of the PVC tube to control the velocity of the outlet air and a thermocouple to control the temperature. This temperature difference is one of the factors that affects the performance of the system. FigureIV.5 shows the positioning of the K-type thermocouples on the heat exchanger immersed in the water of the well. It was also used to measure the air temperature in different sections along the tube. Another instrument, Anemometer TESTO 416, is placed at the exit of the heat exchanger to measure the velocity of the air created by a blower.

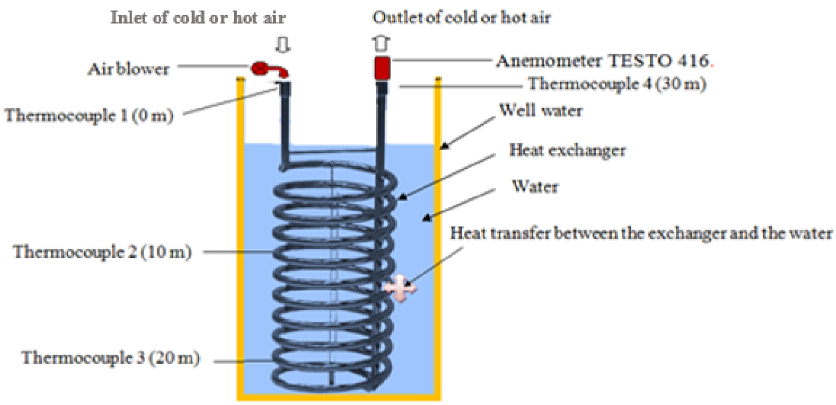


Figure IV.5: General view of the heat exchanger

## IV.2 Thermophysical characteristics of the system

The thermophysical characteristics of pipe air ducts, water and air are shown in Table IV.2, systems based on the water have become an interesting alternative, especially due to the high specific heat and the heat capacity of water.

Table IV.2: Physical and thermal properties used in the present study

| Material | Density ($kg.m^{-3}$) | Thermal Capacity ($J.kg^{-1}.K^{-1}$) | Thermal Conductivity ($W.m^{-1}.K^{-1}$) |
|---|---|---|---|
| **Air(300 K)** | 1.1774 | 1005.7 | 0.02624 |
| **Water(300 K)** | 1000 | 4180 | 0.60 |
| **PVC pipe** | 1380 | 900 | 0.16 |

## IV.3 Measuring equipments

The temperature measurements at the different levels in the "test office" are carried out using a constant-manganin thermocouple (k-type) are represented in figure IV.6. The technical characteristics of the thermocouples are presented in (See Appandix B.Table IV.3).A set of K-type thermocouple were used for measuring the temperature in different locations such as ambient temperature, water well temperature at five different positions, the temperature of air in the inlet and outlet of the HWAHE, seven measuring the temperature detectors (k-type) were used to measure the temperature of the air at different sections along the length of pipe (See Appendix B).

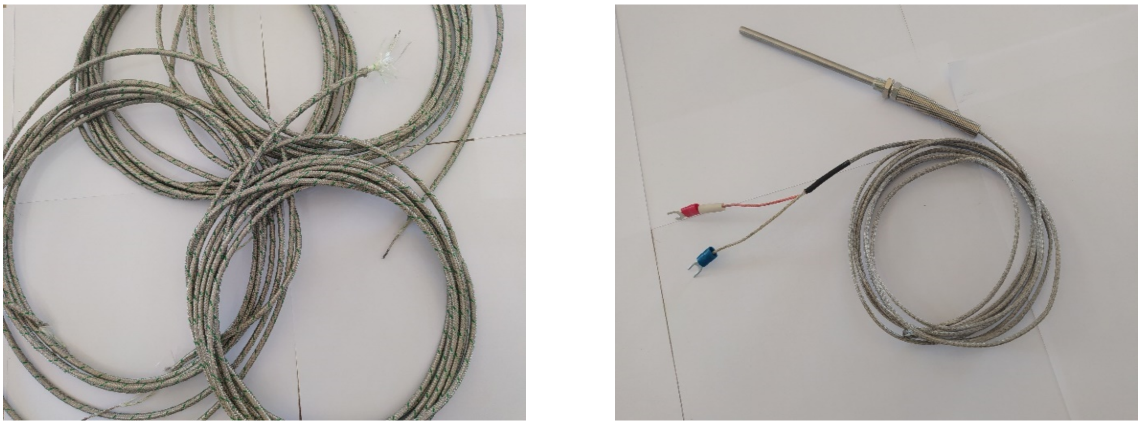

Figure IV.6: Type K thermocouples used

Air flow velocity and flow rate through HWAHE pipe was measured with the help of a vane probe-type anemometer (TESTO 416) as shown in Figure IV.7 small vane anemometers with a fixed telescopic probe, designed for measuring the airflow, wind speed and calculating Volumatic flow rate. The 416 digital anemometer provides accuracy on the spot readings in small ducts, ventilation grilles and air outlets. Compact in design, the hand-held instrument uses a high precision mini rotating vane to deliver readings with a high degree of accuracy. A TESTO 416 type was utilized for measuring the mass flow rate. the anemometer is placed at inlet and outlet of the heat exchanger to measure the velocity of the air created by a blower.

Figure IV.7: Anemometer Testo 416

## IV.4 Experimental uncertainty

Several factors such as instrument selection, state and calibration, environmental condition and experiment plan can cause errors and uncertainties in the experiments. Therefore, an uncertainty analysis should be performed to verify the precision of the equipment and experiment. An uncertainty analysis was performed using the method described [102].

A result R which depending on $W_1$, $W_2$, $W_3$........, $W_n$. In this work, be the uncertainties in the independent variable measured in the experiments, then the uncertainty in the result having these odds is given as:

$$w_R = \left[ \left( \frac{\partial R}{\partial x_1} w_1 \right)^2 + \left( \frac{\partial R}{\partial x_2} w_2 \right)^2 + ........ + \left( \frac{\partial R}{\partial x_n} w_n \right)^2 \right]^{\frac{1}{2}} \tag{IV.1}$$

Each measured and calculated parameters uncertainty is calculated using Eq (IV.1), an example the uncertainty evaluations in the heat exchange rate can be gifted as follows:

$$w_Q = \left[ \left( \frac{\partial Q_e}{\partial \dot{m}} w_{\dot{m}} \right)^2 + \left( \frac{\partial Q_e}{\partial C_P} w_{C_P} \right)^2 + \left( \frac{\partial Q_e}{\partial T_O} w_{T_O} \right)^2 + \left( \frac{\partial Q_e}{\partial T_{in}} w_{T_{in}} \right)^2 \right]^{\frac{1}{2}} \tag{IV.2}$$

Where $W_{\dot{m}}$ and $W_{T_i}$ represent the estimated uncertainties of the mass flow rate and temperature measurements, respectively. The sensitiveness of the thermocouple and anemometer used to carry out these experiments is respectively equal to ± 0.01 $^oC$ and ±0.1 $m.s^{-1}$. To identify tests errors and uncertainties caused by tools chosen in the present study and to prove the accuracy and validity of the experiments, the measurement errors are presented (see Appandixe B Table IV.3). The error investigations, therefore, give the uncertainties for velocity and temperature as ± 2.0% and ± 3.57% respectively. This is an actual instrumental error noted over the measurement as the present study is a comparative analysis of actual experimentation to investigate the performance of several parameters under various different operating conditions.

## IV.5 Climatic conditions of the experiments

The climatic conditions of El Oued experiments were measured for long-term average values: maximum and minimum ambient temperature, monthly average relative humidity, wind speed and average water temperature immersed TableIV.3.

Table IV.3: The climatic conditions of El Oued (May 2017)

| **Day** | **3 May** | **4 May** | **5 May** |
|---|---|---|---|
| **Maximal ambient temperature** | 38,2 | 36 | 37,6 |
| **Minimal ambient temperature** | 17.3 | 19.5 | 20 |
| **Average relative humidity %** | 31 | 32 | 34 |
| **Mean wind velocity** | 3.9 | 4.3 | 4.6 |
| **Average water temperature at 5m** | 24.8 | 25 | 25.1 |

Hourly variance during the month (May $3^{th}$ to $5^{th}$, 2017) of ambient temperature and solar radiation is shown in Figure IV.8. The ambient temperature differed between 15 to 40 $^oC$ during this time, and solar radiation ranged from 900 to 1000 $W.m^{-2}$.

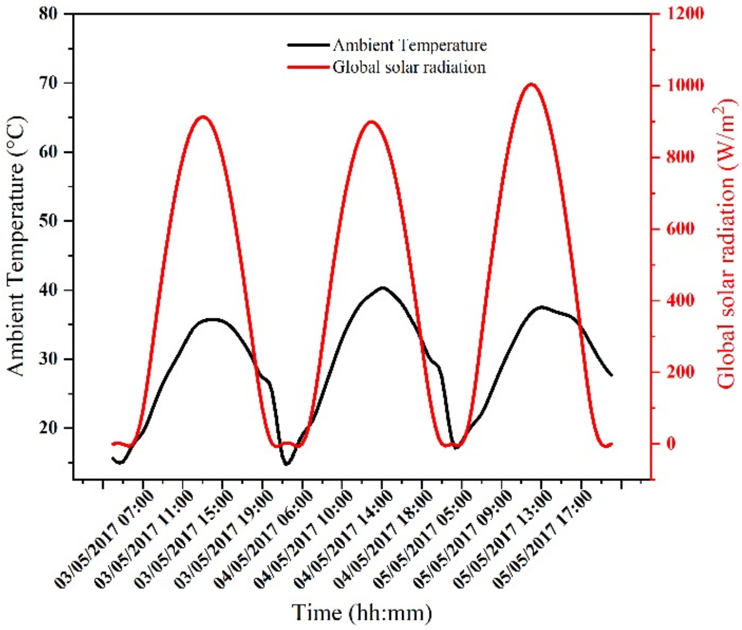


Figure IV.8: Solar radiation and ambient temperature (3 -5 May 2017)

Figure IV.9, presents the average wind speed and relative humidity values at the identical time. It demonstrates that at 07:00 h, the maximum value of relative humidity is reached, equivalent to 77 %. At 16:00 h, its minimum value 19 %. The mean wind speed is 3 $m.s^{-1}$.

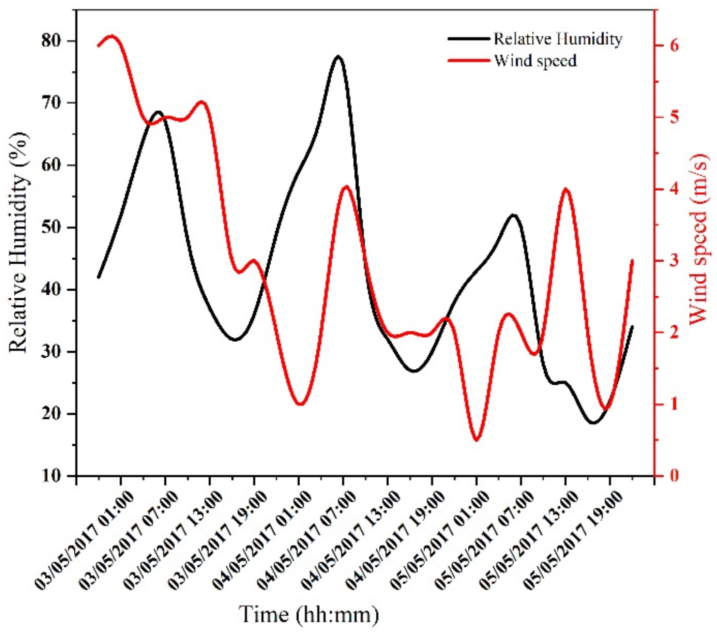


Figure IV.9: Evolution of relative humidity and wind velocity

## IV.6 Conclusion

The thermal behavior and thermal efficiency of the helicoidal water heat exchanger can be determined from experimental tests carried out during the cooling period in the El Oued region.

A data acquisition system was also installed, including the acquisition system and the various measuring instruments. This system allowed us to measure the different parameters: flow rate, soil temperature, input water temperatures, and output of the buried exchanger.

# Chapter V

# Experimental and numerical results

## V.1 Introduction

A significant factor in geothermal system installations is the buried or submerged heat exchanger. Because the efficiency of these systems necessarily starts with a good use of geothermal energy, which is assured by the immersed exchanger being well mounted. The objective of this chapter is to characterize buried exchangers and to determine the output of exchangers of this kind in arid and semi-arid climates. The heat exchange rate, extracted from the earth, is used to express the efficiency of the buried exchangers during this analysis. The effects of various parameters, such as air mass flow rate, burial depth, length and temperature of the inlet, are studied experimentally.

In order to complete the experimental part of the study of the impact of the diameter, the measurement of pressure losses and the exergy study, an analytical study have also been developed and validated.

## V.2 Thermal ground model(Depth ground temperature)

Figures V.1a, V.1b and V.1c show the average annual variation in soil temperature for three different soil types. Table V.1 shows the different thermophysical properties of the three types of soil studied (wet sand, clay and clay-sand silt). We notice that the average temperature of the soil decreases when we increase more into the soil. This behavior appears clearly in soil with a low thermal diffusivity (figure V.1b) than other types of soil (figure V.1a, V.1b and V.1c). The nature of the soil plays a very important role in the burial and the operation of the air-to-soil exchanger.

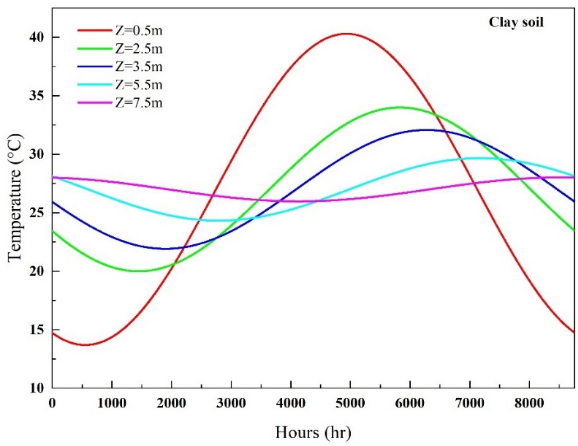


(a) Hourly evolution of soil temperature as a function of depth for clay ground

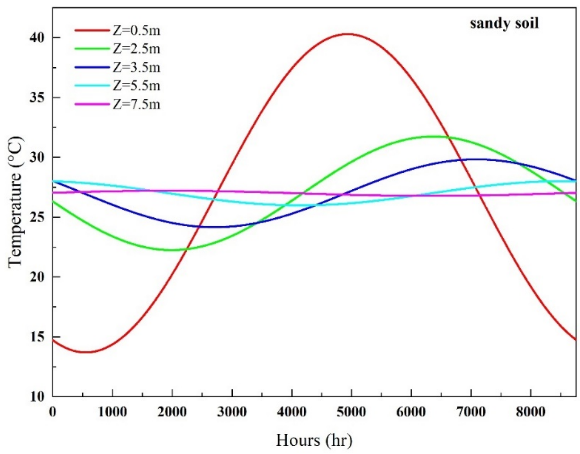


(b) Hourly evolution of soil temperature as a function of depth for sandy ground

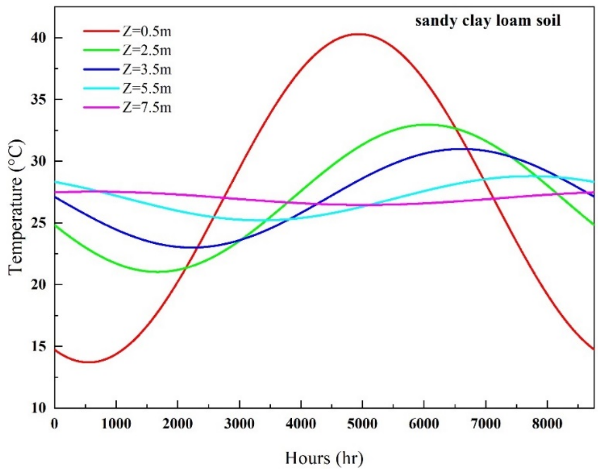


(c) Hourly evolution of soil temperature as a function of depth for a clay-sandy loam ground

Figure V.1: Hourly evolution of soil temperature as a function of depth for all types of soil

Figures V.2, it is remarked that there is a maximum temperature phase shift in the winter period, on the other hand, this phase shift becomes minimal in the summer period for the three soils, this phase shift is due to the thermal diffusivity of each soil, we also notice that as thermal diffusivity increases, the temperature of the soil increases.

Table V.1: Thermal and physical properties of soil

| Type of soil | Density $kg.m^{-3}$ | Thermal diffusivity $m^2.h^{-1}$ | Heat capacity $J.kg^{-1}.K^{-1}$ |
|---|---|---|---|
| **Clay** | 1500 | 0.00348 | 880 |
| **Loam** | 1800 | 0.00223 | 1340 |
| **Sand** | 1780 | 0.00135 | 1390 |

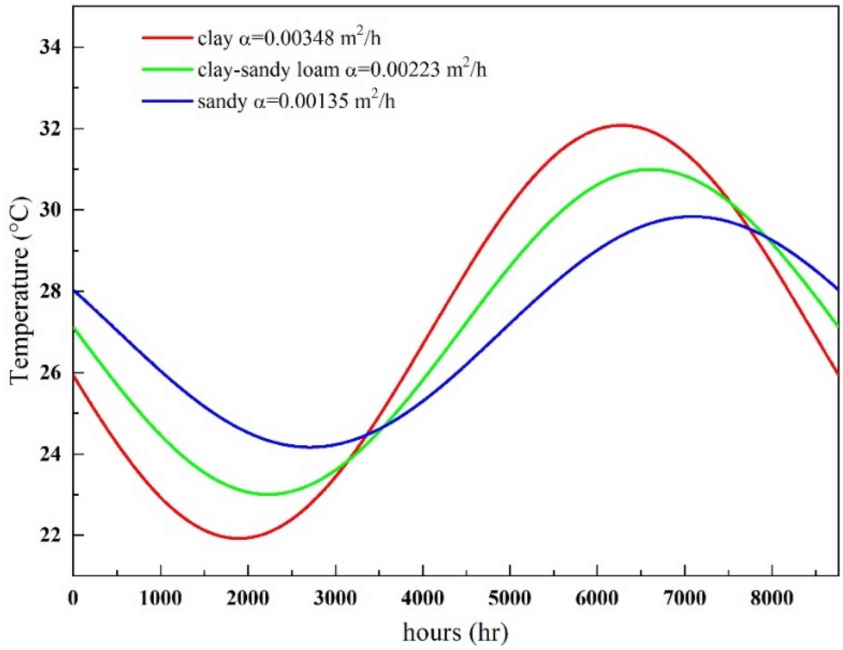


Figure V.2: Hourly evolution of soil temperature for three types of soil for a depth of 3.5m

# V.3 Water well temperature variation

In this work, an experimental study is undertaken to present the potential utilization of a Helicoidal Water-Air Heat Exchanger (HWAHE) in refreshing mode in arid zones, particularly for El-Oued area, Algeria. With this aim, a study of the thermal performance of HWAHE was experimentally analyzed.

## V.3.1 Water well temperature variation

The evolution of ambient temperature and water well temperature for different depths positions, from May 3th to 5th, 2017 is presented in figure V.3. The obtained results demonstrate that the ambient temperature varied from 18 to 38 $^oC$. The temperature of both ambient air and water fluctuates due to solar radiation effect. In addition, the water well temperature was between 23 and 25 $^oC$ for different depth positions.

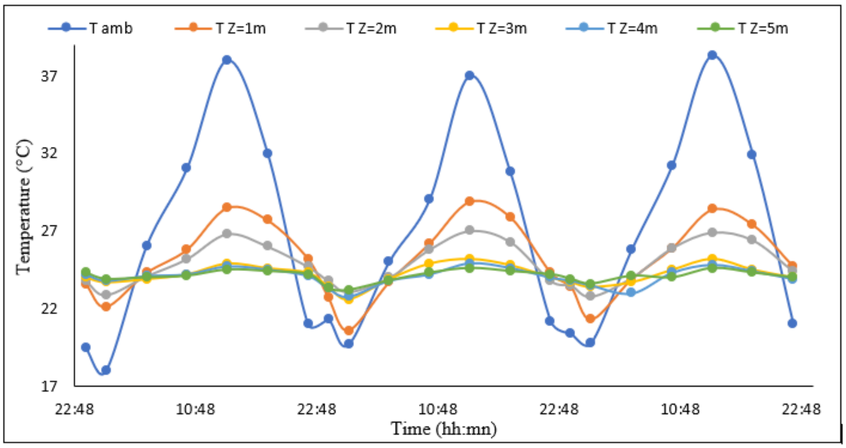


Figure V.3: Experimental soil temperature profile at different depths (May 3th to 5th, 2017)

### V.3.2 Evolution of the air temperature at the outlet of the exchanger

Experiments were performed in the region of El Oued on May 2017 from 10:00 h to 18:00 h. Temperatures were measured each 1hour period for three different air velocities (10, 15 and 20 $m.s^{-1}$). Besides, it is worth to note that the temperature in the water well beyond 3 m was almost constant, varied between 24 and 25 $^oC$. In this regard, the HWAHE was immersed in the water beyond this depth to keep it in a constant temperature environment. Figure V.4 shows side by side the experimental measurements of the inlet temperature, the water temperature and the outlet temperature in the three cases of air velocity 10, 15 and 20 $m.s^{-1}$. From the results of figure V.4, an increase in the air outlet temperature is observed with increasing of air velocity which reaches its highest value at 20 $m.s^{-1}$. The increasing of air velocity causes an increase in the air outlet temperature because of the decreasing of the residence time of air in the HWAHE pipes. Therefore, the thermal performance of the HWAHE deteriorates with increasing of air flow velocity.

Air temperature at the inlet of HWAHE pipe plays a significant role as the rate of heat transfer between air and soil is governed by the temperature difference between

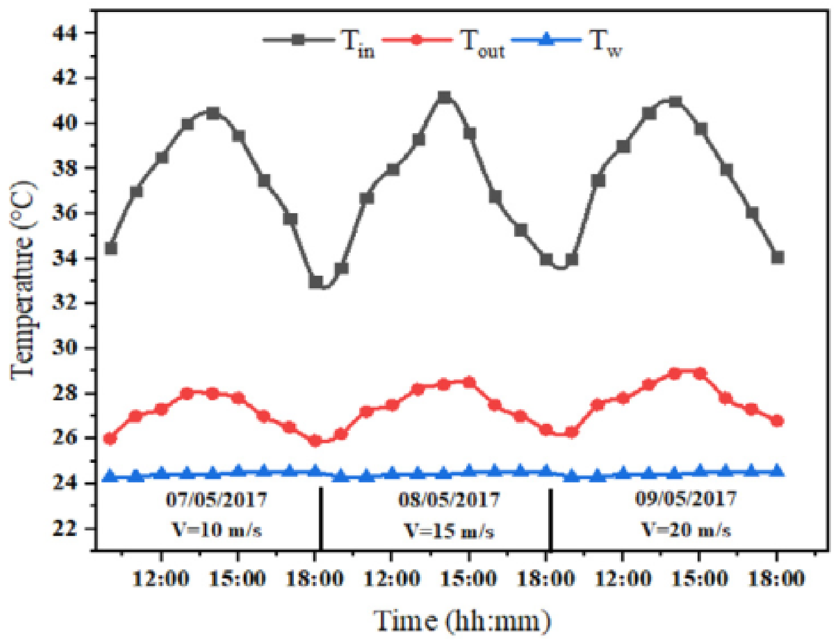


Figure V.4: Variation of the outlet temperatures of the heat exchanger

air and underground soil. The figure V.5, noticed that with the increase in inlet air temperature, the outlet temperature of air increases whereas, the amplitude decreases considerably. As the inlet temperature varied from 33 to 42 $^oC$, outlet air temperature varied from 26 to 29 $^oC$, for a 30 m length exchange, also observed with an increase of mass flow rate, the outlet air temperature increase but total heat gain increases.

### V.3.3 Duration curve of outlet temperature

An important characteristic for passive cooling applications is the temperature ratio RT which describes the temperature damping between inlet and outlet temperature, the effect of the flow rate on the performance of HWAHE was investigated. Figure V.6 shows the air temperature ratio along with the mass flow rate of HWAHE under the different air flow conditions. When the mass flow rate was 0.035 $kg.s^{-1}$ the air temperature decreasing rate was the fastest. The smaller the flow rate was, the faster the air temperature decreasing rate was, and the lower the outlet air temperature was. When the air mass flow rate was low, the time of air staying in the tube was long. Therefore, the heat transfer amount was also more than that of high airflow. The smaller RT, the more cooling energy is supplied to the building. As expected, reaches the smallest RT due to

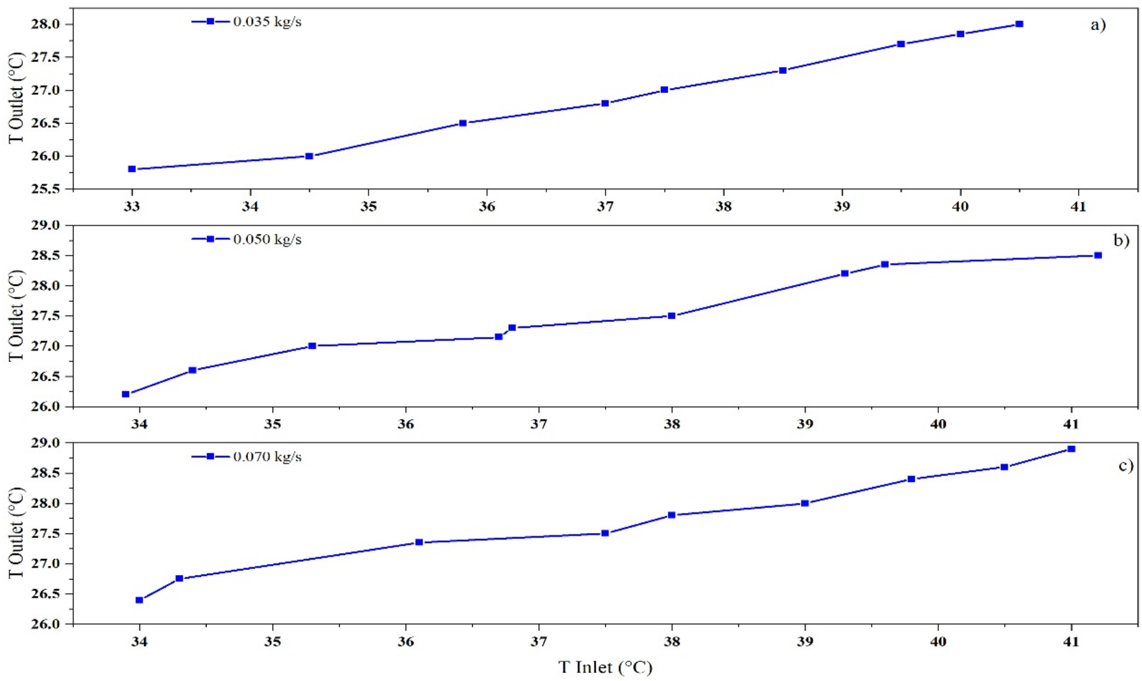


Figure V.5: Outlet air temperature variation versus the inlet air temperature for different mass flow rate

the high specific surface area (high conductive heat transfer between water immersed and pipe) and the comparatively small pipe diameter (high convective heat transfer between pipe and air).

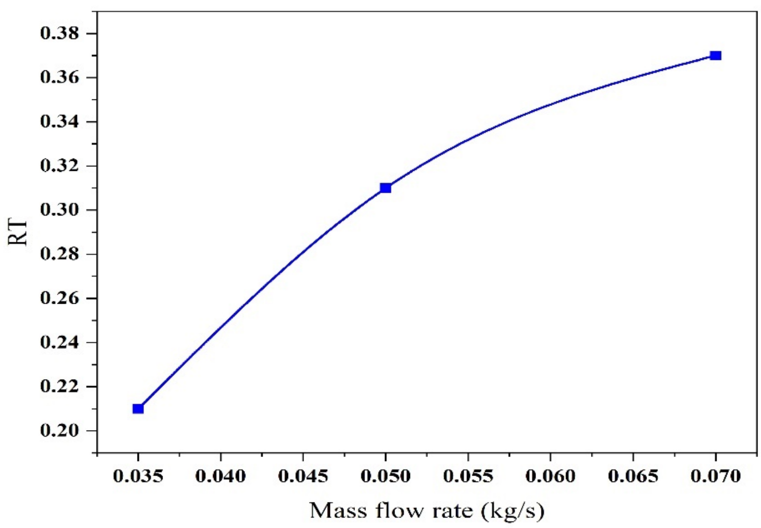


Figure V.6: Temperature ratio at a different flow rate

### V.3.4 Evolutions Heat Exchange Rate

To evaluate the overall heat transfer coefficient, three tests of the thermal potential were performed with varying mass flow rate between 0.035 and 0.07 $kg.s^{-1}$. For estimating heat exchange rate in each experience, the air temperature and mass flow rate in the exchanger inlet were fixed. The heat transfer rate was calculated when the outlet temperature became stable. Figure V.7 demonstrates that the difference of average logarithmic temperature (ΔTLM) has a linear relationship with heat exchanger rate.

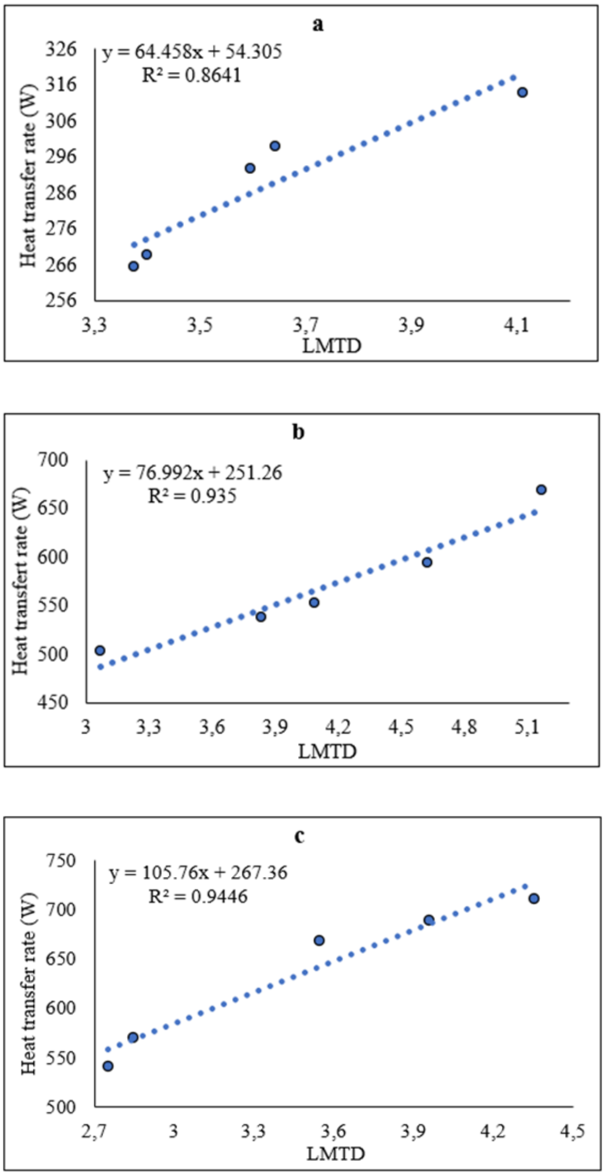


Figure V.7: Heat transfer rate, according to the log mean temperature difference for different flow rates

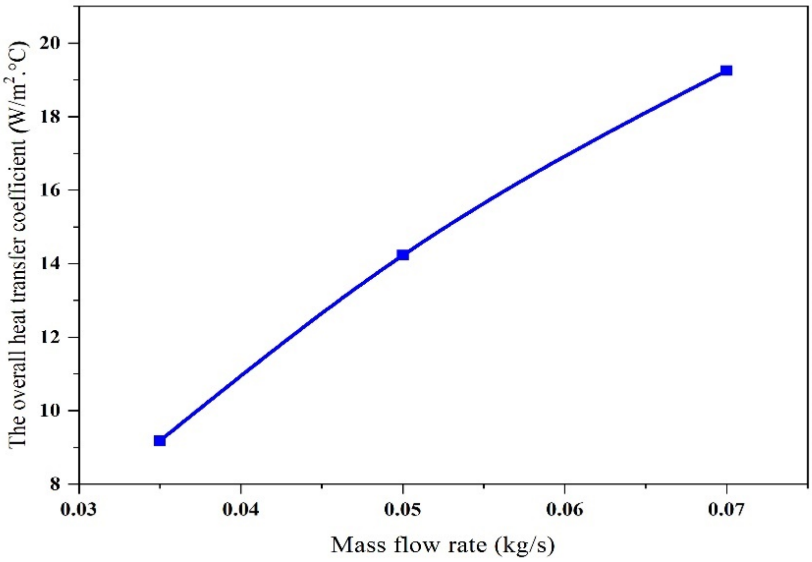


Figure V.8: The overall heat transfer coefficient versus mass flow rate

The calculated overall heat transfer coefficient U of the HWAHE systems is displayed in Figure V.8, this figure shows that the overall heat transfer coefficient, U, increases with the mass flow rate increases, varied from 9 to 19 $W.m^{-2}.^{o}C^{-1}$.

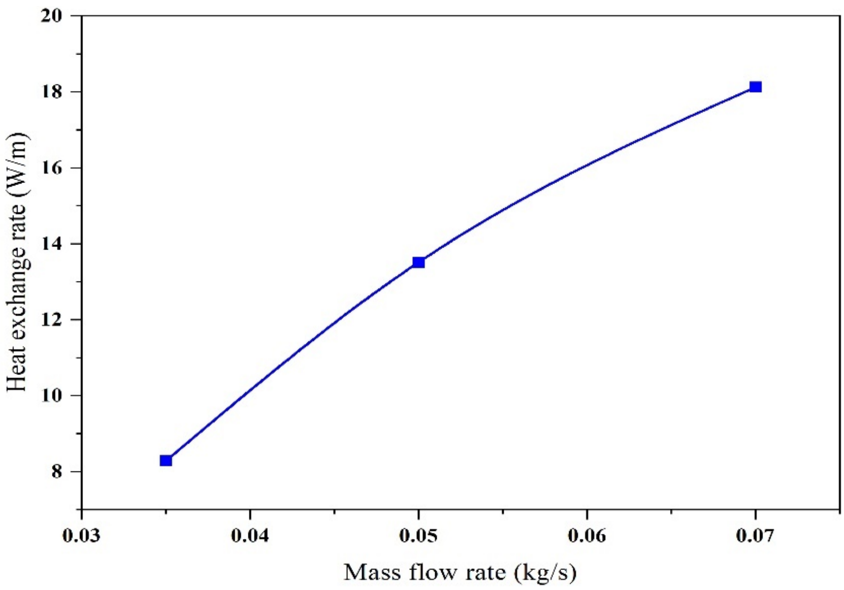


Figure V.9: Heat exchange rate versus mass flow rate

Figure V.9 illustrates the linear relationship between the mass flow rate and the heat exchange rate. The results are showing that when the flow rate is doubled (from 0.035 to 0.07 $kg.s^{-1}$), the heat exchange rate increases from 8 to 18 $W.m^{-1}$. From these results, it is clear that the mass flow rate has a major impact on the rate of heat exchange.

The same is true for the cooling power figure V.10, represents the heat transfer rate varies according to the time for different mass flow rates. An increase of 0.4 kW in cooling power was observed for a change in the mass flow rate of 0.035 to 0.07 $kg.s^{-1}$. As the difference in air temperature between the inlet and the outlet of the buried pipe decreases with the increase in mass flow rate, then the increase in cooling power is due only to the increase in mass air flow. These values confirm the significance of geothermal energy exploitation in El-Oued region.

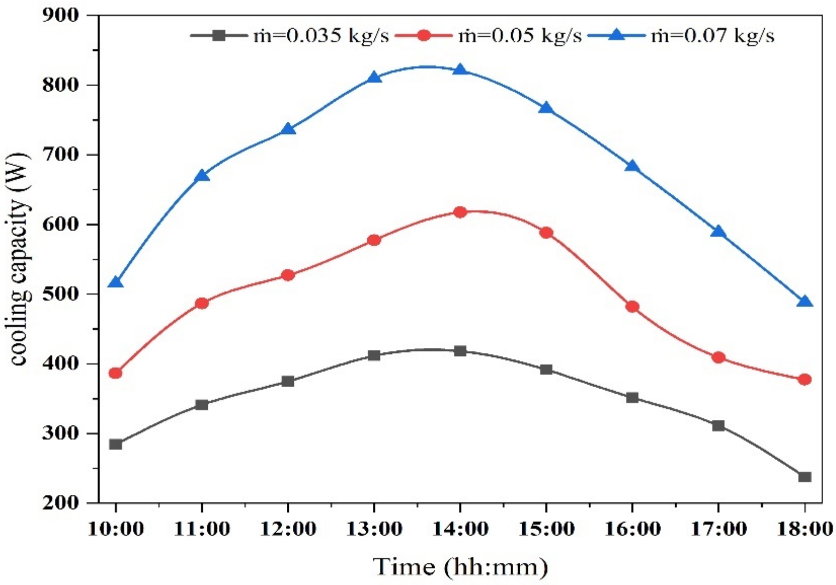


Figure V.10: Heat exchange rate versus time for different mass flow rate

### V.3.5 Energy efficiency

The effect of mass flow rate on energy efficiency, determined by the equation (Eq.III.17), is also studied, the results are shown in figure V.11. We notice in this figure, we note that increasing the mass flow rate decreases energy efficiency, from 92.5 % to 90 %. In addition, the flow rate determines the residence time of the air inside the heat exchanger, so it determines the residence time of the air inside the heat exchanger, so it determines the amount of heat the water immersed can retain. As the flow increases, the temperature differential between the exchanger and the exchanger decreases and thus the energy efficiency decreases.

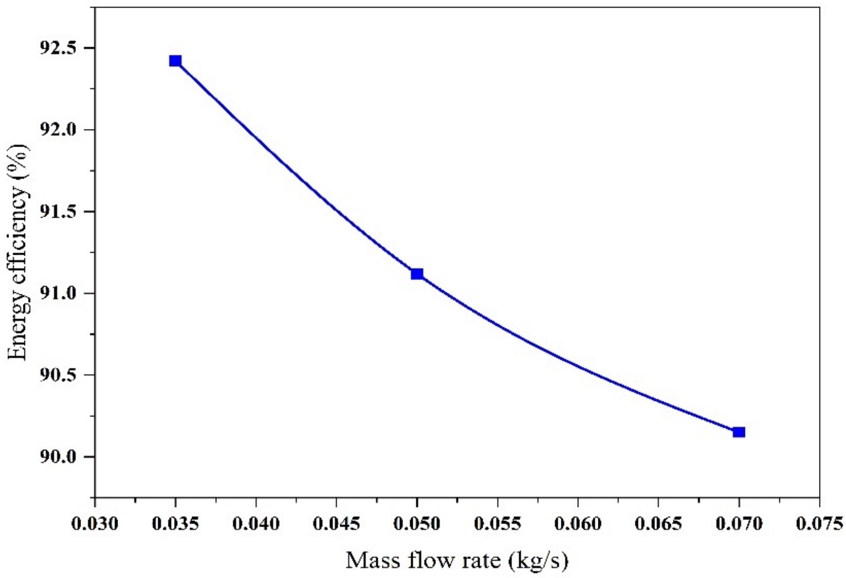


Figure V.11: Energy efficiency versus mass flow rate

## V.4 Effect of the length of the immersed exchanger

Figure V.12 shows the hourly variation of the air temperature inside the HWAHE system at three distances from the inlet (10, 20 and 30 m) for air velocity of 0.035, 0.05 and 0.07 $kg.s^{-1}$. From the results of Figure V.12 it can be noticed that any variation in the inlet temperature will be followed by a variation in the temperature of HWAHE mainly at 10 and 20 meters of distance. However, at the outlet of HWAHE (at 30 m), the air temperature is fairly constant and lower than 29 $^{o}C$ irrespective of the inlet temperature. an increase in the air outlet temperature is observed with increasing of air flow which reaches its highest value at 0.07 $kg.s^{-1}$. At the outlet, a pleasant and favorable temperature level for cooling the buildings in the region of El Oued is achieved at $27^{o}C$.

Figure V.13 represents the results of the experimental measurements. In V.13, the variation of air temperature along the length estimated by measured data for three different mass flow rates of 0.035, 0.05 and 0.07 $kg.s^{-1}$. In this figure, it was observed that increasing the mass flow rate causes a decrease in the air temperature because of the decreasing residence time of the flowing air inside the HWAHE. Therefore, the thermal performance deteriorates proportionally with mass flow rate increases. It was also observed the increase in the length causes an increase in the exchange surface between the fluid and the immersed pipe which increases the heat losses by convection of the air and

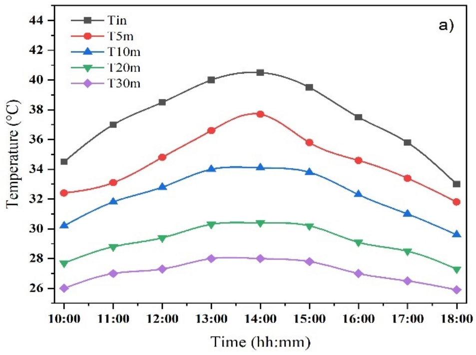


(a) Variation of the air temperature along the HWAHE versus the time 0.035 $kg.s^{-1}$

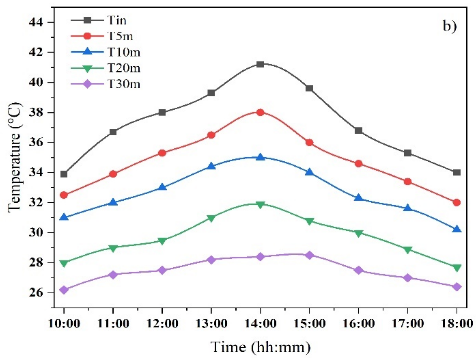


(b) Variation of the air temperature along the HWAHE versus the time 0.05 $kg.s^{-1}$

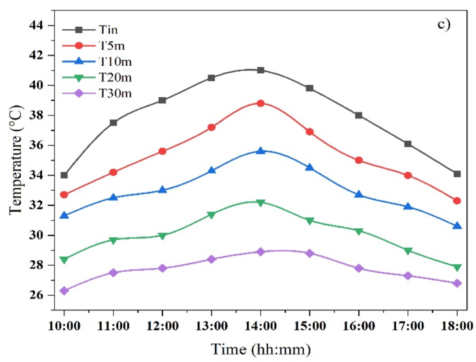


(c) Variation of the air temperature along the HWAHE versus the time 0.07 $kg.s^{-1}$

Figure V.12: HVariation of the air temperature along the HWAHE versus the time for different flow rates

consequently, the air becomes cooled more. and comes out with a temperature closer to the buried tube.

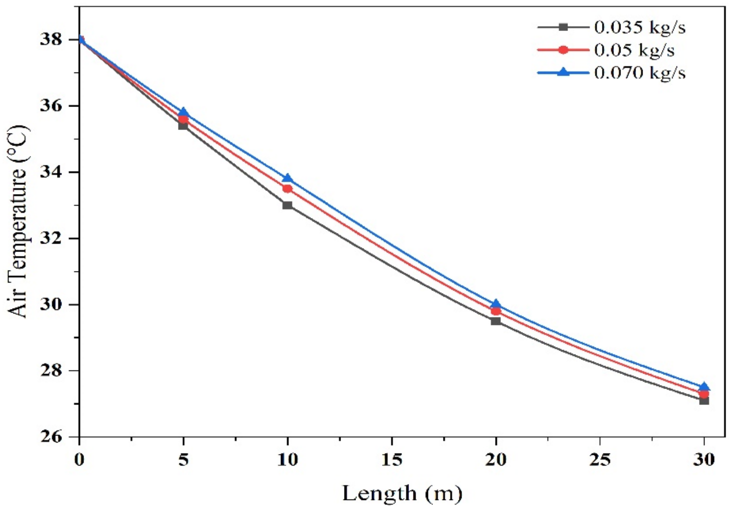


Figure V.13: Variation of air outlet temperature as function of mass flow rate

The efficiency of the system changes according to two variables; temperature and mass flow rate. Figure V.14 shows the results of the efficiency of the system as a function of the length of the heat exchanger. It was observed that when the flow rate increased, the efficiency of the system decreased. Indeed, the residence time influences directly the amount of heat absorbed by the air. Therefore, as the mass flow rate increases, the heat transfer coefficient increases, but on the other hand the residence time of the air in the heat exchanger decreases, so the temperature of the outlet air increases, which finally results in a decrease in the heat exchange efficiency. The efficiency is obtained to be 82%, 81% and 80% for three different mass flow rates of 0.035, 0.05 and 0.07 $kg.s^{-1}$, respectively.

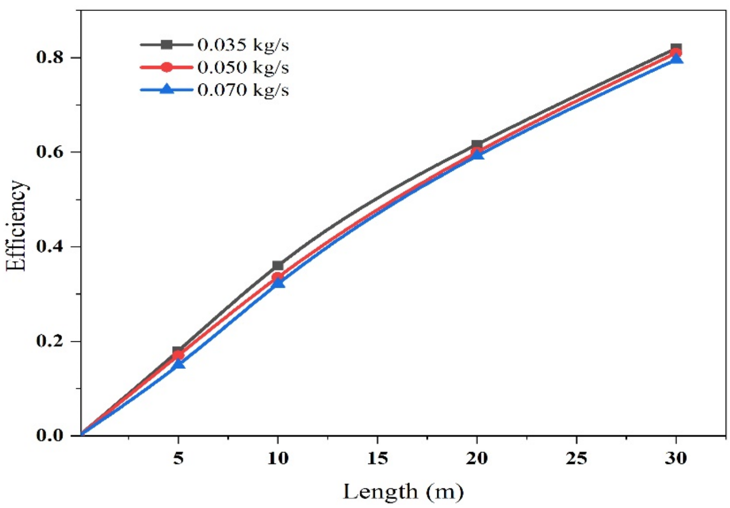


Figure V.14: Efficiency energy versus the exchanger length for different mass flow rate

# V.5 Exploitation of the analytical model

The purpose of the analytical analysis is to research the other parameters not treated in the experimental part, such as the diameter, the length of the immersed exchanger as well as the pressure losses, we will start with a validation of the analytical model followed by its exploitation

#### V.5.0.1 Validation of the analytical model

The validation of the analytical model is limited to the outlet temperature and the energy efficiency of the 30 m length exchanger immersed at a depth of 5 m for the three mass flow rates considered in the experiment. Complete results are grouped in table V.2.

Table V.2: Comparison between exprimental and analytical results

| | **Outlet temperature** | | **Efficiency energy** | |
|---|---|---|---|---|
| **Mass flow rate ($kg.s^{-1}$)** | **Exprimental** | **Analytical** | **Exprimental** | **Analytical** |
| **0.035** | 27.12 | 26.60 | 82 | 83 |
| **0.05** | 27.21 | 27.77 | 81 | 79 |
| **0.07** | 27.53 | 28.04 | 80 | 76 |

It should be noted from Table V.2 that the following analytical values have the same trend as those measured with an acceptable level, in the order of 2% for the outlet temperature and about 4% for the energy efficiency.

# V.6 Exergy performance

The variation of HWAHE exergy efficiency with mass flow rate is plotted in figure V.15. It is remarked that the exergy efficiency declines with the increment in flow rate. The values of exergertic efficiency are calculated as 90, 88 and 87% at respectively 0.035, 0.05 and 0.07 $kg.s^{-1}$, mass flow rates. It is seen that the efficiency of net energy was always higher than that of net energy efficiency. Due to the substantial storage ability of the water well.

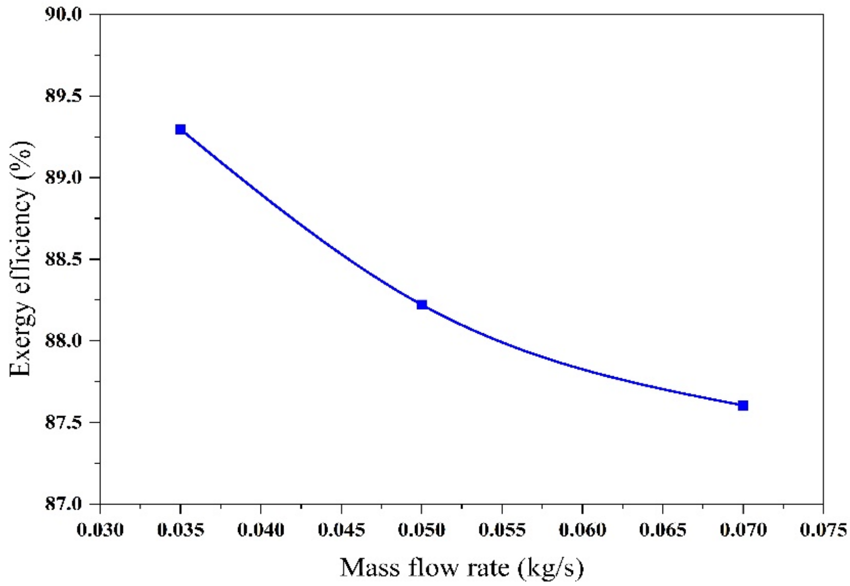


Figure V.15: Exergy efficiency versus mass flow rate

The exergy destruction rate of the HWAHE system is presented in the figureV.16. These results confirm that the increase of mass flow rate leads to an increase in the exergy loss. It is about of 0.9 kW and 3.5 kW at respectively 0.035 $kg.s^{-1}$ and 0.07 $kg.s^{-1}$ mass flow rates. The exergy destruction occurs principally due to blower and HWAHE piping system.

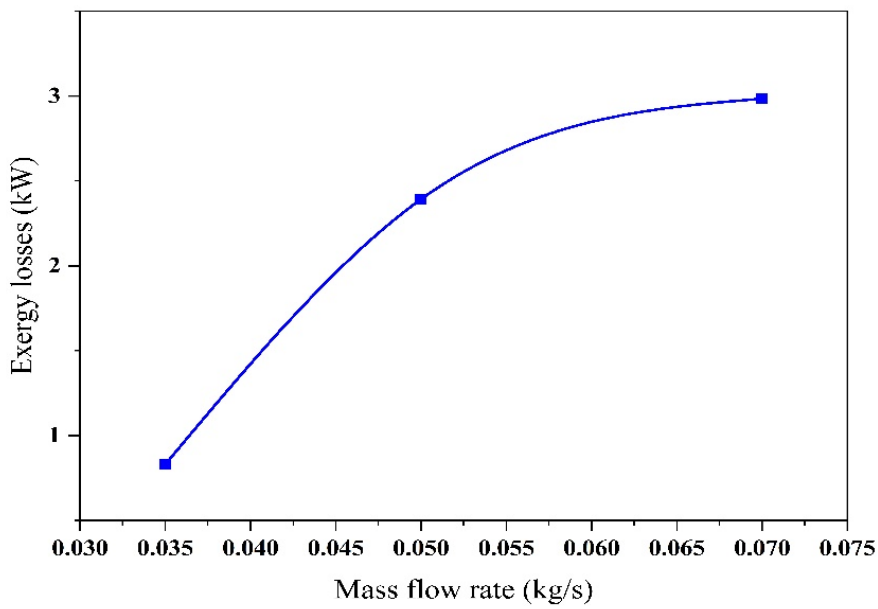


Figure V.16: Exergy losses versus mass flow rate

# V.7 Theoretical process exploitation

## V.7.1 Impact of the diameter of an immersed heat exchanger

In order to illustrate the effect of the exchanger diameter, we have represented on the figure V.17 the variation of the heat exchange rate according to the length of the exchanger for three diameters. The effect of the pipe diameter on the temperature of the air outlet is shown in figure V.17. As noted, an increase in the diameter of the tube leads to an increase in the temperature of the air outlet.

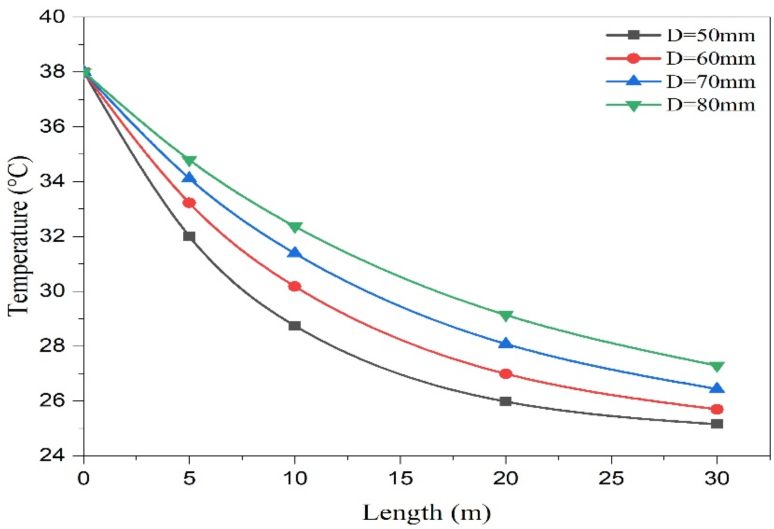


Figure V.17: Influence of pipe diameter on the air outlet temperature

In fact, we observed an increase of 1 $^oC$ and 2 $^oC$ in the maximum air outlet temperature for tube diameter variations of 50 -80 cm respectively. Indeed, the temperature of the air outlet increases because, due to the increase in the diameter of the tube, the mass flow of the circulating air increases, which causes its thermal inertia to rise and therefore the air to lose less heat.

## V.7.2 Calculation of the pressure losses

The differences in the pressure losses as a function of the mass flow rate of air and as a function of the exchanger diameter are grouped in the Table V.3.

These results show that the pressure drop increases with the flow rate and decreases with the diameter of the exchanger.

Table V.3: Analytical pressure loss per unit length

| **Pipe diameter** | **50** | **60** | **70** | **80** |
|---|---|---|---|---|
| **Mass flow rate** ($kg.s^{-1}$) | **Pressure losses** ($Pa.m^{-1}$) | | | |
| **0.035** | 727.46 | 581.05 | 480.80 | 408.28 |
| **0.05** | 1480.89 | 1183.31 | 979.50 | 832.06 |
| **0.07** | 2452.66 | 1960.20 | 1623.01 | 1379.08 |

## V.8 Conclusion

In this study, a new helicoidally waterair heat exchanger (HWAHE) configuration was presented and tested experimentally in refreshing mode in El-Oued region, Algeria. The HWAHE was immersed in 5 m depth water well. Effect of various parameters such as air velocity, exchanger length and inlet air temperature of the HWAHE were examined. Besides, an analytical model was used to predict the evolution of the air temperature inside the HWAHE as function of the main parameters. A good agreement between the experimental measurements and the results of analytical model was found. The main points concluded from this study are as follows:

- The maximum obtained temperature gap between the inlet and the outlet of the HWAHE is of 14.1 $^oC$ with 0.035 $kg.s^{-1}$ of air flow rate;
- The efficiency of the proposed HWAHE decreased with the increase of the air velocity. For the average values of air flow rate used in this study (0.035, 0.05 and 0.07 $kg.s^{-1}$), the HWAHE efficiencies are 82%, 81% and 80%, respectively;
- The analytical study of the exchanger showed a high concordance with those experimental;
- The HWAHE overall exchange coefficient has a positive relationship with mass flow rate and it rises to 19 $W.m^{-2}.K^{-1}$ from 9 $W.m^{-2}.K^{-1}$ when the mass flow rate is varied from 0.035 to 0.07 $kg.s^{-1}$ ;
- The HWAHE heat exchange rate improves to 18 $W.m^{-1}$ from 8 $W.m^{-1}$ with rise in mass flow rate from 0.035 to 0.07 $kg.s^{-1}$ ;

- The obtained results show that the energy provided by the HWAHE is more important in southern Algeria due to a significant difference between ambient temperature and ground temperature.

# Chapter VI

# Techno-economic study

## VI.1 Introduction

The role of geothermal energy in Buildings has received increased attention across a number of disciplines in recent years. Recent developments in the field of geothermal heat exchange uses have led to a renewed interest in energy saving. This chapter investigates the ability to reduce the energy usage for residential buildings located in El Oued region through a techno-economic comparison between three configurations of geothermal heat exchanger. The electricity consumption for cooling and heating of the studied case is calculated with and without the HWAHE system.The outlet air temperatures are calculated by MATLAB software. On this basis, The cooling and heating load for the chosen build with and without the heat exchanger system during the summer and winter are calculated byTRNSYS.

## VI.2 Description of case study

In this case study, the heat exchanger is integrated in the house of 200 $m^2$ as shown in Figure VI.1. The choosen house design is widely used in the arid and semi-arid region, it is selected to demonstrate the possible cooling and heating savings energy consumed when combined with heat exchanger system. The available garden area is used to bury the heat exchanger system.

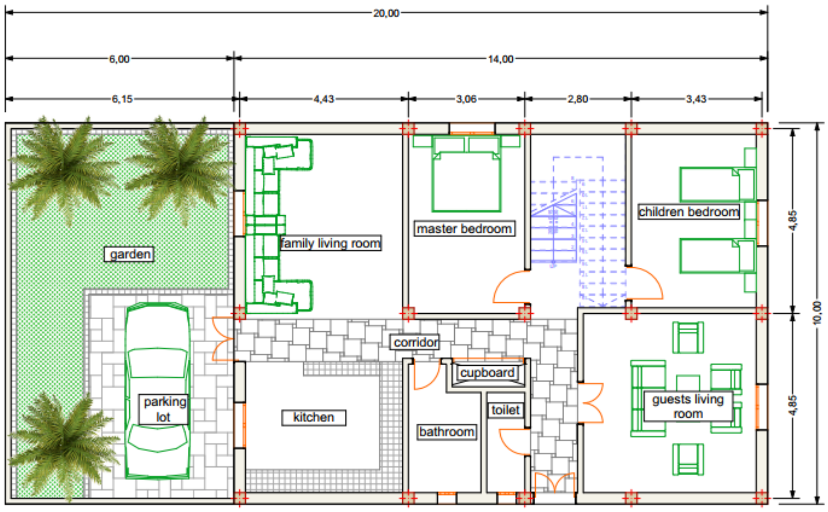


Figure VI.1: Plan of the chosen house for the study

Throughout this study, Three configurations of heat exchanger systems will be studied to demonstrate the economic benefit of geothermal energy integration in buildings:VI.2:

- System 1:This system is designed according to the garden area. It consists of one PVC pipe with 110 mm of diameter and 53.16 m of length, the serpentine pipe buried at 3 m depth, with 2 m spacing and slope of 2% [103];
- System 2: The HWAHE consists of PVC piping with 30 m of length and 0.06 m of diameter immersed into the bottom of a water well at 5 m of depth [69];
- System 3: This system consists of 15 pipes arranged horizontally with 1 m space between them and with 0.1016 m of diameter and 7 m length of each pipe, it buried at 3 m of depth. All the 15 pipes are connected with two header pipes of 0.152 m of diameter and 16 m of length. The method of installation and the size of the three systems GHE studied are shown in Figure VI.2 [110] (see Appendix C).

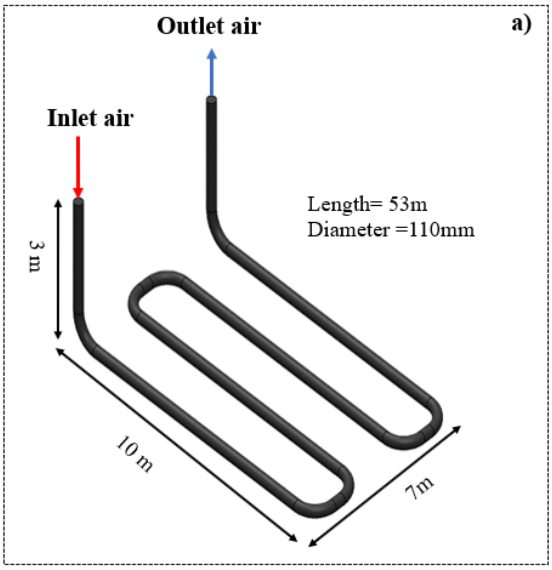


(a) Schematic of heat exchanger for [43]

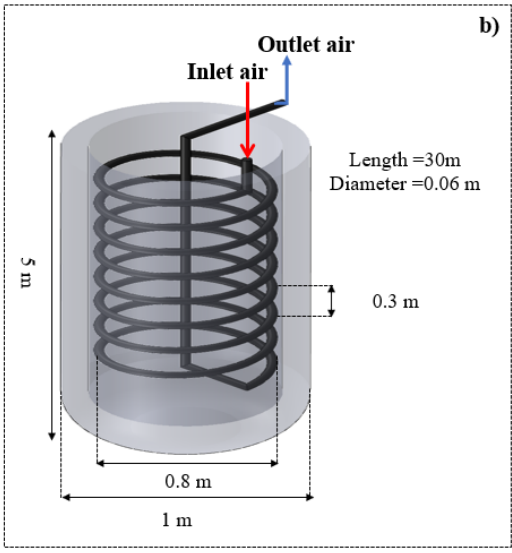


(b) Schematic of heat exchanger for our study [69]

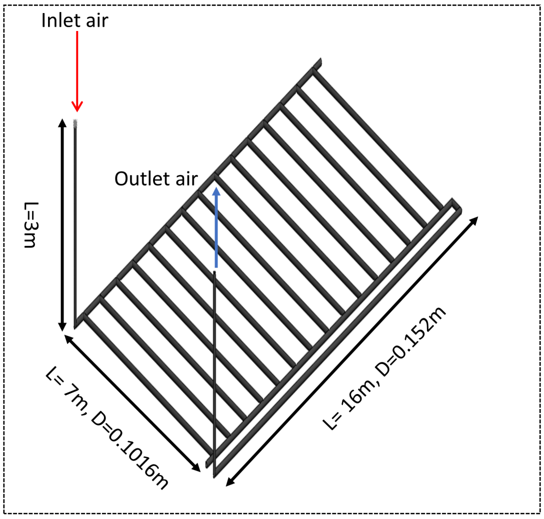


(c) Schematic of heat exchanger for [110]

Figure VI.2: Schematic of the three studied systems of heat exchanger

# VI.3 Governing equations

The heat transfer rate provided by heat exchanger system is given as;

$$Q = \dot{m}\, C_P\, \Delta T \tag{VI.1}$$

The air blower Input Power (IP) is computed by dividing the pumping power by the blower efficiency.

$$IP = \frac{P.P}{\eta} \tag{VI.2}$$

where, $\eta$ is the blower efficiency and it is taken to be equal to 0.8.

The cooling and heating loads of the selected house using the HWAHE system is calculated by subtracting the heat transfer rate provides by the heat exchanger from the cooling and heating load without the HWAHE system [111].

$$\overline{\overline{Q}} = \overline{Q} - Q \tag{VI.3}$$

Where

$\overline{\overline{Q}}$: Cooling or heating load for chosen building with heat exchanger system (kW);

$\overline{Q}$: Cooling or heating load for chosen building without heat exchanger system (kW).

The reduction in cooling and heating loads of the chosen building utilizing the heat exchanger system is determined [110, 111]:

$$Load\,reduction\,(\%) = \left[1 - \frac{\overline{\overline{Q}}}{\overline{\overline{Q}}}\right] \times 100 \tag{VI.4}$$

The energy efficiency ratio (EER) is determined to assess household air-conditioning electricity usage, which reflects the ratio of cooling or heating capacity in $BTU.h^{-1}$ to input power for AC units, varying from 8.5 to 12.5 per air-conditioning (refrence ) For this analysis, EER is assumed to be equivalent to 11.4.

$$EER = \frac{Cooling\,or\,heating\,(BTU/h)}{Power\,input\,(W)} \tag{VI.5}$$

The total consumed electricity (kWh) for cooling and heating of a chosen building with and without the heat exchanger system for 24 hours and 30 days from each month is determined from [110].

$$\overline{T.E.C} = \frac{\overline{Q}(BTU/h)}{EER} \times \frac{1}{1000} \times 24 \times 30 \tag{VI.6}$$

$$\overline{\overline{T.E.C}} = \left[\frac{\overline{\overline{Q}}(BTU/h)}{EER} + IP\right] \times \frac{1}{1000} \times 24 \times 30 \quad \text{(VI.7)}$$

$\overline{T.E.C}$: Total electricity consumption without heat exchanger system (kW).

$\overline{\overline{T.E.C}}$: Total electricity consumption with heat exchanger system (kW).

The energy savings that can be achieved with the heat exchanger system are calculated by:

$$Energy\,saving\,(\%) = \left[1 - \frac{\overline{\overline{T.E.C}}}{\overline{T.E.C}}\right] \times 100 \quad \text{(VI.8)}$$

# VI.4 Boundary conditions

The following conditions were used to complete the model of heat exchanger, where the cooling and heating loads have been calculated according to the design conditions, the construction materials and load components. At the inlet section of the heat exchanger tube, the mass flow rate is constant and equal to (0.07 $kg.s^{-1}$) with constant inlet temperature ($T_{in}$), which equals to the ambient air temperature. The values of the outside air temperature ($T_{in}$) are selected according to the data that was recorded for each month during the period (May 2017-April 2018) in El Oued city in southern Algeria. At the outlet, the relative pressure was taken to be equal to the atmospheric pressure.

# VI.5 Comparison of three proposed systems

## VI.5.1 Cooling season

Figure VI.3 shows Heat transfer rate for three studied systems over the summer season. From this figure it can be remarked that during the summer season the heat transfer from the system and soil increased with increasing of contact surface, thus the maximum heat transfer rate can be obtained from system 3 then system 2, and finally system 1.

The cooling load for the chosen build with and without the heat exchanger system during the summer season is shown in figure VI.4. From this figure, it can be viewed that

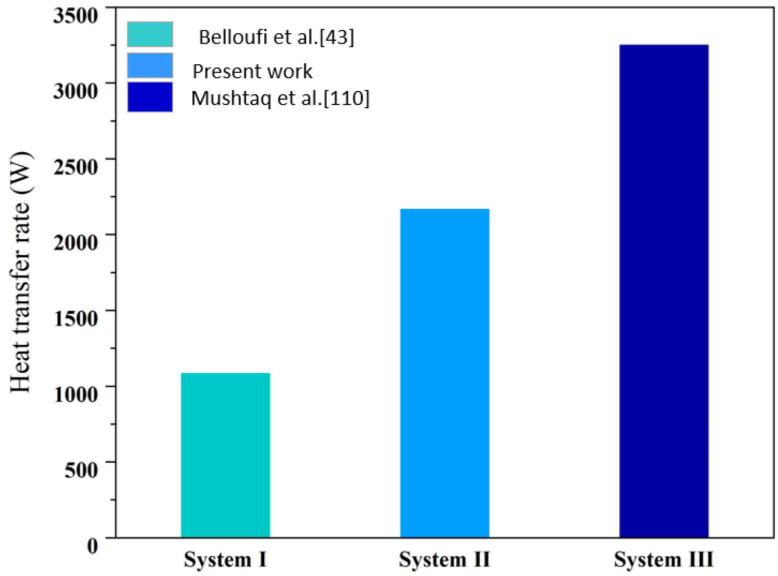


Figure VI.3: Heat transfer rate for the three studied system during summer season

during the summer season, the cooling load for the chosen build decreased using the heat exchanger system, and this drop in cooling load increased with increasing the contact surface of heat exchanger system due to outlet temperature decreasing. So, the minimum cooling load was achieved with using system 3.

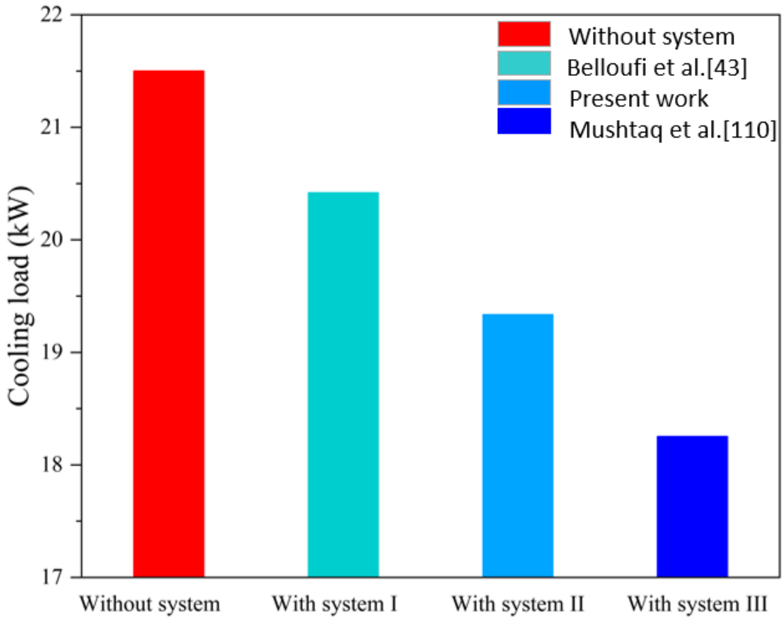


Figure VI.4: The cooling load for the chosen build with and without heat exchanger system for the three studied systems during the summer season

The percentage reduction in the cooling load that can be obtained from each configuration of heat exchanger system is shown in figure VI.5. It seems from this figure that system 3 gives the highest reduction percentage in cooling load, then system 2, which gives a reduction value of 10% ,is greater than system 1 by 6%.

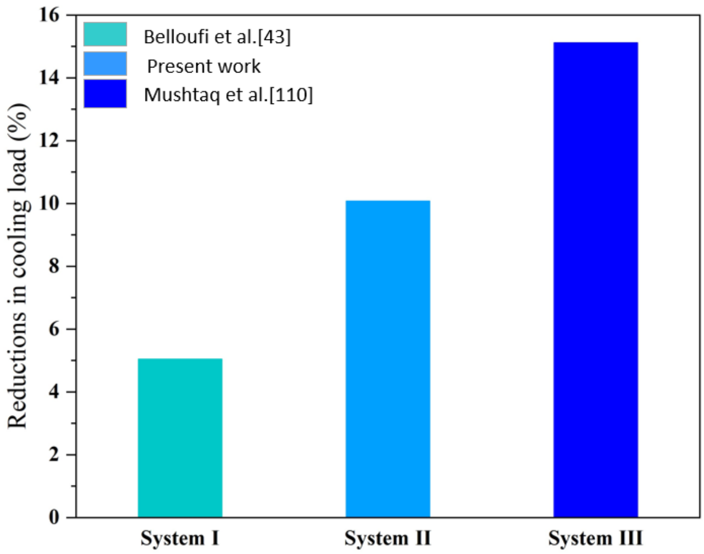


Figure VI.5: The percentage of reduction in cooling load for a chosen building using the heat exchanger system for the three studied systems during summer season

Figure VI.6 , demonstrates the electricity consumption for cooling of the chosen house, with and without the heat exchanger system, for the three systems studied. It is easy to see from this figure that the electricity consumption for cooling of the selected construct is reduced by using the heat exchanger system due to the reduction in the load that needed to be removed by AC units. This figure also shows that the minimum electricity consumption is achieved using System 3 since the maximum reduction in cooling load is given by this system.

For the three tested systems, figure VI.7 shows the energy savings that can be achieved using heat exchanger for the cooling of the chosen house. This figure presents the key advantage of using heat exchanger system, where it can be seen that using the heat exchanger as a passive system for cooling of the selected house during the summer season, there is a saving in energy due to the reduction that occurs in consumed electricity. This figure also shows that a higher energy saving value was reported with system 3 at 15 % , then system 2 at 10 % value, and eventually system 1 at 5% energy saving value in the selected home.

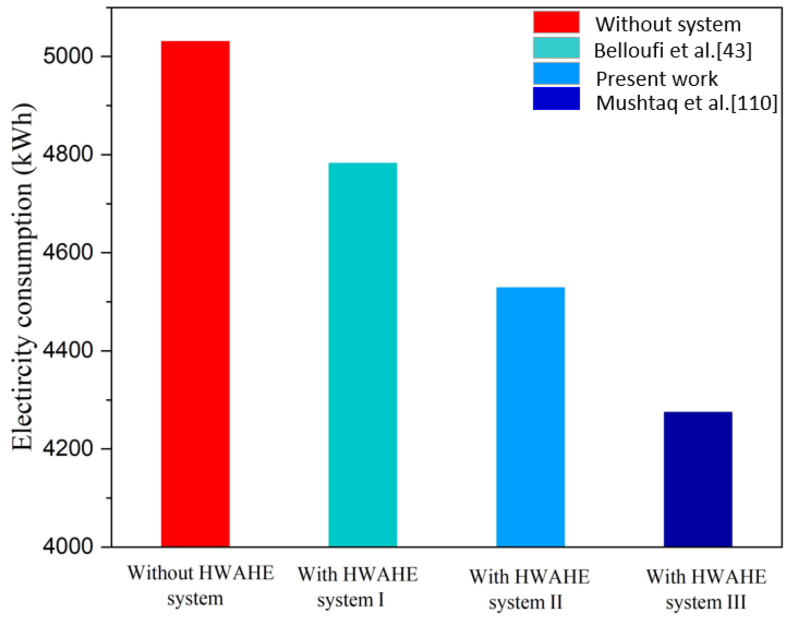


Figure VI.6: The electricity consumption for cooling the chosen build with and without the heat exchanger system for the three studied systems during summer

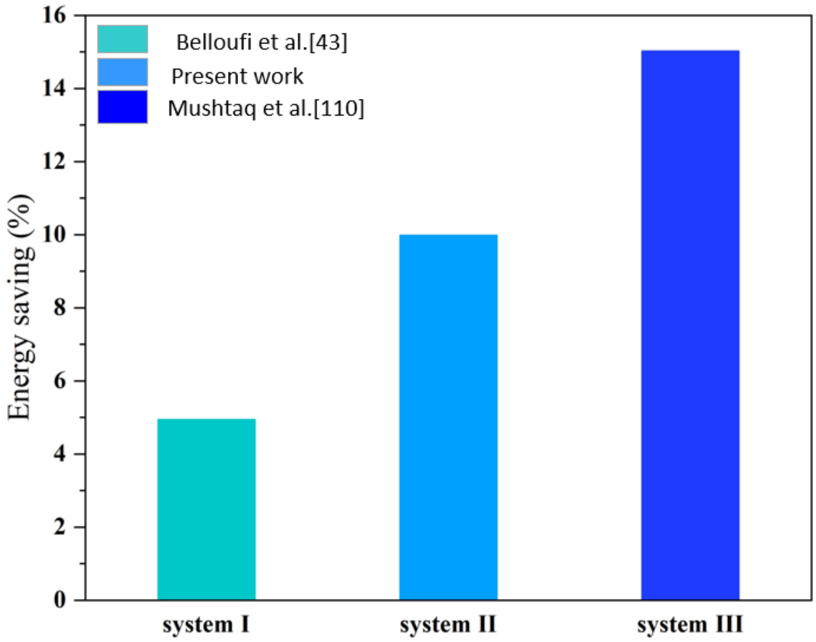


Figure VI.7: Saving in energy occurs with using heat exchanger system for cooling the chosen building

### VI.5.2 Heating season

Figure VI.8 shows the three worked systems over the winter season, the heat transfer rate between air and soil. From this figure it can be found that during the winter season the heat transfer from the air pipe to the soil increasing with the increasing system number of mounted pipes, hence the contact surface, thus the maximum heat transfer rate can be obtained from system 3 then system 2, and finally system 1.

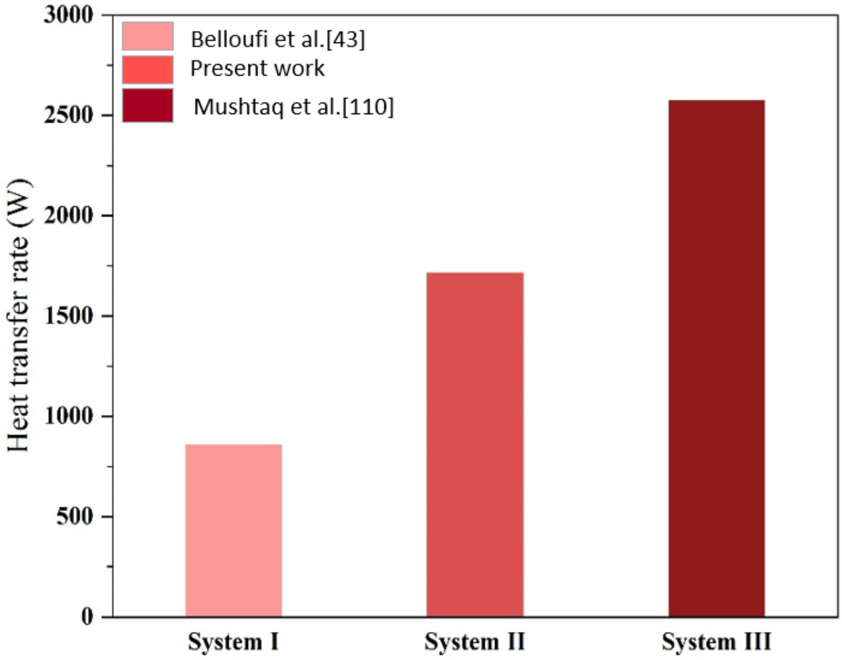


Figure VI.8: Heat transfer rate between three systems during the winter season

Figure VI.9 dipects the heating load for the chosen home with and without the heat exchanger system during the winter season. From this figure, it can be seen that the heating load for the chosen house decreases using the heat exchanger system during this season, and this decrease in heating load increased as the contact surface of heat exchanger system increased due to an increased in the temperature of the air supplied to the house. So, using system 3, the minimum heating load was achieved.

Figure VI.10 displays the percentage reduction in the heating load for the three chosen systems, it seems from this figure that the maximum reduction percentage in heating load is given by system 3, then system 2, which gives a value of reduction close to system 3, and higher than system 1.

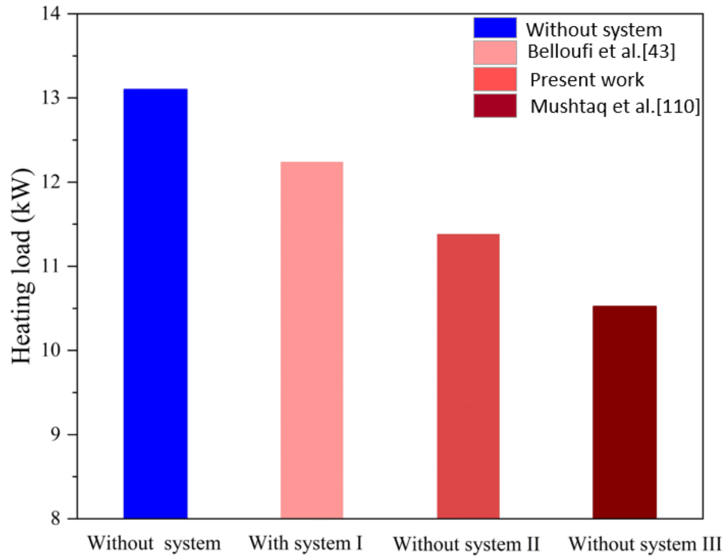


Figure VI.9: The heating load for the chosen home with and without heat exchanger system for the three studied systems during the winter season

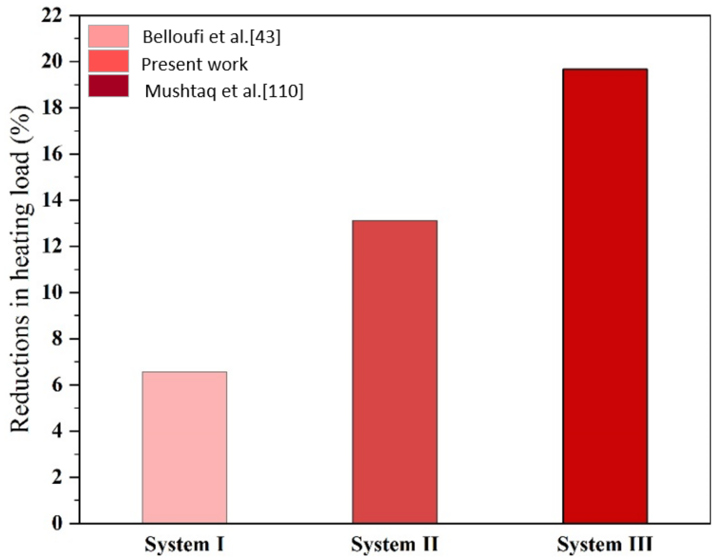


Figure VI.10: The percentage of reduction in heating load for the chosen home using the heat exchanger system for the three studied systems during winter season

Figure VI.11 shows the energy consumed for the heating of the selected house during the winter season with and without a heat exchanger system for the three systems tested. From this figure, it can be seen that the energy consumed has decreased. That by using a geothermal heat exchanger, where the heat exchanger acts as a heating system.

Figure VI.12 shows the saving in energy utilizing for the three systems studied. This figure illustrates that the saving in energy increased with increasing in reduction of

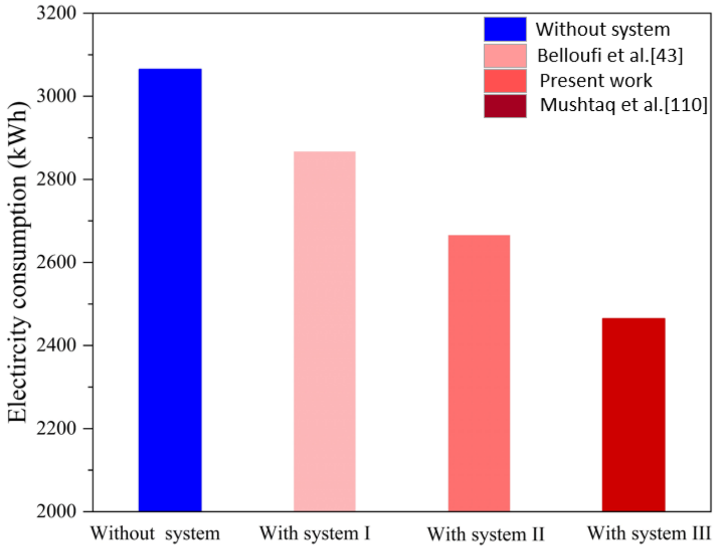


Figure VI.11: The electricity consumption for heating with and without the heat exchanger system for the three studied systems during winter season

electricity consumption, so the maximum energy saving is noted from utilizing system 3 compared with system 2, which gives energy saving higher than system 1.

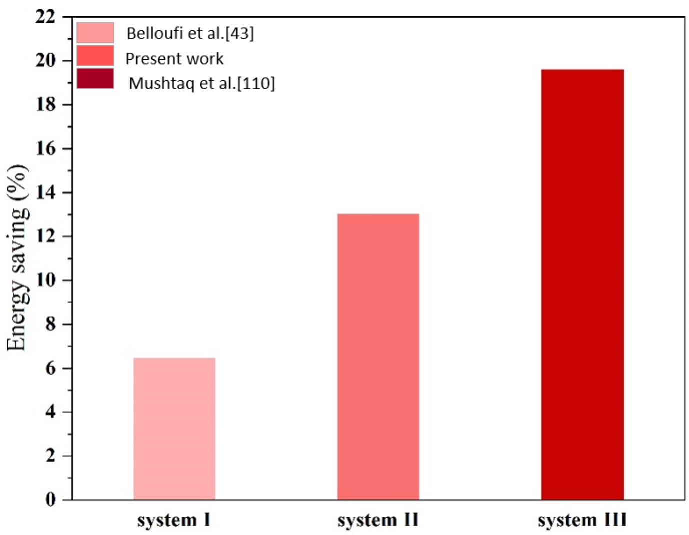


Figure VI.12: Saving energy occurs with using the Earth to air heat exchanger system for heating the selected house

## VI.6 Initial costs of installation

The initial cost of installation of a geothermal heat exchanger device included drilling costs, tubing, elbows, staff, and drawers. The estimates cost for the three systems were made on the basis of the local Algerian market prices, as shown in Table VI.1. From this table, it can be noted that the overall total initial cost of the heat exchanger system in case 3 is 60,310.00 DZD (468 $), while system 1 and heat exchanger system 2 have reached 75,700.00 DZD (588 $) and 97,200.00 DZD (755 $) respectively.

Table VI.1: The total estimated intiale cost of installation of the heat exchanger systems

| **System** | **System 1** | **System 2** | **System 3** |
|---|---|---|---|
| **Item** | | **Prices (DZD)** | |
| **Drilling** | 25000 | 37500 | 50000 |
| **Workers** | 14310 | 16200 | 16200 |
| **Drawer air** | 15000 | 10000 | 25000 |
| **Pipes and elbows** | 6000 | 12000 | 6000 |
| **Total cost (DZD)** | 60310 | 75700 | 97200 |
| **Total cost ($)** | 486.063 | 587.504 | 754.365 |

After analyzing and determining the appropriate system in terms of energy savings of cooling and heating loads for the chosen house during the summer and winter seasons. Where 5 months of summer (May, June, July, August and September) and 3 months of winter (December, January and February) are selected. Studying of the economic impacts of HWAHE utilization on energy saving during the year is important for the future of heating and cooling loads in El Oued region.

The monthly average of inlet and outlet HWAHE air temperature during the period (May 2018- April 2019) is presented in the figure VI.13. It can be noticed from this figure that notwithstanding the difference in the average Ambient air temperature per month, where it ranges from 10.65 $^oC$ in the month of January to 41.72 $^oC$ in August,the temperature of the outlet air of the HWAHE reported for all months is nearly around to 25 $^oC$. The temperature of the outlet air from the HWAHE system reported in January is 22.812 $^oC$ and 28.40 $^oC$ in July. In general, from this figure, it can be inferred that the air temperature supplied by the HWAHE system is more constant compared to fluctuating external air temperature values.

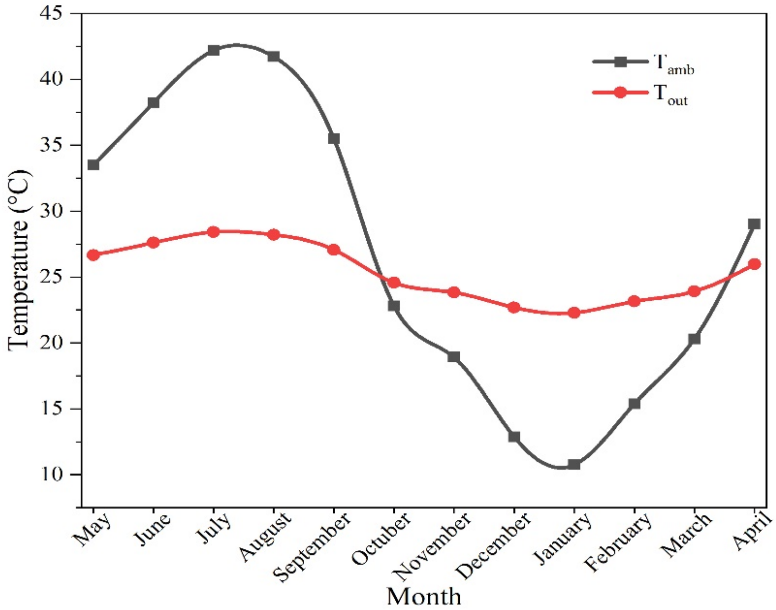


Figure VI.13: Monthly average of outside air temperature and outlet air temperature of HWAHE system

Figure VI.14 presents the monthly average rate of heat transfer between air and water well per month over the course of the year. Heat transfer is measured on the basis of each month's average temperature. From this figure, it can be observed that, due to the difference in external temperature, which reflects the inlet temperature of the HWAHE system, the amount of heat transfer rate varies throughout the year. It reported that the heat transfert rate in January and August was 1942.20 W and 1625.99 W, respectively. This results may be explained by the fact that the highest amount of heat transfer can be obtained during theses monthes due to the minimum and maximum outside temperature.

The amount of cooling load for the chosen home during summer months with and without the HWAHE system is illustrated in Figure VI.15.It can be noticed from this figure that the amount of cooling load varies in summer, depending on the variation in the outside air temperature, where the maximum amount was recorded in August and the minimum was recorded in May because these months have the maximum and minimum outside air temperature, respectively. Also, it can be remarked from this figure that the amount of cooling load for the chosen home was reduced when the heat exchanger system is installed and coupled with the house, whereas, for example, in August, the amount of

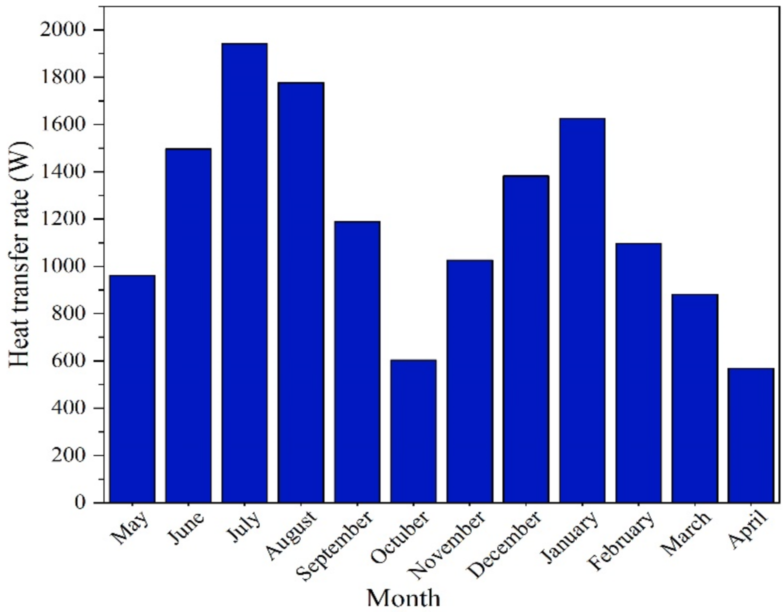


Figure VI.14: The heat transfer rate on the monthly average of the outdoor air temperature per month

cooling load without the heat exchanger system was registered envirent to 14.90 kW, but this value reduced to 13.12 kW using the HWAHE system.

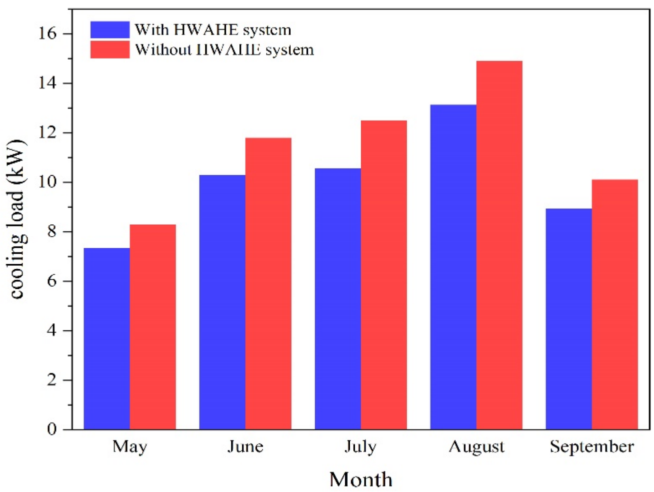


Figure VI.15: Cooling load for the chosen home with and without the HWAHE system during summer months

The percentage of the cooling load reduction is illustrated in Figure VI.16 From this figure, it can be observed that the percentages of cooling load reduction ranged from 11.55 % in May to 15.54 % in August. This figure also demonstrates that the maximum values reported in August and July due to the high outside temperature.

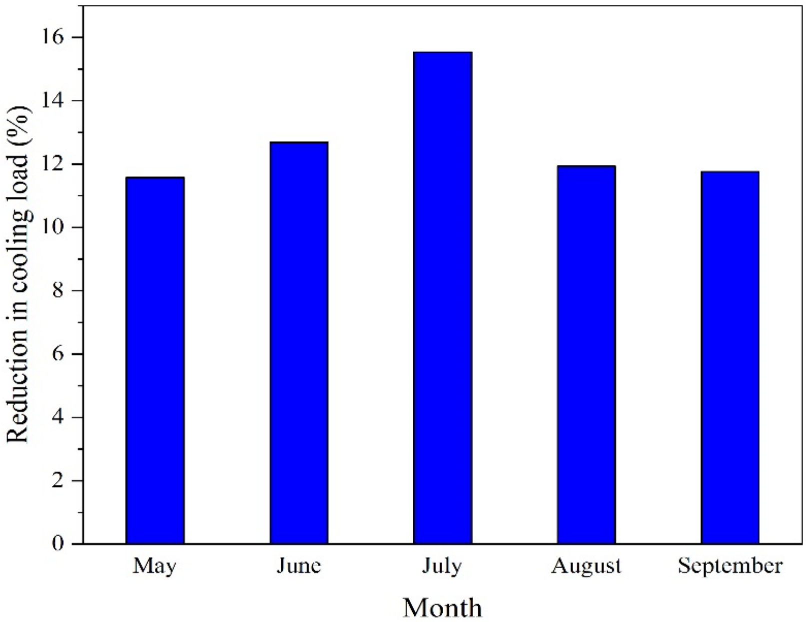


Figure VI.16: Reduction in cooling load for the chosen home using the heat exchanger system during summer months

Figure VI.17 presents the electricity use for the cooling of the chosen home during the summer months, with and without the HWAHE system. It can be observed from this figure that the maximum electricity consumption was stated in August, while the minimum was recounted in May since the consumption of electricity was dependent on the quantity of cooling load in which the maximum and minimum quantity of cooling load is registered in those months. This figure also shows that, due to the reduction in cooling load using the HWAHE system, electricity consumption is decreased compared with electricity consumption without the HWAHE system.

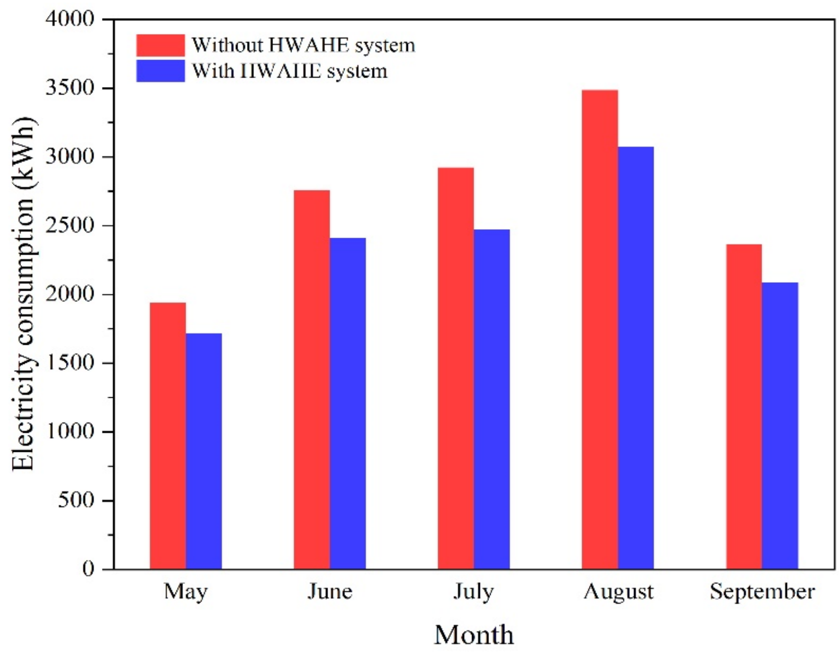


Figure VI.17: Electricity consumption for cooling of the chosen home with and without HWAHE system through summer months

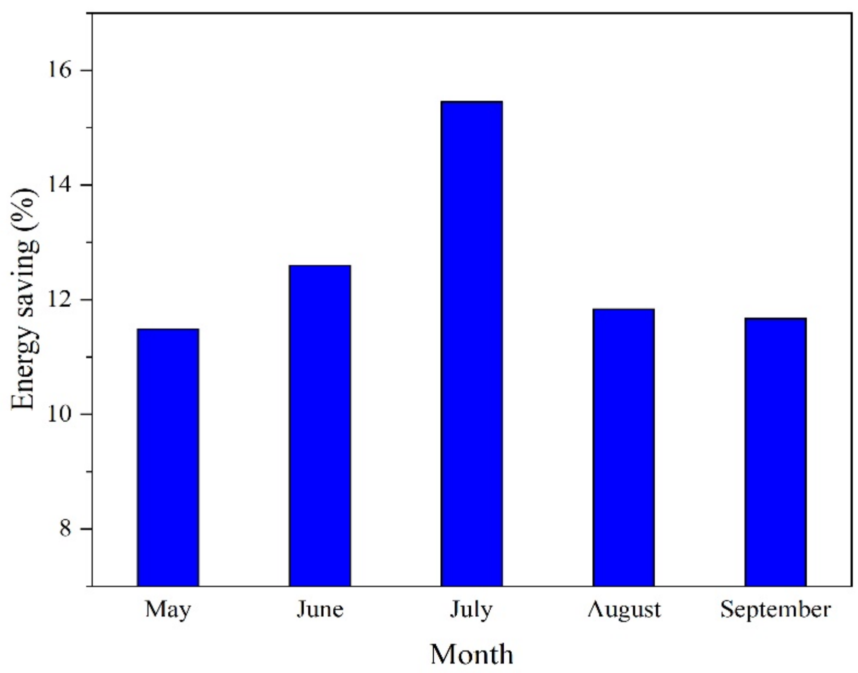


Figure VI.18: Energysaving occurs with using heat exchanger system for cooling the chosen home during the summer months

The energy-saving percentages using the HWAHE method during the summer months are shown in FigureVI.18. This figure presents that the energy-saving percentages are from 11.37% to 15.45%, where the maximum energy saving can be achieved in August, while the minimum amount of energy-saving was recorded in May because in August and May the maximum and minimum reduction in cooling load was recorded. .

Figure VI.19 shows the amount of heating load for the chosen home with and without the HWAHE system during the winter months. It can be remarked that during the months with low outdoor air temperatures, the amount of heating load increased so that the maximum heating load value was reached in January. This figure also indicates a decrease in the required heating with the use of the HWAHE system, where the heating load decreased from 7.41 to 6.01 kW, from 8.20 to 6.57 kW, and from 6.52 to 5.41 kW through December, January, and February, respectively.

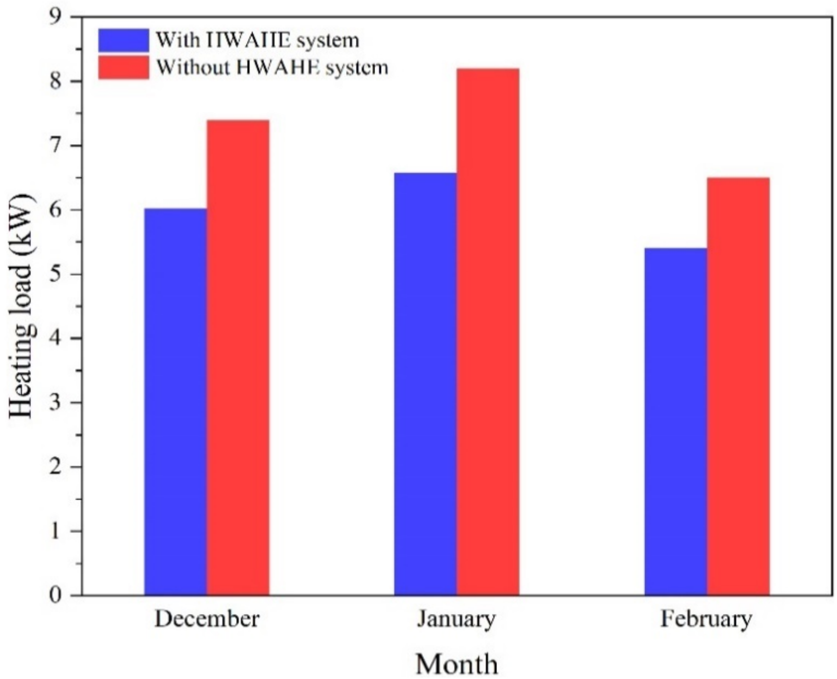


Figure VI.19: Heating load during winter months for the chosen home with and without the HWAHE system

Figure VI.20 shows the heating load reduction during the winter months when it is combined with the HWAHE system. It can be noticed an important reduction in energy use by utilizing the HWAHE system. It is also seen from this that the HWAHE system is very helpful in the winter months, where the reduction percentages are values of 18.67 %, 19.82 %, and 16.86 % for January, December, and February months, respectively.

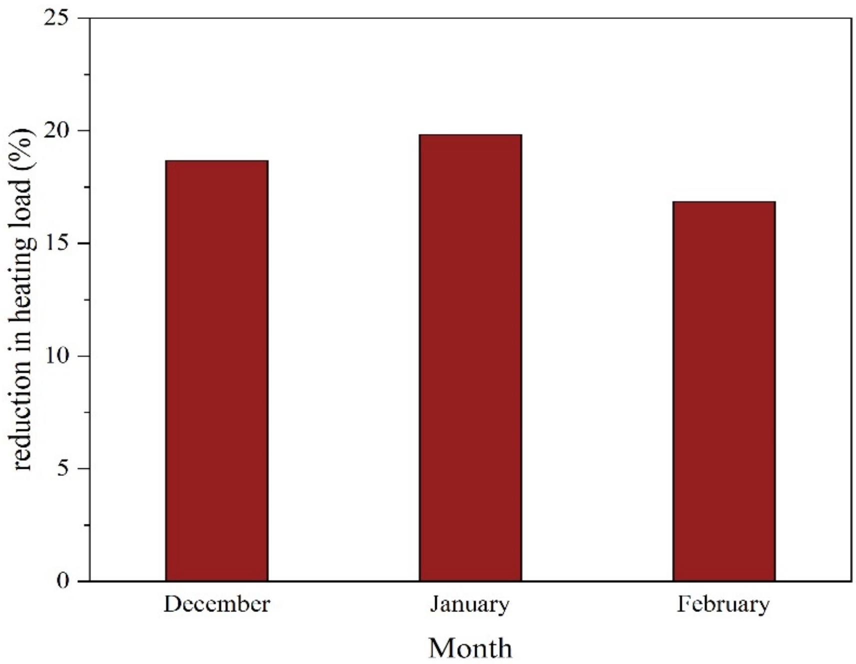


Figure VI.20: Reduction in heating load of the chosen home using the HWAHE system during winter season

Figure VI.21 shows the energy usage for heating the chosen house during the winter months, with and without the HWAHE system. It remarked that the maximum consumed electricity was in January for heating the chosen house. This figure also shows that there is a decrease in electricity usage when HWAHE is used during all the winter months, where usage decreased by 321.89, 378.81 and 255.13 kWh over the months of January, December and February, respectively.

The percentage of energy savings over the winter months using the HWAHE system is shown in figureVI.22. This figure presents that there is a benefit from the use of HWAHE as a passive heating system, where electricity consumption was reduced using the HWAHE system, leading to energy savings reaching a maximum value of 19.74% in January.

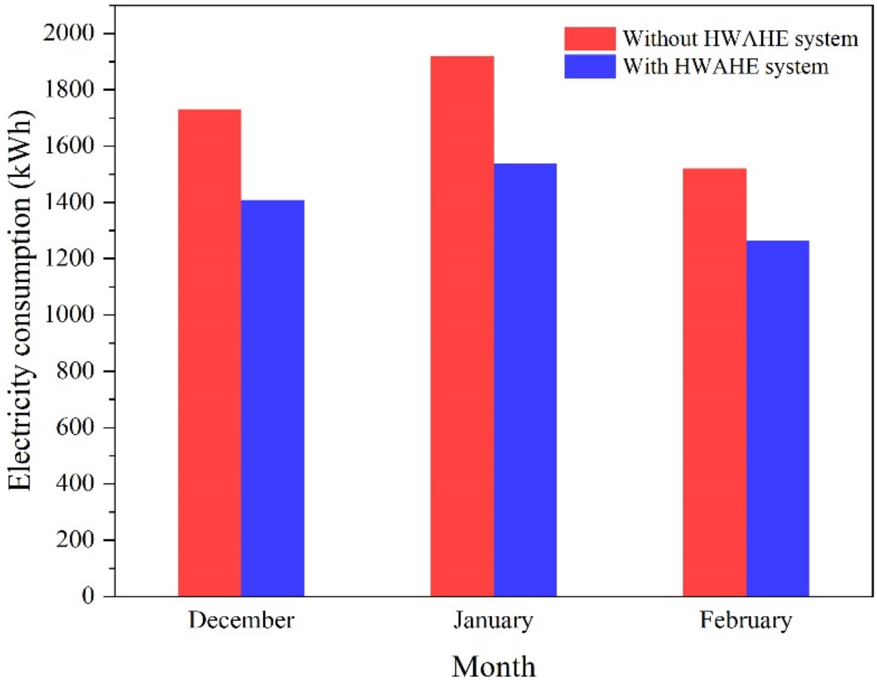


Figure VI.21: Electricity consumption for Heating of the chosen home with and without HWAHE system through winter months

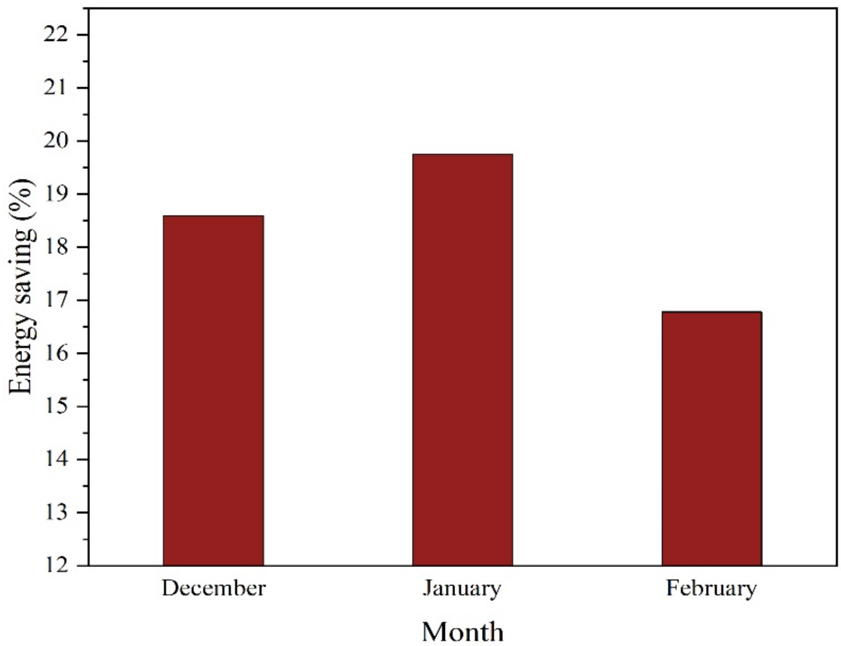


Figure VI.22: Energy saving occurs with using HWAHE system for heating the chosen home during the winter months

## VI.7 Cost saving

The cost saving by using HWAHE as the cooling and heating system is evaluated based on a space with 200 $m^2$. Electrical energy consumption cost for the cooling and heating of the indicated space, with and without the HWAHE system, is determined according to the prices of the Algerian Ministry of Electricity (ME).

Table VI.2 presents the overall cost of energy used for cooling and heating loads in the summer and winter months with and without the HWAHE system. This table shows that the maximum cost saving using the studied system has a range from 1.221,95 DZD (9.48 $) in May to 2.4761,06 DZD (19 $) in July. In addition, the total cost saving has been 14.614,15 DZD (113 $) during the summer and winter months.

From the total initial cost, the installation of the HWAHE system, which values 75700 DZD (587 $ ) the cost-saving of energy consumed for 1 year for both summer and winter months reached 14614 DZA (113$). with the payback time of HWAHE system is around 5 years.

## VI.8 Conclusion

The HWAHE system is used to minimize the energy usage of cooling and heating homes by adding to the method. This chapter presents a modelling inquiry into the reduction of the cooling and heating energy consumption of a specific house coupled with the HWAHE device under the design conditions of the South-East Algerian city of EL Oued. The following can be inferred from the findings:

In the summer season, the maximum decrease in cooling load for a chosen build using the HWAHE system reached 15.53 %. The maximum reduction in heating load was reported at 19.89 % in during the winter season.

The total electricity demand for cooling and heating of the chosen house decreases with the HWAHE method, so energy savings reached a maximum value of 15.45 % in the summer of August and 19.70 % in the winter of January.

The gross total savings of energy consumed for 1 year for both summer and winter months reached 14614.158 DZD (113 $) with an expected payback period of approximately

Table VI.2: The total cost of the consumed electricity with an without the HWAHE system

| **Month** | **Cost without HWAHE** (DZD) | **Cost with HWAHE** (DZD) | **Saving cost** (DZD) | **Saving cost, $** |
|---|---|---|---|---|
| **May** | 9514.798 | 8292.846 | 1221.952 | 9.484 |
| **June** | 14001.839 | 12096.704 | 1905.135 | 14.786 |
| **July** | 14899.247 | 12423.142 | 2476.106 | 19.217 |
| **August** | 17976.076 | 15715.246 | 2260.830 | 17.546 |
| **September** | 11835.239 | 10322.935 | 1512.305 | 11.737 |
| **December** | 8360.987 | 6597.144 | 1763.843 | 13.689 |
| **January** | 9386.596 | 7310.660 | 2075.937 | 16.111 |
| **February** | 7207.176 | 5809.127 | 1398.050 | 10.850 |
| **All month ($)** | 93181.962 | 78567.804 | 14614.158 | 113.420 |

5 years.

# General conclusion

This present work aims to establish technical and economic feasibility of installing a geothermal heat exchanger, it also aims to examine the thermal and energy performance of an air-to-water heat exchanger(HWAHE) used for building cooling. This exchanger consists of a PVC tube submerged at 5m depth in the water well and it is operated under the climatic conditions of the El Oued region.

First, general culture study a accompanied by bibliographical research paper on the extraction of energy from the ground by geothermal systems on the various passive cooling or heating techniques carriedout. geothermal heat exchangers are exhibited. Also, the effect of thermo-physical parameters of soil, thermal and flow parameters of air, geometrical and material properties of pipe, different modes of operation on the performance of earth air tunnel heat exchanger systems have been critically reviewed.

Done the system's thermal modeling. For this, a thermal model based on a semi-infinite medium model, subjected to determine the temperature at the depth of the soil and at the surface has been developed, In this model, an analysis of the Fourier series was implemented that allowed us to obtain a harmonic model for the temperature at soil depth. Three types of soil, namely clay, sandy clay loam, and sand, were also studied. The obtained results show us that, because of its high thermal inertia, the sandy soil is most suitable for cooling applications by air-soil exchangers.

An experimental characterization of the immersed in water well exchanger was carried out,followed by a parametric study and is completed by the development and validation of an analytical model.

This allowed us to draw conclusions as follows:

- The thermal potential of the HWAHE system in the EL Oued area enables the immersed helical vertical heat exchanger to be useful in buildings and agricultural greenhouses or dwellings of farmers in the considered region;

- Indeed, the variation in the temperature of the water well shows that in May, at a depth of 5m, it is less than that of the outside air by 14 $^oC$;
- The maximum obtained temperature gap between the inlet and the outlet of the HWAHE is of 14.1 $^oC$ with 0.035 $kg.s^{-1}$ of mass flow rate;
- The analytical study of the exchanger showed a high concordance with those experimental;
- Energy and exergy efficiency decrease as a function of the mass flow rate for immerged exchangers;
- The maximum reduction in cooling load for a selected home using the HWAHE system reached 15.54 % in July of the summer season, while in the winter season the maximum reduction in heating load was recorded at 19.89 % in January;
- With the HWAHE system, the total required electricity for cooling and heating the selected home decreases, therefore, the saving in energy reached the maximum value of 15.45 % at July in the summer and 19.72 % through January in the winter;
- The gross cost savings of energy consumed for 1 year for both summer and winter months reached 14614.158 DZA (113$) with an expected payback period of approximately 5 years.

# Bibliography

[1] BP. Bp statistical review of world energy. Report, 2019.

[2] MEM. Bilan énergétique national de l'année 2018. Report, 2018.

[3] Bulletin des énergies renouvelables. Report, centre des énergies renouvelables CDER,Algérie, 2011.

[4] F Al-Ajmi, DL Loveday, and Victor Ian Hanby. The cooling potential of earthair heat exchangers for domestic buildings in a desert climate. *Building Environment*, 41(3):235–244, 2006.

[5] Mohammed Benhammou and Belkacem Draoui. Parametric study on thermal performance of earth-to-air heat exchanger used for cooling of buildings. *Renewable and Sustainable Energy Reviews*, 44:348–355, 2015.

[6] Hassen Boughanmi, Mariem Lazaar, Abdelhamid Farhat, and Amenallah Guizani. Evaluation of soil thermal potential under tunisian climate using a new conic basket geothermal heat exchanger: Energy and exergy analysis. *Applied Thermal Engineering*, 113:912–925, 2017.

[7] Fuxin Niu, Yuebin Yu, Daihong Yu, and Haorong Li. Heat and mass transfer performance analysis and cooling capacity prediction of earth to air heat exchanger. *Applied Energy*, 137:211–221, 2015.

[8] Djamel Belatrache, Saïd Bentouba, and Mahmoud Bourouis. Numerical analysis of earth air heat exchangers at operating conditions in arid climates. *International journal of hydrogen energy*, 42(13):8898–8904, 2017.

[9] J Xamán, I Hernández-Pérez, J Arce, G Álvarez, L Ramírez-Dávila, and F Noh-Pat. Numerical study of earth-to-air heat exchanger: The effect of thermal insulation. *Energy and buildings*, 85:356–361, 2014.

[10] MEM. Bilan énergétique national de l'année 2019. Report, 2019.

[11] IEA. A key world energy statistic. Report, 2019.

[12] PRB. World population data sheet. Report, 2019.

[13] MEM. Bilan énergétique national de l'année 2017. Report, 2017.

[14] MEM. Bilan énergétique national de l'année 2008. Report, 2008.

[15] MEM. Bilan énergétique national de l'année 2009. Report, 2009.

[16] MEM. Bilan énergétique national de l'année 2010. Report, 2010.

[17] MEM. Bilan énergétique national de l'année 2011. Report, 2011.

[18] MEM. Bilan énergétique national de l'année 2012. Report, 2012.

[19] MEM. Bilan énergétique national de l'année 2013. Report, 2013.

[20] MEM. Bilan énergétique national de l'année 2014. Report, 2014.

[21] MEM. Bilan énergétique national de l'année 2015. Report, 2015.

[22] MEM. Bilan énergétique national de l'année 2016. Report, 2016.

[23] Amina Ouled-Henia. *Choix climatiques et construction. Zones arides et semi arides. Maison à Bou-Saada.* Thesis, 2003.

[24] D Medjelekh. *Impact de linertie thermique sur le confort hygrothermique et la consommation énergétique du bâtiment cas de lhabitation de lépoque coloniale à Guelma.* Thesis, 2006.

[25] Algerian national weather office.

[26] D Medjelekh. Impact de linertie thermique sur le confort hygrothermique et la consommation énergétique du bâtiment cas de lhabitation de lépoque coloniale à guelma. *Mémoire magister. option: Architecture Bioclimatique. Université Mentouri de Constantine*, 2006.

[27] Joseph Kestin. *Sourcebook on the production of electricity from geothermal energy.* US Department of Energy, 1980.

[28] Leyla Ozgener, Arif Hepbasli, Ibrahim Dincer, and Marc A. Rosen. Exergoeconomic analysis of geothermal district heating systems: A case study. *Applied Thermal Engineering*, 27(8-9):1303–1310, 2007.

[29] John E Mock, Jefferson W Tester, P Michael Wright, and the Environment. Geothermal energy from the earth: its potential impact as an environmentally sustainable resource. *Annual review of Energy*, 22(1):305–356, 1997.

[30] Alger EPAU and Mr SEMAHI Samir. Contribution méthodologique a la conception des logements à haute performance énergétique (hpe) en algérie. 2013.

[31] April 2017.

[32] Abderrahmane Gouareh, Noureddine Settou, Ali Khalfi, Bakhta Recioui, Belkhir Negrou, Soumia Rahmouni, and Boubekeur Dokkar. Gis-based analysis of hydrogen production from geothermal electricity using co2 as working fluid in algeria. *nternational journal of hydrogen energy*, 40(44):15244–15253, 2015.

[33] Michel A Bernier. Uncertainty in the design length calculation for vertical ground heat exchangers/discussion. *Ashrae Transactions*, 108:939, 2002.

[34] Principes de fonctionnement et usages de la géothermie. Report, Juin 2012.

[35] Xavier Moch. *Etude théorique et expérimentale d'échangeurs géothermiques hélicoïdaux: Production de chaud et de froid par pompe à chaleur, et dimensionnement d'installations.* PhD thesis, 2013.

[36] Leyla Ozgener. A review on the experimental and analytical analysis of earth to air heat exchanger (eahe) systems in turkey. *Renewable sustainable energy reviews*, 15(9):4483–4490, 2011.

[37] Kamal Kumar Agrawal, Ghanshyam Das Agrawal, Rohit Misra, Mayank Bhardwaj, and Doraj Kamal Jamuwa. A review on effect of geometrical, flow and soil properties on the performance of earth air tunnel heat exchanger. *Energy Buildings*, 176:120–138, 2018.

[38] Jagjeet Kaur, Prem Singh, and Harminder Kaur. A review on the experimental and analytical analysis of earth air tunnel heat exchanger system. *Environmental Sustainability: Concepts, Principles, Evidences Innovations*, pages 116–120, 2015.

[39] Jaskiran Sobti and Sanjay Kumar Singh. Earth-air heat exchanger as a green retrofit for chandgarha critical review. *Geothermal Energy*, 3(1):1–9, 2015.

[40] Viorel Badescu. Simple and accurate model for the ground heat exchanger of a passive house. *Renewable energy*, 32(5):845–855, 2007.

[41] Panayiotis D. Pouloupatis, Savvas A. Tassou, Paul Christodoulides, and Georgios A. Florides. Parametric analysis of the factors affecting the efficiency of ground heat exchangers and design application aspects in cyprus. *Renewable Energy*, 103:721–728, 2016.

[42] Benjamin David Philip Hepburn. *An investigation of the behaviour of the ground in response to energy extraction.* Thesis, 2013.

[43] Yousef Belloufi, Abdelhafid Brima, Sakina Zerouali, Rachid Atmani, Faris Aissaoui, Amar Rouag, and Noureddine Moummi. Numerical and experimental investigation on the transient behavior of an earth air heat exchanger in continuous operation mode. *International Journal of Heat Technology*, 35(2):279–288, 2017.

[44] Pierre Hollmuller. *Utilisation des échangeurs air/sol pour le chauffage et le rafraîchissement des bâtiments.* Thesis, 2002.

[45] Abdelmalek Atia, Abdessamia Hadjadj, Boubaker Benhaoua, Nacer Lebbihiat, and Abdelhafid Brima. A review of studies on geothermal energy system applied on sub-saharan climate regions. *Water and Energy International*, 60(5):63–68, 2017.

[46] Chiew Shan Anthony Chong, Guohui Gan, Anne Verhoef, Raquel Gonzalez Garcia, and Pier Luigi Vidale. Simulation of thermal performance of horizontal slinky-loop heat exchangers for ground source heat pumps. *Applied Energy*, 104:603–610, 2013.

[47] Nesrine Hatraf, Foued Chabane, Abdelhafid Brima, Noureddine Moummi, and Abdelhafid Moummi. Parametric study of to design an earth to air heat exchanger with experimental validation. *Engineering Journal*, 18(2):41–54, 2014.

[48] Hassen Boughanmi, Mariem Lazaar, Salwa Bouadila, and Abdelhamid Farhat. Thermal performance of a conic basket heat exchanger coupled to a geothermal heat pump for greenhouse cooling under tunisian climate. *Energy Buildings*, 104:87–96, 2015.

[49] M. Saadeddine. *Identification et analyse des principaux facteurs influant le comportement thermique dun échangeur air/sol enterré.* Thesis, 2013.

[50] S. F. Ahmed, M. T. O. Amanullah, M. M. K. Khan, M. G. Rasul, and N. M. S. Hassan. Parametric study on thermal performance of horizontal earth pipe cooling system in summer. *Energy Conversion and Management*, 114:324–337, 2016.

[51] Zhengxuan Liu, Zhun Jerry Yu, Tingting Yang, Letizia Roccamena, Pengcheng Sun, Shuisheng Li, Guoqiang Zhang, and Mohamed El Mankibi. Numerical modeling and parametric study of a vertical earth-to-air heat exchanger system. *Energy*, 172:220–231, 2019.

[52] Rohit Misra, Abhishek Agarwal, Vikas Bansal, and Doraj Kamal Jamuwa. Cfd simulation of earth air tunnel heat exchanger system in continuous and intermittent operation modes during winter season. *International Journal of Engineering Technology, Management and Applied Sciences*, 5(3):2349–4476, 2017.

[53] Vikas Bansal, Rohit Misra, Ghanshyam Das Agrawal, and Jyotirmay Mathur. Performance analysis of earthpipeair heat exchanger for summer cooling. *Energy Buildings*, 42(5):645–648, 2010.

[54] Sayeh Menhoudj, Mohamed-Hichem Benzaama, Chadi Maalouf, Mohamed Lachi, and Mohammed Makhlouf. Study of the energy performance of an earthair heat exchanger for refreshing buildings in algeria. *Energy Buildings*, 158:1602–1612, 2018.

[55] Nabiha Naili, Majdi Hazami, Issam Attar, and Abdelhamid Farhat. In-field performance analysis of ground source cooling system with horizontal ground heat exchanger in tunisia. *Energy*, 61:319–331, 2013.

[56] N Moummi, H Benfatah, N Hatraf, A Moummi, and S Youcef Ali. Le rafraîchissement par la géothermie: étude théorique et expérimentale dans le site de biskra. *Revue des Energies Renouvelables*, 13(3):399–406, 2010.

[57] B Draoui, B Mebarki, S Abdessemed, A Keboucha, S Drici, and A Sahli. Etude dun système de climatisation intégrant un puits canadien dans les zones arides, cas de béchar. *Revue des Energies Renouvelables*, 2015.

[58] Rakesh Kumar, SC Kaushik, and SN Garg. Heating and cooling potential of an earth-to-air heat exchanger using artificial neural network. *Renewable Energy*, 31(8):1139–1155, 2006.

[59] Nabil AS Elminshawy, Farooq R Siddiqui, Qazi U Farooq, and Mohammad F Addas. Experimental investigation on the performance of earth-air pipe heat exchanger for different soil compaction levels. *Applied Thermal Engineering*, 124:1319–1327, 2017.

[60] Fuxin Niu, Yuebin Yu, Daihong Yu, and Haorong Li. Heat and mass transfer performance analysis and cooling capacity prediction of earth to air heat exchanger. *Applied Energy*, 137:211–221, 2015.

[61] Zhongjian Li, Weifeng Zhu, Tian Bai, and Maoyu Zheng. Experimental study of a ground sink direct cooling system in cold areas. *Energy Buildings*, 41(11):1233–1237, 2009.

[62] Czeslaw Oleskowicz Popiel, Janusz Wojtkowiak, and Beata Biernacka. Measurements of temperature distribution in ground. *Experimental thermal fluid science*, 25(5):301–309, 2001.

[63] G. Mihalakakou, M. Santamouris, and D. Asimakopoulos. Modelling the thermal performance of earth-to-air heat exchangers. *Solar Energy*, 53(3):301–305, 1994.

[64] G. Mihalakakou, J. O. Lewis, and M. Santamouris. The influence of different ground covers on the heating potential of earth-to-air heat exchangers. *Renewable Energy*, 7(1):33–46, 1996.

[65] Vikas Bansal, Rohit Misra, Ghanshyam Das Agrawal, and Jyotirmay Mathur. Performance analysis of earthpipeair heat exchanger for winter heating. *Energy and Buildings*, 41(11):1151–1154, 2009.

[66] V. P. Kabashnikov, L. N. Danilevskii, V. P. Nekrasov, and I. P. Vityaz. Analytical and numerical investigation of the characteristics of a soil heat exchanger for ventilation systems. *International Journal of Heat and Mass Transfer*, 45(11):2407–2418, 2002.

[67] Ahmed A Serageldin, Ali K Abdelrahman, and Shinichi Ookawara. Earth-air heat exchanger thermal performance in egyptian conditions: Experimental results, mathematical model, and computational fluid dynamics simulation. *Energy conversion management*, 122:25–38, 2016.

[68] S Barakat, Ahmed Ramzy, AM Hamed, and SH El Emam. Enhancement of gas turbine power output using earth to air heat exchanger (eahe) cooling system. *Energy conversion management*, 111:137–146, 2016.

[69] Abdessamia Hadjadj, Boubaker Benhaoua, Abdelmalek Atia, Abderrahmane Khechekhouche, Nacer Lebbihiat, and Amar Rouag. Air velocity effect on geothermal helicoidally water-air heat exchanger under el oued climate -algeria. *Thermal Science and Engineering Progress*, page 100548, 2020.

[70] Sanjeev Jakhar, MS Soni, and Nikhil Gakkhar. Performance analysis of earth water heat exchanger for concentrating photovoltaic cooling. *Energy Procedia*, 90:145–153, 2016.

[71] G. Mihalakakou, M. Santamouris, and D. Asimakopoulos. Modelling the thermal performance of earth-to-air heat exchangers. *Solar Energy*, 53(3):301–305, 1994.

[72] Fuxin Niu, Yuebin Yu, Daihong Yu, and Haorong Li. Heat and mass transfer performance analysis and cooling capacity prediction of earth to air heat exchanger. *Applied Energy*, 137:211–221, 2015.

[73] Vikas Bansal, Rohit Misra, Ghanshyam Das Agrawal, and Jyotirmay Mathur. Performance analysis of earth–pipe–air heat exchanger for winter heating. *Energy and Buildings*, 41(11):1151–1154, 2009.

[74] Shams Forruque Ahmed, Mohammad Masud Kamal Khan, MTO Amanullah, MG Rasul, and NMS Hassan. Performance assessment of earth pipe cooling system for low energy buildings in a subtropical climate. *Energy conversion and management*, 106:815–825, 2015.

[75] J. Xamán, I. Hernández-Pérez, J. Arce, G. Álvarez, L. Ramírez-Dávila, and F. Noh-Pat. Numerical study of earth-to-air heat exchanger: The effect of thermal insulation. *Energy and Buildings*, 85:356–361, 2014.

[76] Yuebin Yu, Haorong Li, Fuxin Niu, and Daihong Yu. Investigation of a coupled geothermal cooling system with earth tube and solar chimney. *Applied Energy*, 114:209–217, 2014.

[77] F Chlela, A Husaunndee, P Riederer, and Christian Inard. Numerical evaluation of earth to air heat exchangers and heat recovery ventilation systems. *International Journal of Ventilation*, 6(1):31–42, 2007.

[78] Sanjeev Jakhar, Rohit Misra, Vikas Bansal, and MS Soni. Thermal performance investigation of earth air tunnel heat exchanger coupled with a solar air heating duct for northwestern india. *Energy Buildings*, 87:360–369, 2015.

[79] Anil Kumar Misra, Mayank Gupta, Manish Lather, and Himanshu Garg. Design and performance evaluation of low cost earth to air heat exchanger model suitable for small buildings in arid and semi arid regions. *KSCE Journal of Civil Engineering*, 19(4):853–856, 2015.

[80] Kamal Kumar Agrawal, Rohit Misra, Ghanshyam Das Agrawal, Mayank Bhardwaj, and Doraj Kamal Jamuwa. Effect of different design aspects of pipe for earth air tunnel heat exchanger system: A state of art. *International Journal of Green Energy*, 16(8):598–614, 2019.

[81] Trilok Singh Bisoniya. Design of earth–air heat exchanger system. *Geothermal Energy*, 3(1):18, 2015.

[82] VP Kabashnikov, LN Danilevskii, VP Nekrasov, and IP Vityaz. Analytical and numerical investigation of the characteristics of a soil heat exchanger for ventilation systems. *International Journal of Heat and Mass Transfer*, 45(11):2407–2418, 2002.

[83] Genyr Kappler, João Batista Dias, Fernanda Haeberle, Paulo Roberto Wander, Carlos Alberto Mendes Moraes, and Regina Célia Espinosa Modolo. Study of an earth-to-water heat exchange system which relies on underground water tanks. *Renewable Energy*, 133:1236–1246, 2019.

[84] Kwang Ho Lee and Richard K Strand. The cooling and heating potential of an earth tube system in buildings. *Energy and Buildings*, 40(4):486–494, 2008.

[85] H Ben Jmaa Derbel and O Kanoun. Investigation of the ground thermal potential in tunisia focused towards heating and cooling applications. *Applied thermal engineering*, 30(10):1091–1100, 2010.

[86] Ahmed A Serageldin, Ali K Abdelrahman, and Shinichi Ookawara. Earth-air heat exchanger thermal performance in egyptian conditions: Experimental results, mathematical model, and computational fluid dynamics simulation. *Energy conversion and management*, 122:25–38, 2016.

[87] S Barakat, Ahmed Ramzy, AM Hamed, and SH El Emam. Enhancement of gas turbine power output using earth to air heat exchanger (eahe) cooling system. *Energy conversion and management*, 111:137–146, 2016.

[88] M. K. Ghosal and G. N. Tiwari. Modeling and parametric studies for thermal performance of an earth to air heat exchanger integrated with a greenhouse. *Energy Conversion and Management*, 47(13-14):1779–1798, 2006.

[89] M Benhammou, B Draoui, M Zerrouki, and Y Marif. Performance analysis of an earth-to-air heat exchanger assisted by a wind tower for passive cooling of buildings in arid and hot climate. *Energy conversion and management*, 91:1–11, 2015.

[90] Noor Aziah Mohd Ariffin, Aliyah Nur Zafirah Sanusi, Aminuddin Mohd Noor, et al. Materials for the earth air pipe heat exchanger (eaphe) system as a passive cooling technology for hot-humid climate. *Abstract of Emerging Trends in Scientific Research*, 2:1–19, 2014.

[91] M Bojic, N Trifunovic, G Papadakis, and S Kyritsis. Numerical simulation, technical and economic evaluation of air-to-earth heat exchanger coupled to a building. *Energy*, 22(12):1151–1158, 1997.

[92] Sanjeev Jakhar, Rohit Misra, MS Soni, and Nikhil Gakkhar. Parametric simulation and experimental analysis of earth air heat exchanger with solar air heating duct. *Engineering Science Technology, an International Journal*, 19(2):1059–1066, 2016.

[93] Anuj Mathur, Ayushman Srivastava, Jyotirmay Mathur, Sanjay Mathur, and GD Agrawal. Transient effect of soil thermal diffusivity on performance of eathe system. *Energy Reports*, 1:17–21, 2015.

[94] Ruth da Silva Brum, Joaquim Vaz, Luiz Alberto Oliveira Rocha, Elizaldo Domingues dos Santos, and Liércio André Isoldi. A new computational modeling to predict the behavior of earth-air heat exchangers. *Energy and Buildings*, 64:395–402, 2013.

[95] Anuj Mathur, Sanjay Mathur, GD Agrawal, and Jyotirmay Mathur. Comparative study of straight and spiral earth air tunnel heat exchanger system operated in cooling and heating modes. *Renewable Energy*, 108:474–487, 2017.

[96] Anuj Mathur, Ankit Kumar Surana, Poonam Verma, Sanjay Mathur, GD Agrawal, and Jyotirmay Mathur. Investigation of soil thermal saturation and recovery under intermittent and continuous operation of eathe. *Energy Buildings*, 109:291–303, 2015.

[97] Alexandre de Jesus Freire, José Luís Coelho Alexandre, Valter Bruno Silva, Nuno Dinis Couto, and Abel Rouboa. Compact buried pipes system analysis for indoor air conditioning. *Applied Thermal Engineering*, 51(1-2):1124–1134, 2013.

[98] Angui Li, Changqing Yang, and Tong Ren. Modeling and parametric studies for convective heat transfer in large, long and rough circular cross-sectional underground tunnels. *Energy and Buildings*, 127:259–267, 2016.

[99] Michel De Paepe and Arnold Janssens. Thermo-hydraulic design of earth-air heat exchangers. *Energy and buildings*, 35(4):389–397, 2003.

[100] F Al-Ajmi, DL Loveday, and Victor Ian Hanby. The cooling potential of earth–air heat exchangers for domestic buildings in a desert climate. *Building and Environment*, 41(3):235–244, 2006.

[101] Charaf-Eddine Mehdid, Adel Benchabane, Amar Rouag, Noureddine Moummi, Mohammed-Amin Melhegueg, Abdelhafid Moummi, Mohamed-Larbi Benabdi, and Abdelhafid Brima. Thermal design of earth-to-air heat exchanger. part ii a new transient semi-analytical model and experimental validation for estimating air temperature. *Journal of Cleaner Production*, 198:1536–1544, 2018.

[102] H. Ben Jmaa Derbel and O. Kanoun. Investigation of the ground thermal potential in tunisia focused towards heating and cooling applications. *Applied Thermal Engineering*, 30(10):1091–1100, 2010.

[103] Yousef Belloufi, Abdelhafid Brima, Sakina Zerouali, Rachid Atmani, Faris Aissaoui, Amar Rouag, and Noureddine Moummi. Numerical and experimental investigation

on the transient behavior of an earth air heat exchanger in continuous operation mode. *International Journal of Heat and Technology*, 35(2):279–288, 2017.

[104] Jens Pfafferott. Evaluation of earth-to-air heat exchangers with a standardised method to calculate energy efficiency. *Energy and buildings*, 35(10):971–983, 2003.

[105] Nabiha Naili, Majdi Hazami, Sami Kooli, and Abdelhamid Farhat. Energy and exergy analysis of horizontal ground heat exchanger for hot climatic condition of northern tunisia. *Geothermics*, 53:270–280, 2015.

[106] IE IdelCik. *Mémento des Pertes de Charges: Coefficients de Pertes de Charges Singulières et de Pertes de Charge par Frottement Traduit par M.* Meury Editions Eyrolles, Saint-Germain, Paris, 1986.

[107] Narendra Singh, SC Kaushik, and RD Misra. Exergetic analysis of a solar thermal power system. *Renewable energy*, 19(1-2):135–143, 2000.

[108] Rohit Misra, Sanjeev Jakhar, Kamal Kumar Agrawal, Shailendra Sharma, Doraj Kamal Jamuwa, Manoj S Soni, and Ghanshyam Das Agrawal. Field investigations to determine the thermal performance of earth air tunnel heat exchanger with dry and wet soil: energy and exergetic analysis. *Energy and Buildings*, 171:107–115, 2018.

[109] Mokhtar Ghodbane, Boussad Boumeddane, Zafar Said, and Evangelos Bellos. A numerical simulation of a linear fresnel solar reflector directed to produce steam for the power plant. *Journal of cleaner production*, 231:494–508, 2019.

[110] Mushtaq I Hasan and Sajad W Noori. A study of the potential of using the earth to air heat exchanger for cooling and heating of residential buildings in iraq. *Heat TransferAsian Research*, 48(8):3902–3927, 2019.

[111] Mushtaq I Hasan, Abdul A Rageb, M Yaghoubi, and Homayon Homayoni. Influence of channel geometry on the performance of a counter flow microchannel heat exchanger. *International Journal of Thermal Sciences*, 48(8):1607–1618, 2009.

# Appendix

## Appendix A

**Approximate conversion factors**

1 metric tonne = 2204.62 lb.

= 1.1023 short tons

1 kilolitre = 6.2898 barrels

1 kilolitre = 1 cubic metre

1 kilocalorie (kcal) = 4.1868 kJ = 3.968 Btu

1 kilojoule (kJ) = 1,000 joules = 0.239 kcal = 0.948 Btu

1 petajoule (PJ) = 1 quadrillion joules (1 x $10^{15}$)

1 exajoule (EJ) = 1 quintillion joules (1 x $10^{18}$)

1 British thermal unit (Btu) = 0.252 kcal = 1.055 kJ

1 barrel of oil equivalent (boe) = 5.8 million Btu = 6.119 million kJ

1 kilowatt-hour (kWh) = 860 kcal = 3600 kJ = 3412 Btu

**climatic data for the El-Oued region**

Interpretation of climatic data for the El-Oued region (2008-20018)

| **Month** | **Wind** $(m.s^{-1})$ | **Tamb minimal** $(^oC)$ | **Tamb maximal** $(^oC)$ | **Tamb mean** $(^oC)$ | **Humidity %** | **Precipitation (mm)** | **Evaporation (mm)** | **Sunhours period (Hours)** |
|---|---|---|---|---|---|---|---|---|
| **Jan** | 1.6 | 5.42 | 18.16 | 11.75 | 63 | 12.18 | 110 | 263 |
| **Feb** | 2 | 6.52 | 19.66 | 13.08 | 48.5 | 6.65 | 150 | 229 |
| **Mar** | 3.6 | 10.47 | 24.05 | 17.26 | 38 | 8.82 | 165 | 256 |
| **Abr** | 4.3 | 14.77 | 29.02 | 21.93 | 29.4 | 10.24 | 206 | 240 |
| **May** | 4.4 | 19.08 | 33.48 | 26.3 | 27 | 1.23 | 200 | 223 |
| **Jun** | 4.2 | 23.75 | 38.23 | 30.95 | 25.8 | 0.57 | 290 | 337 |
| **Jul** | 4.1 | 27.14 | 42.19 | 34.71 | 24 | 0.18 | 330 | 365 |
| **Aug** | 2.5 | 26.67 | 40.72 | 33.7 | 32.5 | 0.85 | 312 | 351 |
| **Sep** | 2.6 | 23.2 | 36.12 | 29.95 | 40.6 | 8.59 | 220 | 244 |
| **Oct** | 2.7 | 14.85 | 30.32 | 22.6 | 57 | 3.82 | 190 | 196 |
| **Nov** | 2.6 | 10.54 | 23.32 | 16.92 | 60.2 | 5.24 | 139 | 239 |
| **Dec** | 2.2 | 5.92 | 18.57 | 12.21 | 69 | 2.14 | 105 | 222 |

# Appendix B


| **Type de capteur** | **Hélice** |
|---|---|
| Plage de mesure | 0.6 ... 40 m/s |
| Précision<br>± 1 digit | ± (0.2 m/s +1.5% v.m.) |
| Résolution | 0.1 m/s |
| **Caractéristiques techniques générales** | |
| Temp. de service | -20 ... +50 °C |
| Temp. de stockage | -40 ... +70 °C |
| Type de piles | Bloc 9V, 6F22 |
| Autonomie | 80 h |
| Dimensions | 182 x 64 x 40 mm |
| Poids | 325 g |
| Matériau du boîtier | ABS |

Data sheet Testo 416

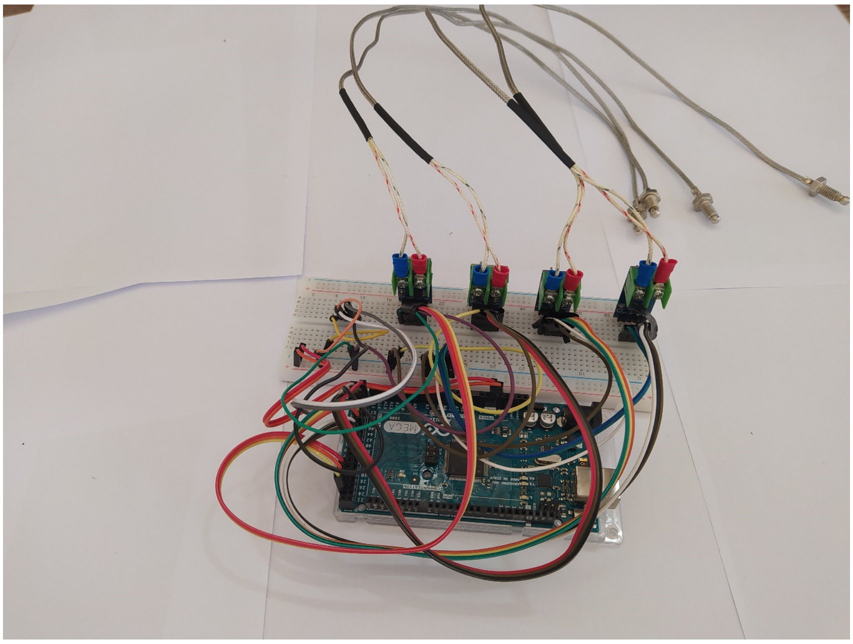

Ardouino

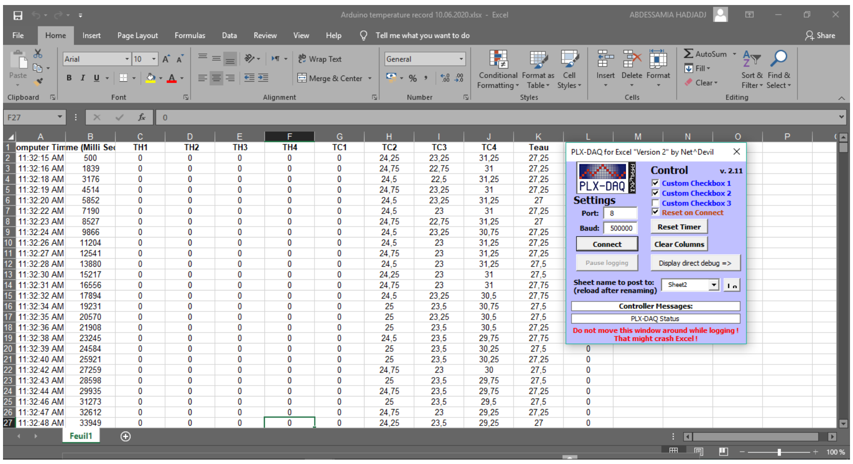

| | A | B | C | D | E | F | G | H | I | J | K | L |
|---|---|---|---|---|---|---|---|---|---|---|---|---|
| 1 | omputer Timme (Milli Sec | | TH1 | TH2 | TH3 | TH4 | TC1 | TC2 | TC3 | TC4 | Teau | |
| 2 | 11:32:15 AM | 500 | 0 | 0 | 0 | 0 | 0 | 24,25 | 23,25 | 31,25 | 27,25 | |
| 3 | 11:32:16 AM | 1839 | 0 | 0 | 0 | 0 | 0 | 24,75 | 22,75 | 31 | 27,25 | |
| 4 | 11:32:18 AM | 3176 | 0 | 0 | 0 | 0 | 0 | 24,5 | 22,5 | 31,25 | 27,25 | |
| 5 | 11:32:19 AM | 4514 | 0 | 0 | 0 | 0 | 0 | 24,75 | 23,25 | 31 | 27,25 | |
| 6 | 11:32:20 AM | 5852 | 0 | 0 | 0 | 0 | 0 | 24,5 | 23,25 | 31,25 | 27 | |
| 7 | 11:32:22 AM | 7190 | 0 | 0 | 0 | 0 | 0 | 24,5 | 23 | 31 | 27,25 | |
| 8 | 11:32:23 AM | 8527 | 0 | 0 | 0 | 0 | 0 | 24,75 | 22,75 | 31,25 | 27 | |
| 9 | 11:32:24 AM | 9866 | 0 | 0 | 0 | 0 | 0 | 24,5 | 23,25 | 30,75 | 27,25 | |
| 10 | 11:32:26 AM | 11204 | 0 | 0 | 0 | 0 | 0 | 24,5 | 23 | 31,25 | 27,25 | |
| 11 | 11:32:27 AM | 12541 | 0 | 0 | 0 | 0 | 0 | 24,75 | 23 | 31,25 | 27,25 | |
| 12 | 11:32:28 AM | 13880 | 0 | 0 | 0 | 0 | 0 | 24,5 | 23 | 31,25 | 27,5 | |
| 13 | 11:32:30 AM | 15217 | 0 | 0 | 0 | 0 | 0 | 24,25 | 23 | 31 | 27,5 | |
| 14 | 11:32:31 AM | 16556 | 0 | 0 | 0 | 0 | 0 | 24,75 | 23 | 31 | 27,75 | |
| 15 | 11:32:32 AM | 17894 | 0 | 0 | 0 | 0 | 0 | 24,5 | 23,25 | 30,5 | 27,75 | |
| 16 | 11:32:34 AM | 19231 | 0 | 0 | 0 | 0 | 0 | 25 | 23,5 | 30,75 | 27,5 | |
| 17 | 11:32:35 AM | 20570 | 0 | 0 | 0 | 0 | 0 | 25 | 23,25 | 30,5 | 27,5 | |
| 18 | 11:32:36 AM | 21908 | 0 | 0 | 0 | 0 | 0 | 25 | 23,5 | 30,5 | 27,25 | |
| 19 | 11:32:38 AM | 23245 | 0 | 0 | 0 | 0 | 0 | 24,5 | 23,5 | 29,75 | 27,75 | |
| 20 | 11:32:39 AM | 24584 | 0 | 0 | 0 | 0 | 0 | 25 | 23,5 | 30,25 | 27,5 | 0 |
| 21 | 11:32:40 AM | 25921 | 0 | 0 | 0 | 0 | 0 | 25 | 23,5 | 30,25 | 27,25 | 0 |
| 22 | 11:32:42 AM | 27259 | 0 | 0 | 0 | 0 | 0 | 24,75 | 23 | 30 | 27,5 | 0 |
| 23 | 11:32:43 AM | 28598 | 0 | 0 | 0 | 0 | 0 | 25 | 23,5 | 29,75 | 27,5 | 0 |
| 24 | 11:32:44 AM | 29935 | 0 | 0 | 0 | 0 | 0 | 24,75 | 23,5 | 29,75 | 27,25 | 0 |
| 25 | 11:32:46 AM | 31273 | 0 | 0 | 0 | 0 | 0 | 25 | 23,5 | 29,5 | 27,5 | 0 |
| 26 | 11:32:47 AM | 32612 | 0 | 0 | 0 | 0 | 0 | 24,75 | 23 | 29,25 | 27,25 | 0 |
| 27 | 11:32:48 AM | 33949 | 0 | 0 | 0 | 0 | 0 | 24,25 | 23,5 | 29,25 | 27 | 0 |

Shows data results

# Appendix C

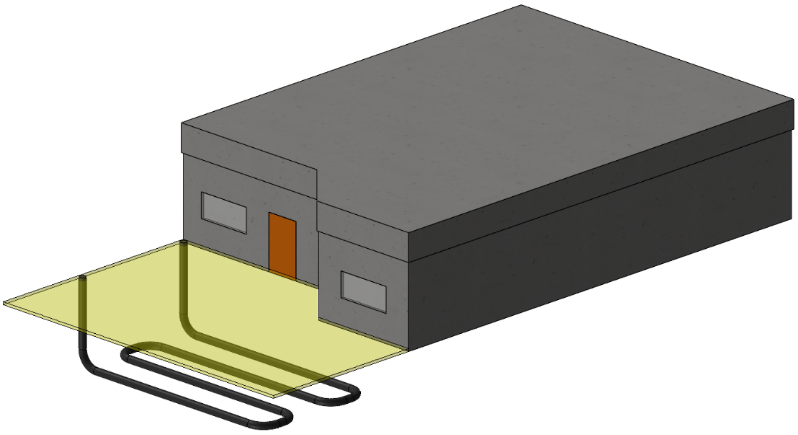

Systeme I

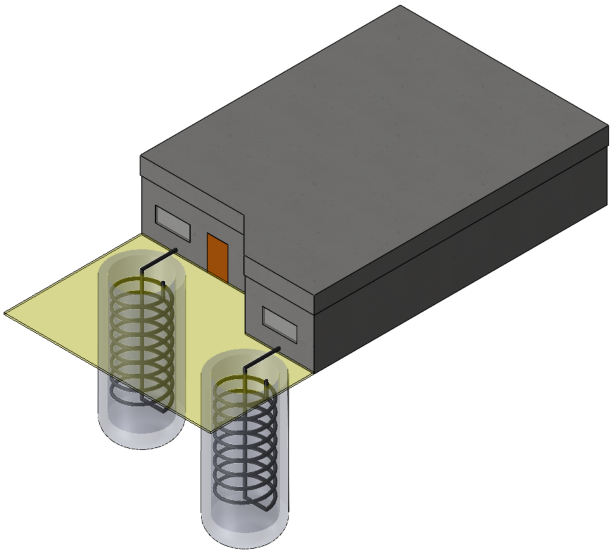

system II

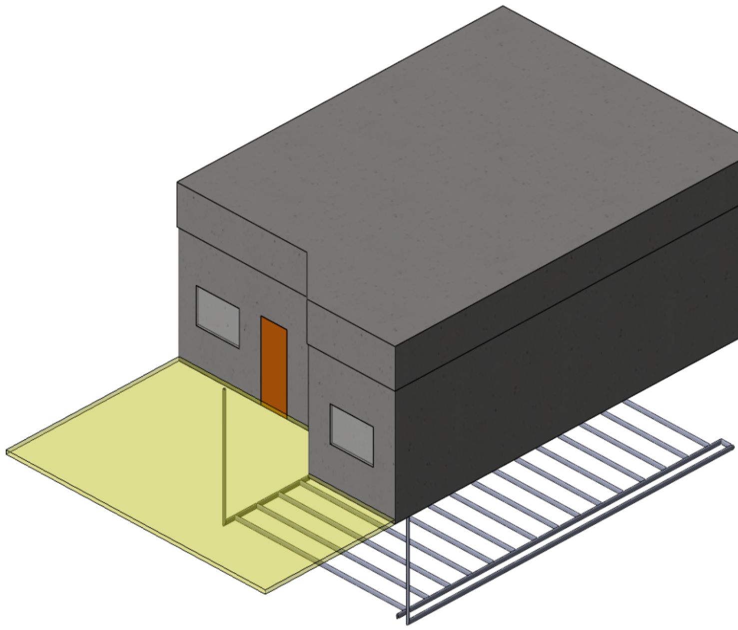

system III

# Abstract

In the present work of this thesis, experimentally and modeling investigations of the effect of mass flow rate on the performance of a Helicoidal Water Air Heat Exchanger (HWAHE) in the region of El-Oued (south-est of Algeria), were undergone. On the basis of the obtained results, an experimental study of the refreshing strategy (HWAHE) system in the El Oued region, it was shown that a great potential of the earth to air heat exchanger technique for buildings and agricultural greenhouses in arid regions preheating or precooling may be ensured.The HWAHE made of PVC piping with 30 m of length and 0.06 m of diameter was immersed into the bottom of a water well at 5 m depth. In addition, a theoretical model was developed to determine the evolution of the air temperature inside the HWAHE as function of the main operating parameters. It is found that the exchanger is mainly depending on the mass flow rate. As results, the maximum heat exchange reached nearly 418 W at 0.035 $kg.s^{-1}$ of mass flow rate while the maximum of temperature gap between the inlet and the outlet air was 14.1 $^oC$. The HWAHE efficiency decreased with the increase of the mass flow rate. The efficiency of heat exchanger was obtained to be 82%, 81% and 80% for the average velocity value of 0.035, 0.05 and 0.07 $kg.s^{-1}$, respectively. In addition, exergitical and economichal investigate were carried out. The HWAHE energy and exergy efficiencies are maximal, and they reach to 92% and 89%, respectively.

**Keywords:** Geothermal energy; Helicoidal Water Air Heat Exchanger; Energy and Exergetic analysis;Thermal performance; Energy saving.

# Résumé

Dans le présent travail de cette thèse, une étude expérimentale et modélisée de l'effet du débit massique sur les performances d'un échangeur de chaleur hélicoïdal eau-air (HWAHE : Helicoidal water-air heat exchanger) dans la région d'El-Oued (sud-est de l'Algérie), a été menée . Sur la base des résultats obtenus, une étude expérimentale de la stratégie de rafraîchissement du système (HWAHE) dans la région d'El Oued, il a été montré qu'un grand potentiel géothermie de la technique des échangeurs de chaleur terre-air pour le préchauffage ou le prérefroidissement des bâtiments et l'agriculture des serres dans les régions arides peuvent être assurés. Le HWAHE constitué de canalisations en PVC de 30 m de longueur et 0.06 m de diamètre a été immergé au fond d'un puits d'eau à 5 m de profondeur. De plus, un modèle théorique a été développé pour déterminer l'évolution de la température de l'air à l'intérieur du HWAHE en fonction des principaux paramètres de fonctionnement (débit massique et température). On constate que l'échangeur dépend principalement du débit massique. En conséquence, l'échange thermique, près de 418 W, maximal a atteint à 0.035 $kg.s^{-1}$ de débit dair tandis que l'écart de température maximal entre l'air d'entrée et celui de sortie était de 14,1$^oC$. L'efficacité de HWAHE diminue avec l'augmentation du débit massique. L'efficacité de l'échangeur de chaleur a été obtenue à 82%, 81% et 80% pour la valeur de débit dair moyenne de 0.035, 0.05 et 0.07 $kg.s^{-1}$, respectivement. En outre, des enquêtes éxergitiques et économiques ont été menées. Les rendements énergétiques et éxergétiques de HWAHE sont maximaux et atteignent respectivement 92% et 89%.

**Mots clés:** L'énergie géothermique; Echangeur de chaleur hélicoïdal eau-air; Analyse énergétique et exergétique; Performance thermique; Economie d'énergie.

**الملخص** :

في العمل الحالي لهذه الرسالة، أجريت دراسات تجريبية ونمذجة لتأثير التدفق الكتلي للهواء على أداء مبادل حراري حلزوني أرضي (Helicoidal water-air heat exchanger :HWAHE) في منطقة الواد (جنوب شرق الجزائر) . على أساس النتائج متحصل عليها ، دراسة تجريبية لاستراتيجية التجديد لنظام المبادل الحراري (HWAHE )في منطقة الوادي ، تبين أن هناك إمكانات كبيرة لتقنية هذا المبادل في التبريد والتسخين للمباني والزراعة. قد يتم ضمان التسخين المسبق أو التبريد المسبق في البيوت الزراعية في المناطق القاحلة. حيث يتم غمر HWAHE المصنوع من أنابيب PVC بطول 30 مترًا وقطرها 0.06 مترًا في قاع بئر ماء على عمق 5 أمتارللتأدية الغرض. بالإضافة إلى ذلك ، تم تطوير نموذج نظري لتحديد تطور درجة حرارة الهواء داخل HWAHE كدالة لمعلمات التشغيل الرئيسية. وجد أن المبادل يعتمد بشكل أساسي على معدل التدفق الشامل. ونتيجة لذلك ، بلغ الحد الأقصى للتبادل الحراري ما يقرب من 418 وات عند تدفق 0.035 كغ / ث من الهواء بينما كانت أقصى فجوة في درجة الحرارة بين مدخل ومخرج المبادل 14.1 درجة مئوية. انخفضت كفاءة HWAHE مع زيادة معدل التدفق الشامل. بلغت كفاءة المبادل الحراري 82٪ و 81٪ و 80٪ لمتوسط قيمة السرعة 0.035 و 0.05 و 0.07 كغ / ثانية على التوالي. بالإضافة إلى ذلك ، تم إجراء دراسة جدوى او تحقيق اقتصادي وتحليل طاقوي. حيث تعد كفاءات طاقة HWAHE وكفاءة الطاقة القصوى ، وتصل إلى 92٪ و 89٪ على التوالي.

**كلمات مفتاحية**: مبادل حراري, التبريد والتسخين, كفاءة المبادل الحراري, تحقيق اقتصادي وتحليل طاقوي , وكفاءة الطاقة.

Thermal Science and Engineering Progress 20 (2020) 100548

Contents lists available at ScienceDirect

Thermal Science and Engineering Progress

journal homepage: www.elsevier.com/locate/tsep

# Air velocity effect on the performance of geothermal helicoidally water-air heat exchanger under El Oued climate, Algeria

Abdessamia Hadjadj[a,*], Boubaker Benhaoua[a,b], Abdelmalek Atia[c], Abderrahmane Khechekhouche[a,b], Nacer Lebbihiat[c], Amar Rouag[d]

[a] University of El Oued, VTRS Laboratory, 39000 El Oued, Algeria
[b] University of El Oued, UDERZA Unit, 39000 El Oued, Algeria
[c] University of El Oued, LEVRES Laboratory, 39000 El Oued, Algeria
[d] University of Ouargla, LENREZA Laboratory, 30000 Ouargla, Algeria

ARTICLE INFO

*Keywords:*
Air velocity
Geothermal energy
Thermal efficiency
Water well
Water–air helical heat exchanger

ABSTRACT

This paper investigates experimentally the effect of air velocity on the performance of a water–air helical heat exchanger (HWAHE) in the region of El-Oued, located in the southeast of Algeria. The HWAHE made of PVC piping with 30 m of length and 0.06 m of diameter was immersed into the bottom of a water well at 5 m depth. In addition, a theoretical model was developed to determine the evolution of the air temperature inside the HWAHE as function of the main operating parameters. Results showed that the maximum heat exchange reached nearly 418 W at 10 m/s of air velocity while the maximum of temperature gap between the inlet and the outlet air was 14.1 °C. The HWAHE efficiency decreased with the increase of the air velocity. The efficiency of heat exchanger was obtained to be 82%, 81% and 80% for the average velocity value of 10, 15 and 20 m/s, respectively. According to the obtained results, the HWAHE presented in this paper may be used for cooling and heating of buildings or greenhouses in the southeastern Algeria.

## 1. Introduction

Algeria has a great potential for renewable energy including geothermal energy, which can be utilized to provide space heating/cooling and even electricity [1–3]. The achievement of indoor thermal comfort and the minimizing energy consumption in buildings are a key challenge in desert climates [4,5]. The geothermal energy system is an environmentally friendly and inexpensive technique that is influenced by the temperature difference $T_{in}$ and $T_{out}$ at the level of the PVC pipe or the heat exchanger. Like any other energy system, the geothermal energy also is influenced by the solar energy [6,7]. Many studies noted that beyond 3 m depth, the temperature can be considered almost constant [8–10]. In the studies of [11–14], numerical simulations and experimentations were performed, and different parameters such as air flow, depth of burial, length and diameter were taken in consideration to calculate the energy performance of earth air heat exchanger (EAHE). The performance of a conventional air/water heat pump system with that of a geothermal heat pump system was compared experimentally in [15,16]. Comparing the two systems, the results show that the geothermal system could save 43% of the energy consumed by the traditional system during the heating period (winter) and 37% during the cooling period (summer).

Many researchers are interested in the development of the EAHEs. Some research has shown the importance of coupling the EAHE to building for air conditioning and found that the temperature at the outlet of the EAHE is very acceptable to provide comfortable indoor environment [17–19]. An experimental and theoretical study was performed to indicate the influence of the burial depth in the ground, length, diameter of exchanger and flow velocity on the performance of geothermal energy in [20]. A transient one-dimensional heat transfer model, for predicting the effect of the operating parameters on the performances of the EAHE was developed in [21,22]. A conic basket ground heat exchanger (CBGHE) coupled to a geothermal heat pump was utilized for greenhouse cooling and it was found that the use of this geometric form of the exchanger provides good results [23–27].

The aim of our study is to reduce the consumption of electric energy used for air conditioning in the buildings in the El Oued region by using renewable energy available in the area, which is geothermal energy. An experimental study was performed with a helicoidally water–air heat exchanger (HWAHE) to select the most appropriate air flow rate for the utilization of geothermal energy effectively. The novelty of this work is the use of abundant wells in the region of El Oued to refresh or heat

* Corresponding author.
*E-mail address:* hadjadjabdessami@gmail.com (A. Hadjadj).

https://doi.org/10.1016/j.tsep.2020.100548
Received 16 August 2019; Received in revised form 9 April 2020; Accepted 10 April 2020
2451-9049/ 

**Nomenclature**

| | |
|---|---|
| $\dot{m}$ | mass flow rate, kg/s |
| $Cp_{air}$ | specific heat capacity of the air, J/kg K |
| Ta | air temperature inside the HWAHE, °C |
| $T_w$ | water temperature, °C |
| $T_{in}$ | air temperature at the inlet duct, °C |
| $T_{out}$ | air temperature at the outlet duct, °C |
| $R_{total}$ | total thermal resistance, m K/W |
| $R_w$ | thermal resistance of water, m K/W |
| $R_{pipe}$ | thermal resistance of buried pipe, m K/W |
| $R_a$ | thermal resistance of the convective heat exchange between air and pipe, m K/W |
| $r_i$ | inner radius of the pipe, m |
| $r_o$ | outer radius of the pipe, m |
| $r_{well}$ | water well radius, m |
| $h_a$ | air convective coefficient, W/m$^2$ K |
| $h_w$ | water convective coefficient, W/m$^2$ K |
| L | length of the pipe, m |
| V | air velocity inside the pipe, m/s |
| S | surface area, m$^2$ |
| $\lambda_{pipe}$ | thermal conductivity of the pipe, W/m K |
| $\lambda_{water}$ | thermal conductivity of the water, W/m K |
| ρ | density of the soil, kg/m$^3$ |

*Subscripts*

| | |
|---|---|
| a | air |
| i | inner |
| o | outer |
| w | water |

*Abbreviations*

| | |
|---|---|
| HWAHE | Helicoidally Water-Air Heat Exchanger |
| EAHE | Earth Air Heat Exchanger |
| CBGHE | Conic Basket Ground Heat Exchanger |

agricultural greenhouses or dwellings of farmers in the region with an environmentally friendly and inexpensive technique.

## 2. Method and experimentation

### 2.1. Experimental setup

The geographical coordinates of El Oued city located in the south-east of Algeria are 33.3676° N latitude and 6.8516° E longitude [28]. The steps in the experimentation performed in the study consist of drilling the well, preparation of the heat exchanger and setting up of the heat exchanger into the water well as detailed below. The tests were done in May 2017. The temperatures were recorded every hour from 10:00 h to 18:00 h with thermocouple type K connected to a small display. The meteorological conditions of the experiment are shown in Table 1.

The geothermal heat exchanger has a helical shape with 0.8 m in diameter and 3 m in length. The heat exchanger is made of PVC pipe of 30 m length and 0.06 m diameter, and it is formed of 12 spires where the space between two consecutive spires is 0.3 m. The heat exchanger is immersed in a water well of 5 m deep as shown in Fig. 1.

### 2.2. Principle of operation

The principle of operation is very intuitive, the air at ambient temperature is blown into the heat exchanger by a blower at a constant velocity. It travels throughout the tube and exchanges heat with water. At the outlet at 30 m, an anemometer is placed at the end of the PCV tube to control the velocity of the outlet air and a thermocouple to control the temperature. This temperature difference is one of the factors that affects the performance of the system. Fig. 2 shows the positioning of the K-type thermocouples on the heat exchanger immersed in the water of the well. Another instrument, flowmeter TESTO 416, is placed at the exit of the heat exchanger to measure the velocity of the air created by a blower. Table 2 shows the experimental parameters used in the system and Table 3 shows the thermal and physical properties of the air, water and PVC pipe.

### 2.3. Experimental uncertainty

To identify tests errors and uncertainties caused by tools chosen in the present study and to prove the accuracy and validity of the experiments, the measurement errors are presented in Table 4.

## 3. Mathematical modeling

The modeling of HWAHE is established with respect to the following assumptions: (a) water properties around the immersed pipe is homogenous, (b) air flow is uniform along the length of the immersed pipe; (d) thermo-physical properties of the air are constants; (e) the air flow is one dimensional.

The energy balance is as follow [29–31]:

$$\dot{m}cp_{air}\frac{dT_a}{dx} = -\left(\frac{T_a - T_w}{R_{total}}\right) \tag{1}$$

The total thermal resistance given by

$$R_{total} = R_a + R_{pipe} + R_w \tag{2}$$

The convective thermal resistance between the air and inner pipe surface $R_a$ is expressed as:

$$R_a = \frac{1}{2\pi r_i h_a} \tag{3}$$

The thermal conductive resistance of the pipe can be expressed as:

$$R_{pipe} = \frac{\ln(r_o/r_i)}{2\,\pi\,\lambda_{pipe}} \tag{4}$$

The convective resistance at water side can be written as follow:

$$R_w = \frac{1}{2\pi r_{well} h_w} \tag{5}$$

where $r_i$ and $r_o$ are the inner and outer radius of the pipe, respectively.

The outlet temperature can be obtained by the following expression [29]:

$$T_{out} = T_w + (T_{in} - T_w)\exp\left(\frac{-1}{\rho\ Cp_a S\ V\ R_{total}}L\right) \tag{6}$$

where $T_{in}$, S and V are the inlet air temperature, inner surface area of the pipe, and air velocity, respectively.The efficiency of the HWAHE

**Table 1**
Experimental conditions.

| Meteorological conditions on May 2017 | |
|---|---|
| Sunrise | 05:41 h |
| Sunset | 19:19 h |
| Ambient temperature | 26–40 °C |
| Atmospheric pressure | 101325 Pa |

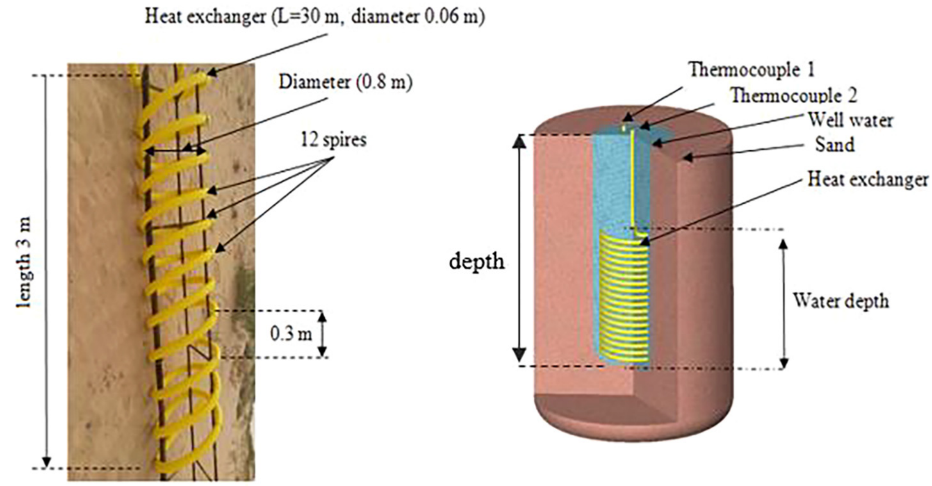


**Fig. 1.** Description of the heat exchanger.

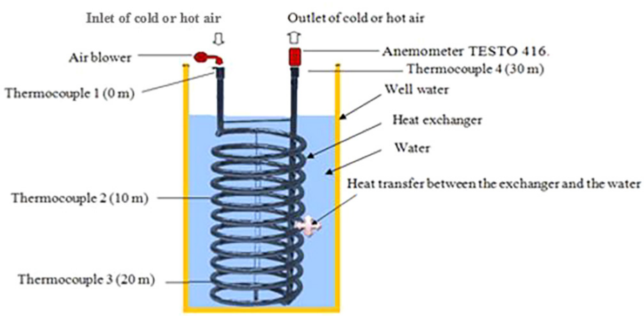


**Fig. 2.** General view of the heat exchanger.

**Table 2**
Experimental parameter.

| | |
|---|---|
| Length of pipe (m) | 30 |
| Diameter of pipe (m) | 0.06 |
| Depth of pipe (m) | 3–5 |
| Thickness of pipe (m) | 0.17 |
| Air velocity (m/s) | 10, 15 and 20 |
| Water temperature (°C) | 24.5 |
| Ambient temperature (°C) | 38 |

**Table 3**
Physical and thermal properties used in the present study.

| Material | Density (kg/m$^3$) | Thermal Capacity (J/kg K) | Thermal Conductivity (W/m K) |
|---|---|---|---|
| Air (300 K) | 1.1774 | 1005.7 | 0.02624 |
| Water | 1000 | 4180 | 0.60 |
| PVC pipe | 1380 | 900 | 0.16 |

**Table 4**
Uncertainties of data readings.

| Device | Accuracy | Range | Error |
|---|---|---|---|
| Anemometer (TESTO 416) | ± 0.2 m/s + 1.5% of | + 0.6 to + 40 m/s | ± 0.1 m/s |
| Thermocouple (Type K) | mV ± 1.1 | − 200 to 1250 °C | ± 1.1 °C |

(ε) is defined as the ratio of the air temperature drop between the outlet and the inlet of the HWAHE, and the difference between water and inlet air temperatures [16].

$$\varepsilon = \frac{T_{out} - T_{in}}{T_w - T_{in}} \tag{7}$$

## 4. Results and discussion

### 4.1. Effect of the air velocity through the tube

Experiments were performed in the region of El Oued on May 2017 from 10:00 h to 18:00 h. Temperatures were measured each 1-hour period for three different air velocities (10, 15 and 20 m/s). Besides, it is worth to note that the temperature in the water well beyond 3 m was almost constant, varied between 24 and 25 °C. In this regard, the HWAHE was immersed in the water beyond this depth to keep it in a constant temperature environment. Fig. 3.a shows side by side the experimental measurements of the inlet temperature, the water temperature and the outlet temperature in the three cases of air velocity 10, 15 and 20 m/s. From the results of Fig. 3.a, an increase in the air outlet temperature is observed with increasing of air velocity which reaches its highest value at 20 m/s. The increasing of air velocity causes an increase in the air outlet temperature because of the decreasing of the residence time of air in the HWAHE pipes. Therefore, the thermal performance of the HWAHE deteriorates with increasing of air flow velocity. Fig. 3.b shows the hourly variation of the air temperature inside the HWAHE system at three distances from the inlet (10, 20 and 30 m) for air velocity of 10 m/s. From the results of Fig. 3.b it can be noticed that any variation in the inlet temperature will be followed by a variation in the temperature of HWAHE mainly at 10 and 20 m of distance. However, at the outlet of HWAHE (at 30 m), the air temperature is fairly constant and lower than 28 °C irrespective of the inlet temperature. At the outlet, a pleasant and favorable temperature level for cooling the buildings in the region of El Oued is achieved.

### 4.2. Heat exchange rate

The air velocity of 10 m/s was used to analyze the impact of the exchanger length on the heat exchange rate as seen in Fig. 4.a. The referred figure shows that the heat exchange rate increases according to the exchanger length for all the considered velocities. Fig. 4.b shows that the HWAHE heat exchange rate is a function of the time. The obtained experimental result gives a maximum value of the heat exchange rate of 418 W at a maximum temperature of 40 °C. This means that our system works well.

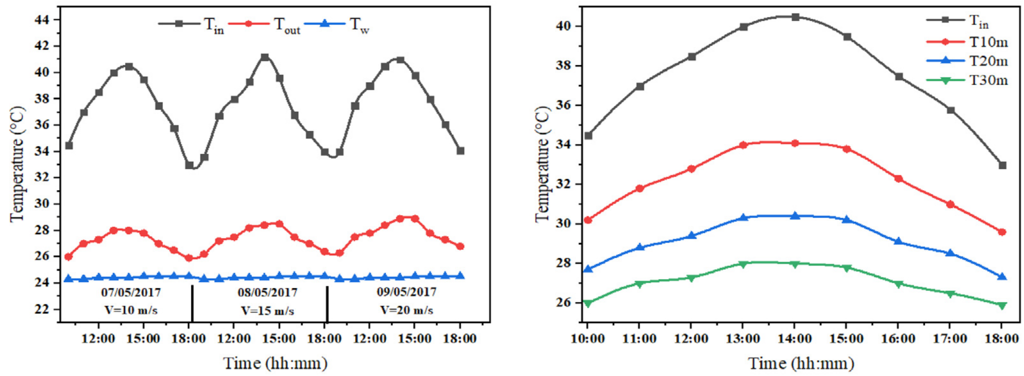


a b

**Fig. 3.** a. Variation of the outlet temperatures of the heat exchanger. b. Variation of the air temperature along the HWAHE versus the time.

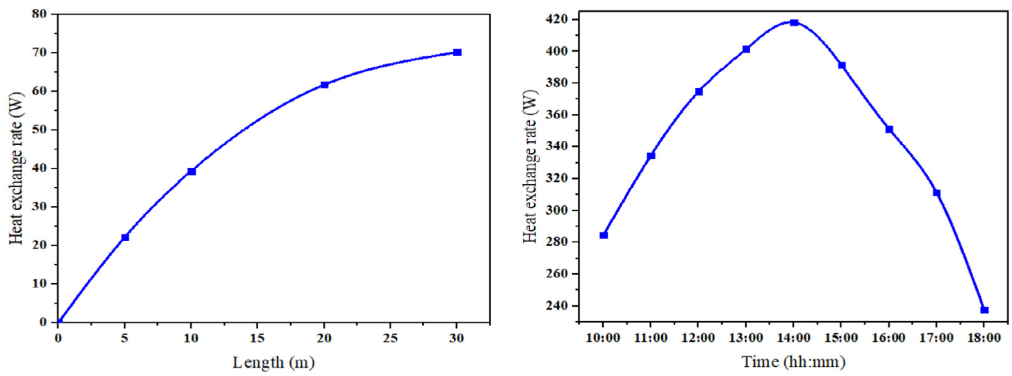


a b

**Fig. 4.** a. Heat exchange rate versus the heat exchanger length. b. Heat exchange rate versus the time.

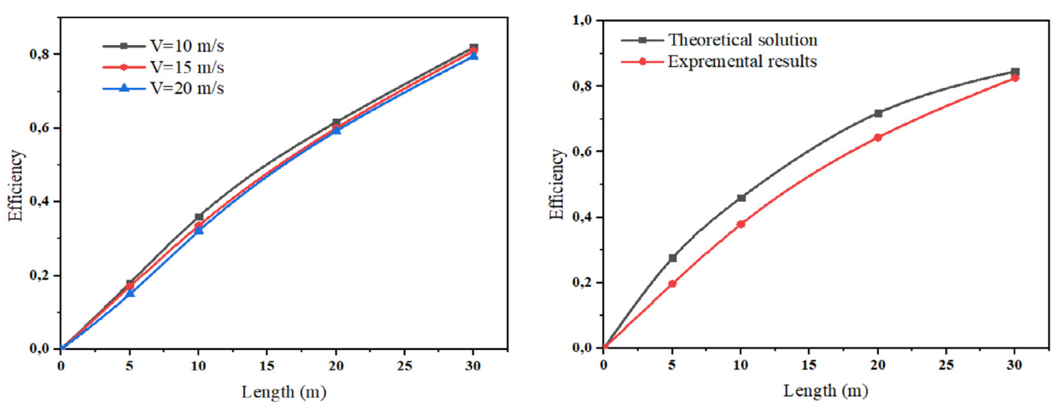


a b

**Fig. 5.** a. Heat exchanger efficiency versus the exchanger length for different air velocities. b. Heat exchanger efficiency versus the exchanger length at air velocity of 10 m/s.

### *4.3. Efficiency*

The efficiency of the system changes according to two variables; temperature and velocity. Fig. 5.a shows the results of the efficiency of the system as a function of the length of the heat exchanger. It was observed that when the velocity increased, the efficiency of the system decreased. Indeed, the residence time influences directly the amount of heat absorbed by the air. Therefore, as the velocity increases, the heat transfer coefficient increases, but on the other hand the residence time of the air in the heat exchanger decreases, so the temperature of the outlet air increases, which finally results in a decrease in the heat exchange efficiency. The efficiency is obtained to be 82%, 81% and 80% for the air velocity of 10, 15 and 20 m/s, respectively. A comparison between numerical and experimental efficiency is presented in Fig. 5.b. We chose the best efficiency (v = 10 m/s, ε = 82%) to validate it with the theoretical results. According to the graph, there is not a big difference between the two efficiencies, which shows that the result obtained is logical and acceptable.

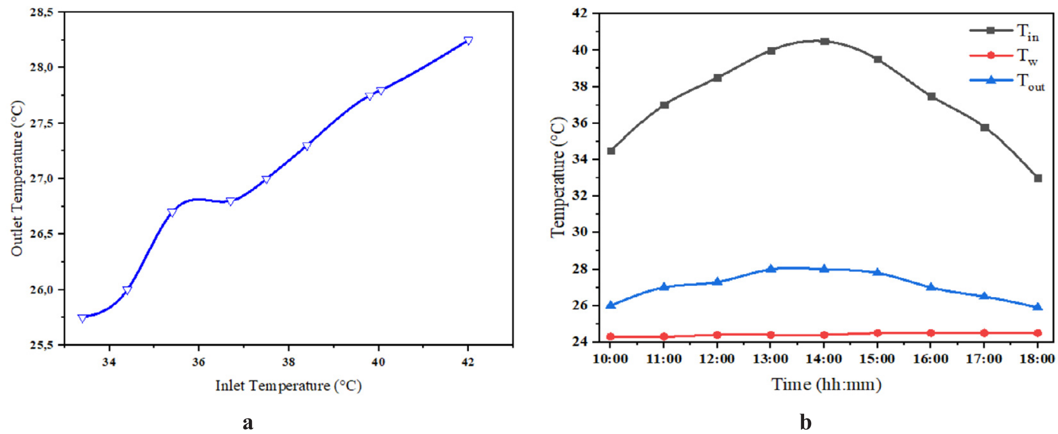


**Fig. 6.** a. Outlet air temperature variation versus the inlet air temperature. b. Variation of inlet air, outlet air and water well temperatures with time.

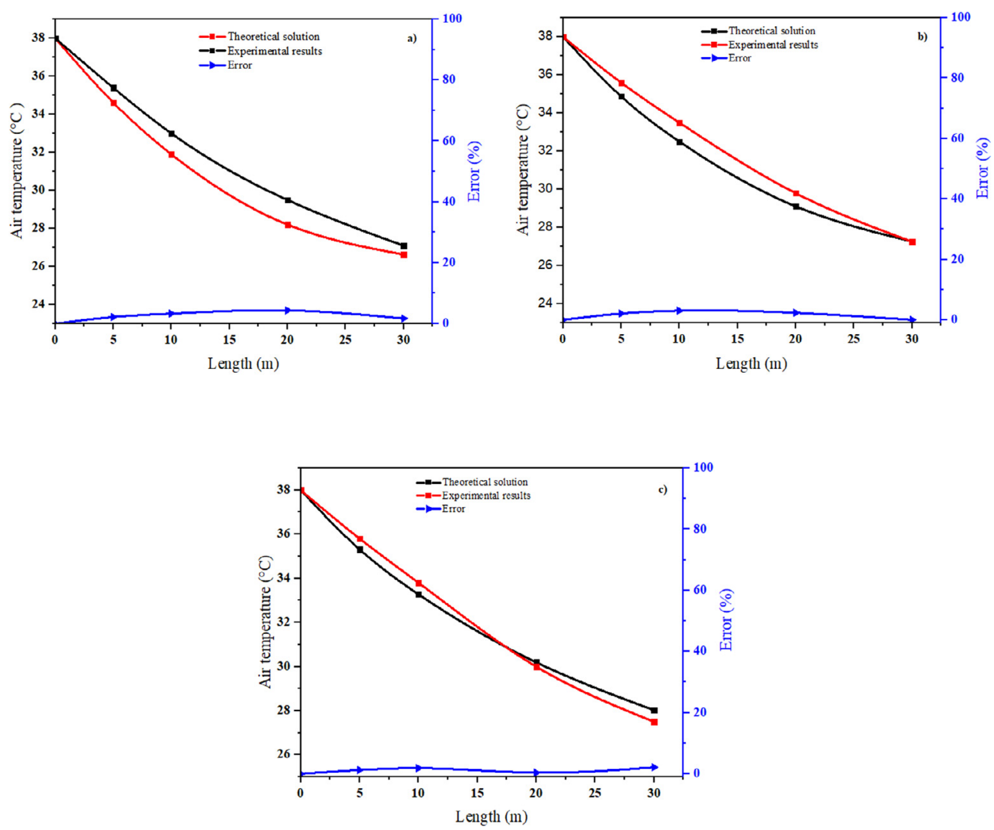


**Fig. 7.** Comparison of the air temperatures between theoretical solutions and experimental results: a) at 10 m/s, b) at 15 m/s, and c) at 20 m/s velocity.

### 4.4. Effect of the heat exchanger on the water well temperature

Fig. 6.a shows the values of the temperature of the air entering the heat exchanger at air velocity of 10 m/s and the values corresponding to the output so that the variation in the temperature level can be observed. Fig. 6.b shows the evolution of the inlet temperature and the outlet temperature (depth is 5 m) as a function of time. Note that the water temperature at this level is nearly constant around 24.5 °C while the outlet temperature varies approximately between 26 and 28 °C with a maximum of 27.9 °C at 14:00 h. On the other hand, the inlet temperature varies between 34 and 42 °C. At 14:00 h precise, we achieved a big difference between the inlet temperature 42 °C and the outlet temperature 27.9 °C which proves that studied system is effective. Furthermore, this confirms the feasibility of the HWAHE where the environment (i.e. the water at 5 m depth) plays the role of the cooling source in summer, and has a potential contribution to the heating in winter.

### 4.5. Comparison between analytical and experimental results

Fig. 7 compares the results of the proposed model with the experimental measurements. In Fig. 7 (a, b and c), the variation of air temperature along the length estimated by the theoretical model is compared with measured data for three different air flow velocities of 10, 15 and 20 m/s. In the figures, the deviation between the numerical and experimental results is also presented. An average relative error of 3.2%, 1.4%, 1.08% % is calculated for air velocity of 10, 15 and 20 m/s, respectively. It can be concluded from this figure that there is a good agreement between numerical and experimental results referring to variation of inlet air temperature over the length of heat exchanger. It was also observed that increasing the air flow velocity causes a decrease in the air temperature because of the decreasing residence time of the flowing air inside the HWAHE, as mentioned above. Therefore, the thermal performance deteriorates proportionally with air flow velocity increasing.

## 5. Conclusion

In this study, a new helicoidally water–air heat exchanger (HWAHE) configuration was presented and tested experimentally in refreshing mode in El-Oued region, Algeria. The HWAHE was immersed in 5 m depth water well. Effect of various parameters such as air velocity, exchanger length and inlet air temperature of the HWAHE were examined. Besides, an analytical model was used to predict the evolution of the air temperature inside the HWAHE as function of the main parameters. A good agreement between the experimental measurements and the results of analytical model was found.

The main points concluded from this study are as follows:

- The maximum heat transfer rate is about 418 W at air velocity of 10 m/s. The lower the air flow rate, the better the heat transfer rate.
- The maximum obtained temperature gap between the inlet and the outlet of the HWAHE is of 14.1 °C with 10 m/s of air velocity.
- The efficiency of the proposed HWAHE decreased with the increase of the air velocity. For the average values of air velocities used in this study (10, 15 and 20 m/s), the HWAHE efficiencies are 82%, 81% and 80%, respectively.
- The analytical study of the exchanger showed a high concordance with those experimental.

It is noted that this study is a starting point for a future development of HWAHE system research in Algeria desert. The obtained results give a good encouragement to use the proposed HWAHE as an air refreshing tool in the region of El-Oued and even in the whole Sahara of Algeria.

## Declaration of Competing Interest

The authors declared no potential conflicts of interest with respect to the research, authorship, and publication of this article.

## Acknowledgment

This study was supported by the Algerian Ministry of Higher Education and Scientific Research. The author are very grateful for the assistance and the enlightening discussions with Dr. Yousef Belloufi.

## References

[1] S. Pahlavan, M. Jahangiri, A. Shamsabadi, A. Khechekhouche, Feasibility study of solar water heaters in Algeria, a review, J. Solar Energy Res. (2018) 135–146.
[2] G. Kappler, J.B. Dias, F. Haeberle, P.R. Wander, C.A.M. Moraes, R.C.E. Modolo, Study of an earth-to-water heat exchange system which relies on underground water tanks, Renewable Energy 133 (2019) 1236–1246.
[3] J. Sobti, S.K. Singh, Earth-air heat exchanger as a green retrofit for Chandīgarh—a critical review, Geothermal Energy 3 (1) (2015) 14.
[4] O. Leyla, A review on the experimental and analytical analysis of earth to air heat exchanger (EAHE) systems in Turkey, Renew. Sustain. Energy Rev.. 15 (9) (2011) 4483–4490.
[5] K.K. Agrawal, M. Bhardwaj, R. Misra, G.D. Agrawal, V. Bansal, Optimization of operating parameters of earth air tunnel heat exchanger for space cooling: Taguchi method approach, Geothermal Energy 6 (1) (2018) 10.
[6] A. Khechekhouche, A. Boukhari, Z. Driss, N. Benhissen, Seasonal effect on solar distillation in the El-Oued region of south-east Algeria, Int. J. Energ. 2 (2) (2017) 42–45.
[7] Adel Laaraba, Abderrahmane Khechekhouche, Numerical simulation of natural convection in the air gap of a vertical flat plat thermal solar collector with partitions attached to its glazing, Indonesian J. Sci. Technol. 3 (2) (2018) 14–23.
[8] Zhengxuan Liua, hun (Jerry)Yu, Tingting Yang, Letizia Roccamena Pengcheng Sun, Shuisheng Li, Guoqiang Zhang, Mohamed El Mankibi, "Numerical modeling and parametric study of a vertical earth-to-air heat exchanger system," Energy vol. 172, pp. 220-231, 2019.
[9] M. Rohit, B. Vikas, A.G. Das, M. Jyotirmay, A.T.K, CFD analysis based parametric study of derating factor for Earth Air Tunnel Heat Exchanger, Appl. Energy 103 (2013) 266–277.
[10] V. Bansal, R. Misra, G.D. Agrawal, J. Mathur, Performance analysis of earth–-pipe–air heat exchanger for summer cooling, Energy Build. 42 (5) (2010) 645–648.
[11] S. Menhoudj, M.-H. Benzaama, C. Maalouf, M. Lachi, M. Makhlouf, Study of the energy performance of an earth—Air heat exchanger for refreshing buildings in Algeria, Energy Build. 158 (2018) 1602–1612.
[12] M. Benhammou, B. Draoui, Parametric study on thermal performance of earth-to-air heat exchanger used for cooling of buildings, Renew. Sustain. Energy Rev. 44 (2015) 348–355.
[13] J.F. Urchueguía, M. Zacarés, J.M. Corberán, Á. Montero, J. Martos, H. Witte, Comparison between the energy performance of a ground coupled water to water heat pump system and an air to water heat pump system for heating and cooling in typical conditions of the European Mediterranean Coast, Energy Convers. Manag. 49 (10) (2008) 2917–2923.
[14] Ł. Amanowicz, J. Wojtkowiak, Validation of CFD model for simulation of multi-pipe earth-to-air heat exchangers (EAHEs) flow performance, Thermal Sci. Eng. Progress 5 (2018) 44–49.
[15] N. Naili, I. Attar, M. Hazami, A. Farhat, First in situ operation performance test of ground source heat pump in Tunisia, Energy Convers. Manag. 75 (2013) 292–301.
[16] N. Naili, M. Hazami, S. Kooli, A. Farhat, Energy and exergy analysis of horizontal ground heat exchanger for hot climatic condition of northern Tunisia, Geothermics 53 (2015) 270–280.
[17] A. Sehli, A. Hasni, M. Tamali, The potential of earth-air heat exchangers for low energy cooling of buildings in South Algeria, Energy Procedia 18 (2012) 496–506.
[18] S.N. Saifi, B. Negrou, A. Hadjadj, Design and functional analysis of earth- air heat exchanger (EAHE) coupled with solar chimney in South East Algeria, Acad. J. Sci. Res. 5 (12) (2017) 732–744.
[19] Yousef Belloufi, Abdelhafid Brima, Sakina Zerouali, Rachid Atmani, Faris Aissaoui, Amar Rouag, Moummi Noureddine., "Numerical and experimental investigation on the transient behavior of an earth air heat exchanger in continuous operation mode, " International Journal of heat and Technology, vol. 35, no. 2, pp. 279-288, 2017.
[20] P. Hollmuller, B. Lachal, Air–soil heat exchangers for heating and cooling of buildings: Design guidelines, potentials and constraints, system integration and global energy balance, Appl. Energy 119 (2014) 476–487.
[21] A. Atia, A. Hadjadj, B. Benhaoua, N. Lebbihiat, A. Brima, A review of studies on geothermal energy system applied on sub-saharan climate regions, Water Energy Int. 60 (5) (2017) 63–68.
[22] M. Benhammou, B. Draoui, M. Hamouda, Improvement of the summer cooling induced by an earth-to-air heat exchanger integrated in a residential building under hot and arid climate, Appl. Energy 208 (2017) 428–445.
[23] M.H. Benzaama, S. Menhoudj, C. Maalouf, A. Mokhtari, M. Lachi, Experimental and numerical analysis of the energy performance of a water/soil exchanger coupled to a cooling floor for North Africa, Geothermics 80 (2019) 8–19.
[24] S. Barakat, A. Ramzy, A. Hamed, S. El Emam, Enhancement of gas turbine power output using earth to air heat exchanger (EAHE) cooling system, Energy Convers. Manage. 111 (2016) 137–146.
[25] N. Naili, I. Attar, M. Hazami, and A. Farhat, "Experimental analysis of horizontal ground heat exchanger for Northern Tunisia," 2012.
[26] H. Boughanmi, M. Lazaar, S. Bouadila, A.J.E. Farhat, Buildings, Thermal performance of a conic basket heat exchanger coupled to a geothermal heat pump for greenhouse cooling under Tunisian climate, Energy Build. 104 (2015) 87–96.
[27] H. Boughanmi, M. Lazaar, A. Farhat, A. Guizani, Evaluation of soil thermal potential under Tunisian climate using a new conic basket geothermal heat exchanger: Energy and exergy analysis, Appl. Therm. Eng. 113 (2017) 912–925.
[28] A. Khechekhouche, B. B. Haoua, A. E. Kabeel, M. E. H. Attia, and W. M. El-Maghlany, "Improvement of Solar Distiller Productivity by a Black Metallic Plate of Zinc as a Thermal Storage Material," Journal of Testing Evaluation, vol. 49, no. 2, 2019.
[29] D. Belatrache, S. Bentouba, M. Bourouis, Numerical analysis of earth air heat exchangers at operating conditions in arid climates, Int. J. Hydrogen Energy 42 (13) (2017) 8898–8904.
[30] E. Neshat, S. Hossainpour, F. Bahiraee, Experimental and numerical study on unsteady natural convection heat transfer in helically coiled tube heat exchangers, Heat Mass Transf. 50 (6) (2014) 877–885.
[31] M. Moawed, Experimental investigation of natural convection from vertical and horizontal helicoidal pipes in HVAC applications, Energy Convers. Manage. 46 (18–19) (2005) 2996–3013.